LIST OF PUBLICATIONS

1. Mayur G. Sankalia, Rajshree C. Mashru, Jolly M. Sankalia, and Vijay B. Sutariya. "Stability improvement of alpha-amylase entrapped in kappa-carrageenan beads: physicochemical characterization and optimization using composite index", *International Journal of Pharmaceutics*, 2006, *xx (x)*, xxx-xxx (in press).

2. Mayur G. Sankalia, Rajshree C. Mashru, Jolly M. Sankalia, and Vijay B. Sutariya. "Papain entrapment in alginate beads for stability improvement and site specific delivery: physicochemical characterization and factorial optimization using neural network modeling", *AAPS PharmSciTech*, 2005, *6 (2)*, article 31, E209-E222. (doi:10.1208/pt060231).

3. Sankalia MG., Mashru RC., Sankalia JM. and Sutariya VB. "Evaluation and simultaneous optimization of papain entrapped in crosslinked alginate beads using 3^3 factorial design and the desirability function", *ARS Pharmaceutica*, 2004, *45 (3)*, 253-279.

4. Mayur G. Sankalia, Rajshree C. Mashru, Jolly M. Sankalia, and Vijay B. Sutariya. "Papain entrapped in ionotropically crosslinked kappa-carrageenan gel beads for stability improvement: physicochemical characterization and factorial optimization using Doehlert Shell Design", *Journal of Pharmaceutical Sciences* (accepted with minor revision).

MANUSCRIPTS COMMUNICATED

1. M. G. Sankalia, R. C. Mashru, J. M. Sankalia, and V. B. Sutariya. "Reversed chitosan-alginate polyelectrolyte complex for stability improvement of alpha-amylase: Optimization and physicochemical characterization", *Pharmaceutical Research.*

2. M. G. Sankalia, R. C. Mashru, J. M. Sankalia, and V. B. Sutariya. "Reversed chitosan-alginate polyelectrolyte complex for stability improvement of papain: Physicochemical characterization and optimization using composite index", *Journal of Pharmacy and Pharmaceutical Sciences.*

3. M. G. Sankalia, R. C. Mashru, J. M. Sankalia, and V. B. Sutariya. "Physicochemical characterization and factorial optimization of alpha-amylase entrapment in alginate beads for stability improvement and site specific delivery", *Drug Development and Industrial Pharmacy.*

4. Mayur G. Sankalia, Rajshree C. Mashru, Jolly M. Sankalia, and Vijay B. Sutariya. "Ionotropically crosslinked kappa-carrageenan gel beads of pepsin for stability improvement: optimization and physicochemical characterization using box-behnken design", *ARS Pharmaceutica.*

5. Sankalia MG., Mashru RC., Sankalia JM. And Sutariya VB. "Application of artificial neural networks (ANN) modeling in pharmaceutical research: a review article", *ARS Pharmaceutica.*

PAPERS PRESENTED

1. Mayur G. Sankalia*, Rajshree C. Mashru, Jolly M. Sankalia, Vijay B. Sutariya and Yogesh M. Rane. "Alpha-amylase encapsulated in biodegradable calcium alginate pellets for shelf-life improvement and site-specific delivery to the gastrointestinal tract", at *National Seminar on Polymers, Surfactants and Gels 2005*, Vadodara, March 11-13, 2005 (Poster Present[n] PP-18).

2. Mayur G. Sankalia, Rajshree C. Mashru, Jolly M. Sankalia* and Vijay B. Sutariya. "Neural Network Modeling for Prediction and Simultaneous Optimization of Papain Entrapped in Crosslinked Alginate Beads", at *56th Indian Pharmaceutical Congress 2004*, Kolkata, December 3-5, 2004 (Oral Presentation: A-64).

3. M. G. Sankalia* and R. C. Mashru. "Immobilization of alpha-amylase in calcium alginate gel for improvisation of shelf-life", at *54th Indian Pharmaceutical Congress 2002*, Poona, December 13-15, 2001 (Poster Presentation: HP-11).

Evaluación y optimización simultánea de papaína inmovilizada en gránulos de alginato entrecruzado mediante un diseño factorial 3x3 y la función de deseabilidad

Evaluation and simultaneous optimization of papain entrapped in crosslinked alginate beads using 3^3 factorial design and the desirability function

SANKALIA MG.[1], MASHRU RC.*, SANKALIA JM. AND SUTARIYA VB.

Center of relevance and excellence in NDDS, Pharmacy Department, G. H. Patel building, The M. S. University of Baroda, Vadodara - 390 002, Gujarat, India. Telephone: +91-265-2434187 / 2794051. Fax: +91-265-2418928.
[1]E-mail: sankalia_mayur@hotmail.com
* Author for correspondence.

RESUMEN

En este artículo se investiga el entrecruzamiento del alginato sódico con iones de calcio a través de la gelación ionotrópica para capturar la papaína mediante disolventes «benignos para el entorno». Se empleó un diseño factorial completo 3x3 para investigar el efecto de las tres variables del proceso, que son la concentración de alginato sódico, la concentración de cloruro cálcico y el tiempo de endurecimiento sobre el porcentaje de captura, el tiempo necesario para la liberación de un 50% (T_{50}) y un 90% (T_{90}) de la enzima, la distribución y el ángulo de reposo. Los gránulos se prepararon mediante el uso de un dispositivo de goteo para el vertido de gotas de solución de alginato sódico que contiene la enzima en la solución de cloruro cálcico agitada magnéticamente. Además, se empleó la función de deseabilidad para optimizar el proceso sometido a estudio. Se demostró que los valores óptimos de las respuestas se pueden obtener en los niveles inferiores de las tres variables del proceso. La caracterización topográfica se realizó mediante microscopía electrónica de barrido (SEM) y la captura se confirmó a través de una calorimetría diferencial de barrido (DSC). Se concluyó que la selección adecuada de concentración de alginato con control de la velocidad de liberación y su potencial interactivo para el entrecruzamiento es importante y determina el tamaño y la forma general de los gránulos, los perfiles de patrón de disolución y duración, la sensibilidad al pH y la capacidad de carga de la enzima.
PALABRAS CLAVE: Gránulos de alginato cálcico. Función de deseabilidad. Captura. Diseño factorial. Optimización. Papaína. Alginato sódico.

ABSTRACT

This paper investigates the crosslinking of sodium alginate with calcium ions through ionotropic gelation to entrap papain using "environmentally benign" solvents. A 3^3 full factorial design was employed to investigate the effect of three process variables namely sodium alginate concentration, calcium chloride concentration and hardening time on % entrapment, time required for 50% (T_{50}) and 90% (T_{90}) of enzyme release, particle size and angle of repose. The beads were prepared by dropping the sodium alginate solution containing enzyme from dropping device to magnetically stirred calcium chloride solution. Furthermore, the desirability function was employed in order to optimize the process under study. It was found that the optimum values of the responses could be obtained at the low levels of all three process variables. Topographical characterization was carried out by taking SEM and entrapment was confirmed using DSC. It was concluded that the proper selection of rate-controlling alginate concentration and their interactive potential for crosslinking is important, and will determine the overall size and shape of beads, the duration and pattern of dissolution profiles, pH sensitivity and enzyme loading capacity.
KEY WORDS: Calcium alginate beads. Desirability function. Entrapment. Factorial design. Optimization. Papain. Sodium alginate.

INTRODUCCIÓN

La papaína (EC 3.4.22.2) es una tiol-proteasa y su centro activo es Cis-25, His-159 y Asp-158. La papaína presenta una amplia actividad proteólica ante las proteínas, péptidos de cadena corta, enlaces amidas y ésteres de aminoácidos[1] y se utiliza de manera muy extendida en el ámbito de la alimentación y la medicina[2]. La reacción inversa de la hidrólisis de la papaína se puede emplear también en la síntesis de péptidos y oligómeros basados en aminoácidos[2-4], especialmente la papaína inmovilizada, empleada en la síntesis enzimática de péptidos y sus derivados en disolventes orgánicos[5]. El pH óptimo para la actividad de la papaína se sitúa en un intervalo de entre 3 y 9, el cual varía según el sustrato[6,7]. No obstante, la papaína es casi inactiva con un pH gástrico de 1,2, por lo que el lugar ideal para su administración es el intestino delgado.

Los sistemas de administración de fármacos en un punto específico son populares y pueden formularse como formas de dosificación de una o varias unidades. Las ventajas relativas que presentan las formas de dosificación de varias unidades (p. ej. un tiempo de tránsito gastrointestinal predecible, menos molestias gastrointestinales localizadas y una mayor seguridad del producto) frente a los productos de una unidad están ampliamente establecidas. Desde el punto de vista de la fabricación, con independencia de los tipos de forma de dosificación (de una o varias unidades), en la actualidad es común el uso de ingredientes hidrófilos que se puedan dilatar en el diseño de sistemas de liberación modificados y proporcionan una gran flexibilidad a la tecnología farmacéutica[8-13]. A la vista de las múltiples ventajas que ofrecen las formas de dosificación de varias unidades, se especula sobre el hecho de que tales sistemas pueden resultar particularmente útiles: (i) para la administración de fármacos muy irritantes, como son los fármacos antiinflamatorios no esteroides (AINE)[14,15]; (ii) para la administración en un punto específico del tracto gastrointestinal[16]; y (iii) para la administración de enzimas, péptidos/proteínas y vacunas[17,18].

El alginato es un copolímero natural de ácido â-D-manurónico (M) y á-L-gulurónico (G) unidos por enlaces 1-4 y es un polisacárido con una elevada masa molecular que se extrae de las algas pardas(Phaeophyceae, principalmente Laminaria)[19]. Se descubrió que las unidades G y M se unen en bloques y, como tales, se pueden encontrar tres tipos de bloques: bloques G homopolímeros (GG), bloques M homopolímeros (MM) y bloques heteropolímeros con secuencias alternantes (MG). La reactividad con el calcio y la consiguiente capacidad para la formación de geles es una función directa de la longitud de cadena media de los bloques G[20]. Por lo tanto, los alginatos que contienen las fracciones de GG mayores presentan la más alta capacidad para la formación de geles. Esto se deriva inicialmente de la capacidad del catión calcio divalente para ajustarse en las estructuras gulurónicas de forma similar a como lo hacen los huevos en una «caja de huevos». Por consiguiente, esto une las cadenas de alginato mediante la formación de zonas de unión, lo que conduce a continuación a la gelación de la solución y a la formación de gránulos. Al añadir una solución acuosa de alginato sódico en forma de gotas a una solución acuosa de cloruro cálcico, se obtiene un gel esférico de forma y tamaño regulares. El gel esférico se denomina «gránulo de alginato». Los gránulos de alginato presentan la ventaja de no ser tóxicos por vía oral y de poseer una elevada biocompatibilidad[21,22]. Otra propiedad ventajosa es su incapacidad para volver a dilatarse en entornos ácidos mientras que sí lo hacen con facilidad en entornos alcalinos, de modo que los fármacos sensibles al ácido que se incorporen a los gránulos estarían protegidos ante los jugos gástricos[23]. Por lo tanto, el alginato se emplea como una matriz de captura para células y enzimas, así como para aditivos farmacéuticos y alimentarios[24-26]. No obstante, la porosidad de los gránulos de alginato resulta en una rápida liberación del contenido incorporado.

En el pasado, se han realizado investigaciones de los gránulos de alginato cálcico entrecruzados convencionales para el desarrollo de un sistema de administración de fármacos de varias unidades[27-32]. Se puede afirmar que los factores más importantes que regulan la administración de fármacos son el grado de relajación de polímeros, el mantenimiento de los límites de la capa del gel, la erosión del gel y la disolución de polímeros[12]. Por consiguiente, para identificar de forma lógica estos mecanismos de regulación, en este artículo se analizan los estudios de disolución de los gránulos y se evalúan y caracterizan los parámetros fisicoquímicos que afectan a

INTRODUCTION

Papain (EC 3.4.22.2) is one of the thiol proteases, and its active site consists of Cys-25, His-159 and Asp-158. Papain shows extensive proteolytic activity towards proteins, short-chain peptides, amino acid esters and amide links[1], and is applied extensively in the fields of food and medicine[2]. The reverse reaction of hydrolysis of papain also can be employed in the synthesis of peptides and oligomers based on amino acids[2-4], especially immobilized papain, which has been employed in the enzymic synthesis of peptides and their derivatives in organic solvents[5]. Optimum pH for activity of papain is in the range of 3-9 which varies with different substrate[6,7]. However, papain is almost inactive at gastric pH of 1.2 so the ideal place for papain delivery is small intestine.

Site-specific drug delivery systems are popular and can be formulated as single or multiple unit dosage forms. The relative merits of multiple unit dosage forms (e.g. predictable gastrointestinal transit time, less localized gastrointestinal disturbances and greater product safety) over single unit products are well established. From a manufacturing point of view, irrespective of the types of the dosage form (single or multiple unit), currently the utilization of hydrophilic swellable ingredients in the design of modified release systems are common and offer significant flexibility in pharmaceutical technology[8-13]. In view of the many benefits offered by multiple unit dosage forms, it is speculated that such systems are particularly useful: (i) for delivering highly-irritant drugs such as nonsteroidal anti-inflammatory drugs (NSAIDs)[14,15]; (ii) for site-specific targeting within the gastrointestinal tract[16]; and (iii) for delivery of enzymes, peptides/proteins and vaccines[17,18].

Alginate is a natural copolymer of 1,4-linked â-D-mannuronic acid (M) and á-L-guluronic acid (G) and is a high-molecular-mass polysaccharide extracted from brown seaweeds (Phaeophyceae, mainly Laminaria)[19]. It has been shown that the G and M units are joined together in blocks and as such, three types of blocks may be found: homo-polymeric G blocks (GG), homo-polymeric M blocks (MM) and heteropolymeric sequentially alternating blocks (MG). The reactivity with calcium and the subsequent gel formation capacity is a direct function of the average chain length of the G blocks[20]. Hence, alginates containing the highest GG fractions possess the strongest ability to form gels. This initially arises from the ability of the divalent calcium cation to fit into the guluronate structures like eggs in an "egg box junctions". Consequently, this binds the alginate chains together by forming junction zones, and sequentially leading to gelling of the solution mixture and bead formation. When an aqueous solution of sodium alginate is added dropwise to an aqueous solution of calcium chloride, a spherical gel with regular shape and size is obtained. The spherical gel is termed an "alginate bead". Alginate beads have the advantages of being nontoxic orally and having high biocompatibility[21,22]. Another advantageous property is their inability to reswell in acidic environment while easily reswells in alkaline environment, so acid-sensitive drugs incorporated into the beads would be protected from gastric juice[23]. Therefore, alginate is used as an entrapment matrix for cells and enzymes as well as pharmaceutical and food adjuvants[24-26]. However, the porosity of alginate beads results in a fast release of incorporated content.

In the past, conventional crosslinked calcium–alginate beads have been investigated for the development of a multiple unit drug delivery system[27-32]. It may be postulated that the most crucial factors regulating drug release are degree of polymer relaxation, maintenance of gel layer boundary, gel erosion and polymer dissolution[12]. Consequently, in order to logically identify these regulating mechanisms, this paper will deal with dissolution studies of beads and with evaluating and characterizing those physicochemical parameters which affect bead formation and its release behavior.

MATERIALS AND METHODS

Materials

Purified papain, sodium alginate, calcium chloride dihydrate, dibasic sodium phosphate and citric acid were purchased from S. D. Fine-Chem Ltd., Mumbai, India. Hammersten type casein (Himedia Laboratories Pvt. Ltd., Mumbai, India) and trichloroacetic acid (Qualigens Fine Chemicals, Mumbai, India) were used as received. All the other chemicals and solvents were

la formación de gránulos y al comportamiento de liberación correspondiente.

MATERIALES Y MÉTODOS

Materiales

La papaína purificada, el alginato sódico, el cloruro cálcico dihidratado, el fosfato sódico dibásico y el ácido cítrico se adquirieron en S. D. Fine-Chem Ltd., Mombai, India. La caseína tipo Hammerstein (Himedia Laboratories Pvt. Ltd., Mombai, India) y el ácido tricloroacético (Qualigens Fine Chemicals, Mombai, India) se utilizaron como se recibieron sin modificación alguna. Todos los demás productos químicos y disolventes eran de grado analítico y se utilizaron sin una posterior purificación. Para el estudio se utilizó agua desionizada sometida a doble destilación.

Preparación de los gránulos

La solución de alginato sódico concentrado se preparó antes de que fuera necesario mediante la disolución de alginato sódico en agua destilada. La cantidad de enzima requerida (200 mg de papaína en 50 ml de solución de alginato sódico final) se disolvió en una pequeña cantidad de agua y se mezcló con la solución de alginato sódico concentrado. La concentración final de alginato sódico se ajustó en un intervalo de 1-2% p/v y utilizó tras su desgasificación en vacío. La preparación de los gránulos se realizó mediante el vertido de gotas de la solución de alginato sódico (50 ml) que contiene la enzima desde un dispositivo de goteo como una jeringa con una aguja hipodérmica de punta plana con un calibre de 26» en una solución de cloruro cálcico agitada magnéticamente (200 ml) y se dejó que se endureciera durante un período de tiempo específico. Se seleccionaron distintos niveles (Tabla 1) de alginato sódico, cloruro cálcico y tiempo de endurecimiento. Los gránulos se obtuvieron mediante la decantación de la solución de cloruro cálcico, se lavaron con agua desionizada y se secaron en un desecador de vacío (Tarsons Products Pvt. Ltd., Kolkata, India) durante 36 horas. El proceso descrito anteriormente se realizó a una temperatura ambiente controlada (20°C).

of analytical grade and were used without further purification. Deionized double-distilled water was used through out the study.

Preparation of beads

Concentrated sodium alginate solution was prepared well before required by dissolving sodium alginate in distilled water. Required quantity of enzyme (200 mg papain in 50 ml of final sodium alginate solution) was dissolved in small quantity of water and mixed with concentrated sodium alginate solution. Final concentration of sodium alginate was adjusted in the range of 1-2% w/v and was used after being degassed under a vacuum. The beads were prepared by dropping of the sodium alginate solution (50 ml) containing enzyme from the dropping device such as syringe with 26G" flat-tip hypodermic needle to a magnetically stirred calcium chloride solution (200 ml) and were allowed to harden for specific time. Different levels (Table 1) of sodium alginate, calcium chloride and hardening time were selected. The beads were collected by decanting calcium chloride solution, washed with deionized water and dried in vacuum desiccator (Tarsons Products Pvt. Ltd., Kolkata, India) for 36 hours. Above process was carried out at controlled room temperature (20°C).

TABLA I. Factorial 3x3: factores y niveles correspondientes.

TABLE 1. Factorial 3^3: factors and their levels.

Factores Factors	Nivel bajo Low level	Nivel medio Middle level	Nivel alto High level
A: Alginato sódico (% p/v) A: Sodium alginate (% w/v)	1,0	1,5	2,0
B: Cloruro cálcico (M) B: Calcium chloride (M)	0,05	0,10	0,15
C: Tiempo de endurecimiento (min) C: Hardening time (min)	20	25	30

Evaluación de los gránulos

Determinación de la eficacia de captura

La eficacia de captura constituía el parámetro de evolución importante para la optimización de la captura. La cantidad total de enzima capturada en los gránulos se determinó mediante la disolución de éstos en un fluido intestinal simulado y agitado magnéticamente durante 45 min. La solución se centrifugó a 2500 rpm durante 10 min (Remi Instruments Ltd, Mombai, India) y la parte flotante se sometió a ensayo (n=3) en busca de contenido enzimático mediante el método de digestión de la caseína de USP XXVI. La eficacia de captura se calculó como:

$$\text{Eficacia de captura} = \frac{\text{Carga enzimática}}{\text{Carga enzimática teórica}} \times 100 \quad (1)$$

Determinación del perfil de liberación dependiente del pH

Los estudios de disolución «in vitro» se realizaron mediante el aparato 2 de disolución de USP XXVI (TDT-60T, Electrolab, Mombai, India) en 500 ml en medios con diferentes pH que oscilaban entre 1,2 y 8,0 en un lote experimental a 37±0,5°C con el agitador de paletas a una velocidad de 50 rpm. Se introdujeron muestras pesadas con precisión (n=3) equivalentes a unos 40 mg de papaína en el medio de disolución y se obtuvieron muestras de 2 ml a las 0, 0,25, 0,50, 0,75, 1,0, 1,5, 2,0, 2,5, 3,0, 3,5, 4,0, 4,5, 5,0, 5,5 y 6,0 horas. Las muestras se filtraron a través de un filtro de membrana de 0,4 lm y se sometieron a estudio en busca de contenido enzimático tal y como se hizo con anterioridad. Los gránulos de alginato demostraron tener un perfil de liberación dependiente del pH, obteniéndose el valor

Evaluation of beads

Determination of entrapment efficiency

Entrapment efficiency was the important evolutionary parameter for optimization of entrapment. Total amount of enzyme entrapped in beads was determined by dissolving the beads in magnetically stirred simulated intestinal fluid without enzyme for about 45 min. The solution was centrifuged at 2500 rpm for 10 min (Remi Instruments Ltd, Mumbai, India) and supernatant was assayed (n=3) for enzyme content by casein digestion method of USP XXVI. Entrapment efficiency was calculated as:

$$\text{Entrapmentefficiency} = \frac{\text{Enzymeloading}}{\text{Theoratical enzymeloading}} \times 100 \quad (1)$$

Determination of pH dependent release profile

'In vitro' dissolution studies were carried out using the USP XXVI dissolution apparatus 2 (TDT-60T, Electrolab, Mumbai, India) in 500 ml of different pH media ranging from 1.2 to 8.0 on one experimental batch at 37±0.5°C with paddle speed of 50 rpm. Accurately weighed samples (n=3) equivalent to about 40 mg of papain were introduced to dissolution media and samples of 2 ml were collected at 0, 0.25, 0.50, 0.75, 1.0, 1.5, 2.0, 2.5, 3.0, 3.5, 4.0, 4.5, 5.0, 5.5 and 6.0 hr. Samples were filtered through 0.4 lm membrane filter and assayed for enzyme content as before. Alginate beads showed pH dependant release profile and it was maximum in simulated intestinal fluid without enzyme.

máximo en el fluido intestinal simulado sin enzima.

Determinación de los valores T_{50} y T_{90}

El tiempo necesario para la liberación del 50 (T_{50}) y el 90 (T_{90}) por ciento de la enzima son parámetros importantes para el estudio de la liberación enzimática. Para una mayor optimización, se realizó un estudio de disolución de todos los lotes en 500 ml de fluido intestinal simulado sin enzima, tal y como se realizó anteriormente. Se sometieron a la disolución las muestras pesadas con precisión (n=3) equivalentes a unos 40 mg de papaína y se sometieron a estudio alícuotas de 2 ml cada 0, 5, 10, 15, 20, 30, 45, 60, 90 y 120 min. Los valores T_{50} y T_{90} se obtuvieron a partir del porcentaje de enzima liberada en relación a una línea de tiempo mediante el trazado de una línea de proyección en los ejes de tiempo en los valores de liberación del 50% y 90% respectivamente.

Mediciones del tamaño de partículas

El tamaño de las partículas se determinó con el analizador de tamaño de partículas por difracción láser (MAN 0244/ HYDRO 2000 SM, Malvern Instruments Ltd., RU) con alcohol isopropílico como vehículo.

Mediciones del ángulo de reposo

Para medir el ángulo de reposo se hicieron pasar los gránulos a través de un embudo situado sobre la superficie horizontal. Se midió la altura (h) del montón con un catetómetro y se determinó también el radio (r) de la base del cono. El ángulo de reposo (Φ) se calculó a partir de la ecuación:

$$\tan \Phi = \frac{h}{r} \qquad (2)$$

Calorimetría diferencial de barrido (DSC)

El análisis calorimétrico diferencial de barrido se utilizó para caracterizar el comportamiento térmico de las sustancias aisladas, gránulos cargados y vacíos. Los termogramas DSC se obtuvieron mediante un sistema de análisis térmico automático (DSC-60, Shimadzu, Japón). Las calibraciones de temperatura se realizaron utilizando indio como estándar. Las muestras se colocaron en una cubeta de aluminio estándar y se calentaron de 30°C a 400°C a incrementos de 10°C/min con un purgado constante de nitrógeno seco a razón de 30 ml/min. Se utilizó como referencia una cubeta vacía, sellada de la misma forma que la muestra.

Determination of T_{50} and T_{90}

Time required for 50 (T_{50}) and 90 (T_{90}) percent of enzyme release are important parameters for enzyme release study. For optimization purpose, dissolution study of all batches was carried out in 500 ml of simulated intestinal fluid without enzyme as before. Accurately weighed samples (n=3) equivalent to about 40 mg of papain were subjected to dissolution and aliquots of 2 ml were assayed at 0, 5, 10, 15, 20, 30, 45, 60, 90 and 120 min. T_{50} and T_{90} were found from % enzyme released versus time plot by drawing a projection line on the time axes at 50% and 90% release respectively.

Particle size measurements

Particle size was determined with the laser diffraction particle size analyzer (MAN 0244/ HYDRO 2000 SM, Malvern Instruments Ltd., UK) using isopropyl alcohol as a vehicle.

Angle of repose measurements

Angle of repose was measured by passing beads through a funnel on the horizontal surface. The height (h) of the heap formed was measured with a cathetometer and the radius (r) of the cone base was also determined. The angle of repose (Φ) was calculated from:

$$\tan \Phi = \frac{h}{r} \qquad (2)$$

Differential scanning calorimetry (DSC)

Differential scanning calorimetric analysis was used to characterize the thermal behaviour of the isolated substances, empty and loaded beads. DSC thermograms were obtained using an automatic thermal analyzer system (DSC-60, Shimadzu, Japan). Temperature calibrations were performed using indium as a standard. Samples were crimped in a standard aluminium pan and heated from 30–400°C at 10°C/min under constant purging of dry nitrogen at 30 ml/min. An empty pan, sealed in the same way as the sample, was used as a reference.

Microscopía electrónica de barrido (TEM)

La finalidad del estudio mediante SEM era la de obtener una caracterización topográfica de los gránulos. Los gránulos se montaron en portamuestras de latón mediante cinta adhesiva por ambas caras. Las imágenes SEM se tomaron con un microscopio electrónico de barrido (JSM-5610LV, Jeol Ltd., Japón) con el aumento requerido a temperatura ambiente. Se mantuvo una distancia de trabajo de 39 mm y se utilizó un voltaje de aceleración de 15 kV, con la imagen de electrones secundarios (SEI) como detector.

Diseño factorial y función de deseabilidad

Para este estudio se utilizó un diseño factorial completo 3x3 para determinar el efecto de la concentración de alginato sódico (% p/v), la concentración de cloruro cálcico (M) y el tiempo de endurecimiento (min). Con anterioridad a la aplicación del diseño, se realizó cierto número de pruebas preliminares para determinar las condiciones a las que se producían gránulos durante el proceso. Los factores implicados y los niveles correspondientes se muestran en la Tabla 1.

La matriz de los experimentos y el resultado de las respuestas se muestran en la Tabla 2. para determinar el error experimental, se repitió el experimento en el punto medio cinco veces en días diferentes. La media del porcentaje de captura, T_{50}, T_{90}, el tamaño de las partículas y el ángulo de reposo de estos experimentos fue 85,88±1,02, 15,57±0,28, 82,43±0,33, 261,130±0,868 y 20,61±0,29 respectivamente. Estos valores mostraron la excelente reproducibilidad del proceso. La evaluación estadística de los resultados se realizó mediante el análisis de varianza con un paquete de software de análisis estadístico disponible en el mercado (DESIGN EXPERT V 6.0.10, Minneapolis, EE.UU.). Se seleccionó el modelo cuadrático para este análisis.

Scanning electron microscopy (SEM)

The purpose of SEM study was to obtain a topographical characterization of beads. The beads were mounted on brass stubs using double-sided adhesive tape. SEM photographs were taken with scanning electron microscope (JSM-5610LV, Jeol Ltd., Japan) at the required magnification at room temperature. The working distance of 39 mm was maintained and acceleration voltage used was 15 kV, with the secondary electron image (SEI) as a detector.

Factorial design and the desirability function

In this study a 3^3 full factorial design was used to determine the effect of the concentration of sodium alginate (% w/v), the concentration of calcium chloride (M) and the hardening time (min). Before the application of the design a number of preliminary trials were conducted to determine the conditions at which the process resulted to beads. The factors and their levels are shown in Table 1.

The matrix of the experiments and the results of the responses are listed in Table 2. To determine the experimental error, the experiment at the centre point was replicated five times at different days. The mean % entrapment, T_{50}, T_{90}, particle size and angle of repose of these experiments were 85.88±1.02, 15.57±0.28, 82.43±0.33, 261.130±0.868 and 20.61±0.29 respectively. The above-mentioned values showed good reproducibility of the process. The statistical evaluation of the results was carried out by analysis of variance (ANOVA) using a commercially available statistical software package (DESIGN EXPERT V 6.0.10, Minneapolis, USA). The quadratic model was selected for this analysis.

TABLA 2.- Factorial 3x3: matriz de experimentos y resultados de la deseabilidad y las respuestas medidas.
TABLE 2.- Factorial 3^3: matrix of the experiments and results for the measured responses and the desirability.

Factores/Niveles Factors/ levels				Respuestas Responses					Deseabilidad general Overall desira-bility
SE* ESa	Alginato sódico (% p/v) *Na. Alginate (% w/v)*	Cloruro cálcico (M) *Calcium chloride (M)*	Tiempo de endurecimiento (min) *Harde-ning Time (min)*	% de captura *% Entrap-ment*	T50	T90	Tamaño (µm) *Size (µm)*	Ángulo de reposo *Angle of repose*	
1	1,0	0,05	20	91,80	6,50	23,80	211,136	22,62	0,962
10	1,0	0,05	25	89,00	8,30	25,70	207,319	22,88	0,913
19	1,0	0,05	30	86,20	9,35	28,40	202,628	23,27	0,868
4	1,0	0,10	20	85,00	7,80	27,50	184,327	23,39	0,878
13	1,0	0,10	25	82,60	9,10	30,55	181,059	23,75	0,831
22	1,0	0,10	30	80,71	10,70	34,00	178,289	24,15	0,781
7	1,0	0,15	20	68,80	8,60	34,60	175,983	24,07	0,599
16	1 0	0,15	25	67,79	10,30	39,00	171,384	24,94	0,533
25	1,0	0,15	30	65,28	12,05	59,25	169,737	26,33	0,000
2	1,5	0,05	20	93,40	13,35	48,00	297,039	19,50	0,815
11	1,5	0,05	25	90,80	14,45	57,40	291,606	19,76	0,747
20	1,5	0,05	30	88,00	16,30	57,40	285,497	20,02	0,694
5	1,5	0,10	20	87,70	14,35	75,00	266,941	20,27	0,648
29	1,5	0,10	25	87,01	15,30	82,50	261,453	20,56	0,579
32	1,5	0,10	25	86,29	15,90	82,90	259,825	20,20	0,563
31	1,5	0,10	25	85,06	15,20	82,40	260,348	20,98	0,569
28	1,5	0,10	25	84,35	15,80	81,90	261,874	20,44	0,561
14	1,5	0,10	25	86,78	15,70	82,30	262,013	20,89	0,572
30	1,5	0,10	25	85,80	15,50	82,60	261,265	20,58	0,568
23	1,5	0,10	30	83,50	16,80	87,65	255,367	20,97	0,489
8	1,5	0,15	20	77,30	15,55	80,55	258,163	21,20	0,522
17	1,5	0,15	25	75,30	16,90	83,50	252,709	21,84	0,464
26	1,5	0,15	30	72,00	19,30	86,50	246,003	22,20	0,366
3	2,0	0,05	20	94,40	15,90	83,80	715,268	16,14	0,599
12	2,0	0,05	25	91,39	17,05	91,50	708,007	16,49	0,476
21	2,0	0,05	30	88,50	18,60	95,60	701,294	16,87	0,339
6	2,0	0,10	20	88,40	17,70	90,80	682,689	17,00	0,464
15	2,0	0,10	25	86,00	18,60	94,20	677,136	17,26	0,375
24	2,0	0,10	30	84,00	20,20	96,15	671,935	17,77	0,270
9	2,0	0,15	20	79,50	19,40	95,60	673,543	18,03	0,293
18	2,0	0,15	25	76,60	20,40	96,30	668,162	18,56	0,233
27	2,0	0,15	30	73,70	22,80	97,20	662,736	18,89	0,000

* SE: Secuencia experimental – *ES, experimental sequence.*

Por último, se utilizó la función de deseabilidad para el proceso de optimización. La aplicación de la función de deseabilidad conjuga todas las respuestas en una medición y ofrece la posibilidad de predecir los niveles óptimos de las variables independientes. La combinación de las respuestas en una función de deseabilidad requiere el cálculo de la función de deseabilidad de forma individualizada. En este estudio concreto no existía ningún requisito especial en cuanto al tamaño de partículas de la formulación óptima, de modo que se seleccionó el intervalo de valores de las formulaciones producidas. La formulación óptima de este estudio debe tener un tamaño de partículas entre 169,737 y 715,268 lm, con una captura mínima y máxima de T_{50} y T_{90} y un ángulo de reposo. La deseabilidad individual de cada respuesta se calculó mediante los métodos siguientes[33].

Finally the desirability function was used for the optimization process. The application of the desirability function combines all the responses in one measurement, and gives the possibility to predict the optimum levels for the independent variables. The combination of the responses in one desirability function requires the calculation of the individual desirability function. In this particular study there was no special requirement for the particle size of the optimum formulation, so the range of the values of the produced formulations was selected. The optimum formulation of this study should have a particle size ranging between 169.737 and 715.268 lm, with maximum entrapment and minimum T_{50}, T_{90} and angle of repose. The individual desirability for each response was calculated using the following methods[33].

Se maximizó el valor del porcentaje de captura en el procedimiento de optimización debido a que era deseable obtener los valores más elevados de este parámetro. La función de deseabilidad de este parámetro se calculó mediante la ecuación siguiente:

$$d_1 = \frac{Y_1 - Y_{min}}{Y_{max} - Y_{min}} \qquad (3)$$

donde d_1 es la deseabilidad individual del porcentaje de captura e Y_1 es el resultado experimental. Los valores de Y_{max} e Y_{min} para el porcentaje de captura eran 94,40 y 65,28 respectivamente.

El valor T_{50} y T_{90} se minimizó en el procedimiento de optimización, ya que los valores inferiores de estos parámetros suponen una liberación más rápida y completa de las enzimas de los gránulos. El cálculo de la función de deseabilidad se realizó mediante la ecuación:

$$d_2 \text{ ó } d_3 = \frac{Y_{max} - Y_1}{Y_{max} - Y_{min}} \qquad (4)$$

donde d_2 es la deseabilidad individual de T_{50}, d_3 es la deseabilidad individual de T_{90} e Y_1 es el resultado experimental. Los valores de Y_{max} e Y_{min} eran 22,8 y 6,5 para T_{50} y 97,2 y 23,8 para T_{90} respectivamente.

Las formulaciones con un tamaño de partículas dentro del intervalo 169,737-715,268 lm tienen una función de deseabilidad de 1, mientras que las formulaciones con valores fuera de este rango presentan un valor de deseabilidad de 0. Éstos se describen mediante las ecuaciones siguientes:

$$d_4 = 0 \quad \text{para} \quad Y_1 < Y_{min} \qquad (5)$$

$$d_4 = 1 \quad \text{para} \quad Y_{min} < Y_1 < Y_{max} \qquad (6)$$

$$d_4 = 0 \quad \text{para} \quad Y_1 > Y_{max} \qquad (7)$$

donde d_4 es la deseabilidad individual del tamaño de partículas e Y_1 es el resultado experimental.

Se seleccionó la función de deseabilidad parcial no lineal para el ángulo de reposo que era menos importante en la optimización. El valor se minimizó ya que era deseable el menor ángulo de reposo. En este caso, todos los valores

The % entrapment value was maximized in the optimization procedure, as the higher values of this parameter are desirable. The desirability function of this parameter was calculated by using the following equation:

$$d_1 = \frac{Y_1 - Y_{min}}{Y_{max} - Y_{min}} \qquad (3)$$

where d_1 is the individual desirability of % entrapment and Y_1 is the experimental result. The values of Y_{max} and Y_{min} for % entrapment were 94.40 and 65.28 respectively.

The T_{50} and T_{90} value were minimized in the optimization procedure, as lower values of these parameters give quicker and complete release of enzyme from the beads. The calculation of the desirability function was carried out using the equation:

$$d_2 \text{ or } d_3 = \frac{Y_{max} - Y_1}{Y_{max} - Y_{min}} \qquad (4)$$

where d_2 is the individual desirability of T_{50}, d_3 is individual desirability of T_{90} and Y_1 is the experimental result. The values of Y_{max} and Y_{min} were 22.8 and 6.5 min for T_{50} and 97.2 and 23.8 min for T_{90} respectively.

Formulations that have a particle size within the range of 169.737-715.268 lm have a desirability function of 1, while the formulations that have values out of this range have a desirability value of 0. These can be described by the following equations:

$$d_4 = 0 \quad \text{for} \quad Y_1 < Y_{min} \qquad (5)$$

$$d_4 = 1 \quad \text{for} \quad Y_{min} < Y_1 < Y_{max} \qquad (6)$$

$$d_4 = 0 \quad \text{for} \quad Y_1 > Y_{max} \qquad (7)$$

where d_4 is the individual desirability of the particle size and Y_1 is the experimental result.

Non-linear partial desirability function was selected for angle of repose which was less important in the optimization. The value was minimized as lower angle of repose was desirable. In this case all the experimental values were acceptable, however, the values far from the target, are little penalized, by choosing $0<s<1$ (0.1 in this case) in the following equations:

experimentales eran aceptables; no obstante los valores muy alejados del destino se penalizaron levemente mediante la selección de 0<s<1 (0,1 en este caso) en las ecuaciones siguientes:

$$d_5 = 1 \qquad \text{si } Y_1 \le Y_{min} \quad (8)$$

$$d_5 = \left(\frac{Y_{max} - Y_1}{Y_{max} - Y_{min}}\right)^s \qquad \text{si } Y_{min} \le Y_1 \le Y_{max} \quad (9)$$

$$d_5 = 0 \qquad \text{si } Y_{max} \le Y_1 \quad (10)$$

donde d_5 es la deseabilidad individual del ángulo de reposo e Y_1 es el resultado experimental. Los valores de Y_{max} e Y_{min} para el ángulo de reposo eran 26,326 y 16,137 respectivamente.

Los valores de deseabilidad general se calcularon a partir de los valores individuales mediante la ecuación siguiente:

$$D = (d_1 \times d_2 \times d_3 \times d_4 \times d_5)^{1/5} = \left[\prod_{i=1}^{5} d_i\right]^{1/5} \quad (11)$$

RESULTADOS Y DISCUSIÓN

Perfil de liberación dependiente del pH

Normalmente, los fármacos con un mayor peso molecular y que se disuelven con más dificultad en el agua no se liberan de los gránulos de alginato cálcico debido a su estabilidad y capacidad para no dilatarse en entornos ácidos, mientras que se dilatan y se desintegran en el pH intestinal[23,34,35]. La dilatación y desintegración de gránulos de alginato cálcico depende de la composición del medio de disolución como, por ejemplo, el sodio y el fosfato, y la solubilidad del fármaco capturado en los gránulos de alginato. La papaína no se liberó de los gránulos de alginato debido a un mayor peso molecular. La dilatación y desintegración de los gránulos de alginato en el fluido intestinal se debió a la afinidad del calcio con el fosfato y al intercambio sodio/calcio[9,36]. El efecto del pH en la liberación de papaína de los gránulos de alginato cálcico en tampones con distinto pH que simulaban el tracto gastrointestinal de los seres humanos se muestra en la Figura 1. El perfil de liberación del lote optimizado en el fluido intestinal simulado sin enzima se muestra en la Figura 2.

$$d_5 = 1 \qquad \text{if } Y_1 \le Y_{min} \quad (8)$$

$$d_5 = \left(\frac{Y_{max} - Y_1}{Y_{max} - Y_{min}}\right)^s \qquad \text{if } Y_{min} \le Y_1 \le Y_{max} \quad (9)$$

$$d_5 = 0 \qquad \text{if } Y_{max} \le Y_1 \quad (10)$$

where d_5 is the individual desirability of angle of repose and Y_1 is the experimental result. The values of Y_{max} and Y_{min} for angle of repose were 26.326 and 16.137 respectively.

The overall desirability values were calculated from the individual values by using the following equation:

$$D = (d_1 \times d_2 \times d_3 \times d_4 \times d_5)^{1/5} = \left[\prod_{i=1}^{5} d_i\right]^{1/5} \quad (11)$$

RESULT AND DISCUSSION

pH dependent release profile

Generally, higher molecular weight and poorly water-soluble drugs are not released from calcium alginate beads due to stability and non swelling property in acidic environment while swell and disintegrate in intestinal pH[23,34,35]. The swelling and disintegration of calcium alginate beads are dependent on compositions of dissolution medium, e.g. sodium and phosphate, and solubility of drug entrapped into alginate beads. Papain was not released from alginate beads due to higher molecular weight. The swelling and disintegration of alginate beads in intestinal fluid were due to the affinity of calcium to phosphate and sodium/calcium exchange[9,36]. The effect of pH on the release of papain from calcium alginate beads in different pH buffers simulating the human gastrointestinal tract is given in Figure 1. Release profile of optimized batch in simulated intestinal fluid without enzyme is shown in Figure 2.

FIGURA 1. Determinación del perfil de liberación dependiente del pH a través de un estudio de disolución «in vitro».

FIGURE 1. Determination of pH dependent release profile by 'In vitro' dissolution study.

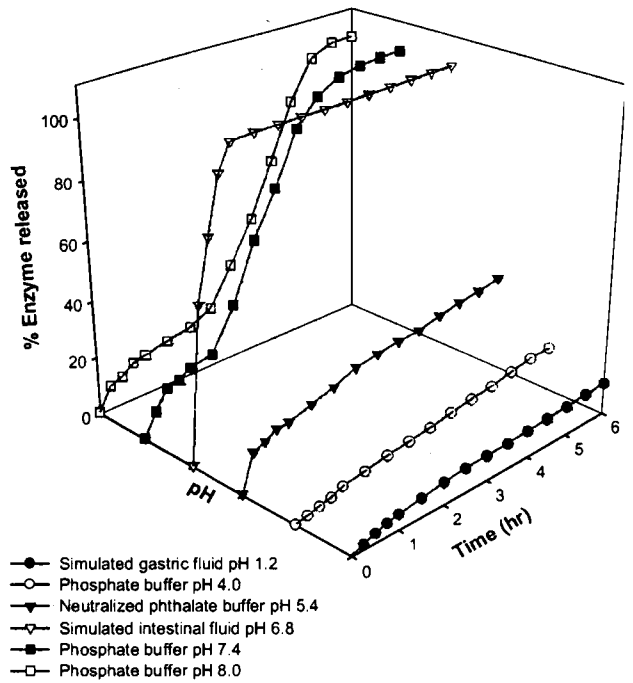

FIGURE 2. Perfil de liberación del lote optimizado (formulación 1) en el fluido intestinal simulado sin enzima.

FIGURE 2.- Release profile of optimized batch (formulation 1) in simulated intestinal fluid without enzyme.

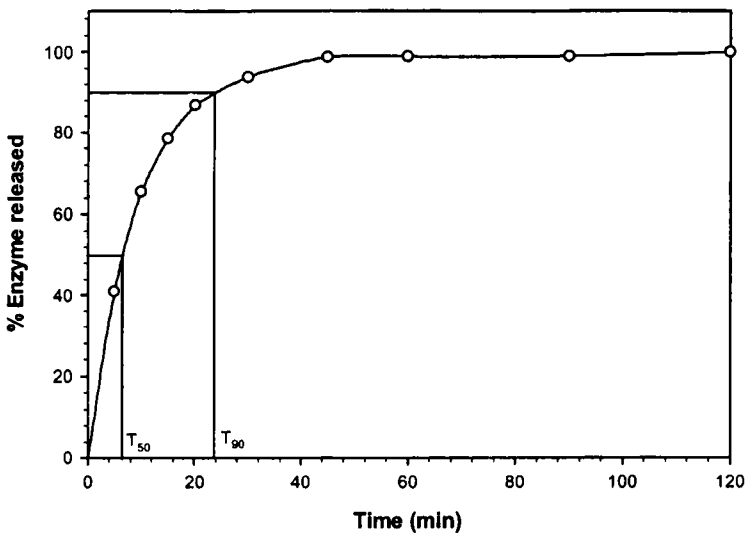

Efecto de los factores sobre las respuestas

Porcentaje de captura

Los resultados del análisis de varianza y los coeficientes de regresión de las variables de respuesta se muestran en la Tabla 3 de la que se derivan que los efectos de los tres factores que inciden sobre el porcentaje de captura fueron significativos desde un punto de vista estadístico (P <0,05). Los resultados que se obtienen de la Tabla 2 mostraron que el mayor valor porcentual de captura se obtuvo a un nivel superior (2% p/v) de la concentración de alginato sódico, sobre todo cuando al elevado nivel de la concentración de alginato sódico se sucedían niveles bajos de los otros dos factores (Experimento 3).

En la adición de la solución de alginato sódico a una solución de cloruro cálcico, se produjo un entrecruzamiento superficial instantáneo con la precipitación del alginato cálcico seguida de una gelación más gradual del interior que provocó la pérdida de enzima de la superficie de los gránulos. La pérdida de enzima superficial fue proporcional al grado de entrecruzamiento. La mayor viscosidad con concentraciones más elevadas de alginato sódico retrasó la penetración del calcio hacia el interior del gránulo. Esto resultó en un descenso del entrecruzamiento y una mayor eficacia de captura, favorecida en mayor medida por el coeficiente positivo del factor A (Tabla 3). El grado de entrecruzamiento aumentó al incrementar la concentración de cloruro cálcico y el tiempo de endurecimiento[37] y resultó en una menor capacidad de captura[38], que se corresponde con el coeficiente negativo de los factores B y C de la Tabla 3. La concentración de cloruro cálcico fue el factor más influyente (42,23%) de los tres.

Effect of the factors on responses

% Entrapment

ANOVA results and regression coefficients of response variables are shown in Table 3 from which it can be concluded that the effects of all three factors on the % entrapment were statistically significant (P <0.05). The results obtained from the Table 2 showed that the highest % entrapment value was obtained at the high level (2% w/v) of the sodium alginate concentration especially when the high level of the sodium alginate concentration was followed by the low levels of the other two factors (experiment 3).

On addition of sodium alginate solution to a calcium chloride solution, instantaneous interfacial crosslinking took place with precipitation of calcium alginate followed by a more gradual gelation of the interior which caused loss of enzyme from the surface of the beads. Loss of surface enzyme was proportional to the degree of crosslinking. Increased viscosity at higher sodium alginate concentration retarded penetration of calcium to the interior of the bead. This resulted in decrease of crosslinking and increased entrapment efficiency which was further supported by the positive coefficient of factor A (Table 3). Degree of crosslinking increased with increase in calcium chloride concentration and hardening time[37] and resulted in decreased entrapent[38] which correspond to negative coefficient for factor B and C in Table 3. Calcium chloride concentration was the most influential (42.23%) factor amongst all three factors.

TABLA 3. Resultados del análisis de varianza (Valores P): efecto de las variables en el porcentaje de captura, T_{50}, T_{90}, el tamaño de partículas y el ángulo de reposo.

TABLE 3. ANOVA results (P values): effect of the variables on % entrapment T50, T90, particle size and angle of repose.

	% de captura / *% Entrapment*		T50		T90		Tamaño de partículas / *Particle size*		Ángulo de reposo / *Angle of repose*	
Factores / Factors	Coeficiente / Coeffici-ent	P	Coeficiente / Coefficient	P	Coeficiente / Coeffi-cient	P	Coeficiente / Coefficient	P	Coeficiente / Coefficient	P
A	2,517	<0,0001*	4,886	<0,0001*	29,908	<0,0001*	248,828	<0,0001*	-1,244	<0,0001*
B	-8,734	<0,0001*	1,417	<0,0001*	8,939	<0,0001*	-18,965	<0,0001*	1,028	<0,0001*
C	-2,467	<0,0001*	1,497	<0,0001*	4,583	0,0071*	-5,089	<0,0001*	0,458	<0,0001*
A^2	-1,532	0,0003*	-1,766	<0,0001*	-11,39	0,0001*	167,526	<0,0001*	-0,028	0,7433
B^2	-3,184	<0,0001*	0,193	0,0764	-4,694	0,0682	10,123	<0,0001*	0,172	0,0485*
C^2	-0,112	0,7569	0,218	0,0474*	-1,744	0,4836	0,183	0,6531	0,019	0,8450
AB	1,720	<0,0001*	0,354	0,0002*	-3,063	0,1194	-1,346	0,0003*	-0,149	0,4462
AC	-0,2245	0,4249	-0,050	0,5386	-1,417	0,4614	-1,229	0,0007*	-0,109	0,0987
BC	0,190	0,4981	0,175	0,0397*	0,533	0,7804	0,401	0,2106	0,185	0,0078*
Constante	85,933	-	15,567	-	79,231	-	261,305	-	20,590	-
r^2_{adj}	0,968	-	0,996	-	0,935	-	0,999	-	0,993	-

Los coeficientes de regresión se expresan mediante valores codificados. * Significativo estadísticamente (P <0,05)
Regression coefficients are in coded values. *, Statistically significant (P <0.05)

T_{50}

El tiempo necesario para la liberación del 50% de la enzima (T_{50}) se empleó para evaluar el inicio de la acción de las formulaciones. Tal y como se aprecia en la Tabla 3, los tres valores tuvieron un importante efecto positivo en el valor de respuesta (es decir, el valor de respuesta aumentó al incrementar el nivel del factor). La concentración de alginato (factor A) tuvo el efecto más significativo (46,26%) sobre el valor T_{50}. No obstante, la liberación inmediata de enzima para que el inicio de la acción fuera más rápido, y obtener así un valor T_{50} más breve, constituía el criterio deseable para la formulación óptima. La liberación de papaína de los gránulos resultó inversamente proporcional al grado de entrecru-

T_{50}

The time required for 50 % of enzyme release (T_{50}) was used to evaluate the onset of action of the formulations. As shown in Table 3, all three factors had significant positive effect on response value (i.e. response value increase with increase in factor level). The concentration of alginate (factor A) had the most significant (46.26%) effect on T_{50}. However, immediate release of enzyme for quicker on set of action and hence shorter T_{50} was the desirable criteria for the optimum formulation. Release of papain from beads was inversely proportional to the degree of crosslinking. Higher calcium concentration and hardening time also resulted in higher T_{50} due to higher degree of crosslinking[38].

zamiento. Una concentración de calcio y un tiempo de endurecimiento mayores supuso también un valor de T_{50} superior debido al mayor grado de entrecruzamiento[38].

T_{90}

El 90% de la enzima debía liberarse en el menor tiempo posible para producir el máximo efecto en el lugar de la liberación. Los tres factores tuvieron un efecto positivo sobre el valor de respuesta que se puede apreciar en la Tabla 3. La concentración de alginato (factor A) fue el factor con una mayor influencia (45,14%). El valor T_{90} fue proporcional al grado de entrecruzamiento y el tamaño de partículas. A concentraciones de alginato mayores se correspondían gránulos de mayor tamaño con valores T_{90} elevados. Una concentración de calcio y un tiempo de endurecimiento mayores supuso un valor de T_{90} superior debido al mayor grado de entrecruzamiento[38].

Tamaño de partículas

Tal y como se muestra en la Tabla 3, los tres parámetros fueron significativos para el tamaño de partículas; de ellos, la concentración de alginato de sodio resultó ser el factor más relevante (54,84%). En el tamaño de los gránulos influyó el tamaño de la abertura a través de la cual se permitió pasar a la solución de alginato (con una cantidad constante) y la viscosidad de la solución de alginato. La viscosidad aumentó con la concentración de alginato de sodio, lo que resultó en partículas de mayor tamaño. La concentración de cloruro cálcico y el tiempo de endurecimiento tuvieron un efecto negativo (es decir, la respuesta se redujo al aumentar los niveles de los factores) en el tamaño de las partículas. Un grado de entrecruzamiento debido a una mayor concentración de cloruro cálcico y un tiempo de endurecimiento mayores causaron la contracción de los gránulos y que el tamaño de partículas fuera menor[38].

Ángulo de reposo

Se midió el ángulo de reposo para estimar la capacidad de fluencia de los gránulos. Si el ángulo supera los 50°, el material no fluye satisfactoriamente mientras que los materiales con valores cercanos al mínimo fluyen fácil y correctamente[39]. Cuanto más irregular y rugosa sea la superficie de las partículas, mayor será el ángulo de reposo. El ángulo también aumenta al reducirse el tamaño de partículas.

Aquí también, los tres factores mostraron tener un efecto significativo sobre el ángulo de reposo. El tamaño de partículas aumentó con el incremento de la concentración de alginato sódico y resultó en un ángulo menor. Esto se confirmó de una forma más sólida por la existencia de un coeficiente negativo para el factor A de la Tabla 3. Una concentración de cloruro cálcico y un tiempo de endurecimiento mayores produjeron gránulos de menor tamaño con una superficie irregular debido a la contracción y al ángulo de mayor tamaño mostrado. La concentración de alginato sódico fue el factor con mayor incidencia (61,33%) de los tres.

Interacción de los factores

Un interacción hace que un factor no produzca el mismo efecto en la respuesta cuando se varían los niveles de otro factor[40]. Los resultados del análisis de varianza (Tabla 3) mostraron que la interacción AB influyó de forma significativa en el porcentaje de captura, el valor T_{50} y el tamaño de partículas. La interacción AC influyó significativamente sólo en el tamaño de partículas mientras que la interacción BC influyó en gran medida en el valor T_{50} y en el ángulo de reposo.

El análisis de los resultados de la Tabla 2 por regresión múltiple conduce a ecuaciones que describen adecuadamente la influencia de los factores seleccionados en el porcentaje de captura, los valores T_{50} y T_{90}, el tamaño de partículas y el ángulo de reposo. En la Tabla 3 se muestran los coeficientes de regresión de estas ecuaciones.

Optimización del proceso mediante la función de deseabilidad

Generalmente, la optimización de las formulaciones farmacéuticas tiene la finalidad de encontrar los niveles óptimos de las variables que afectan a un proceso en el que se podrían gene-

T_{90}

90% of enzyme should be released in minimum time to exert maximum action at the site of release. All three factors had positive effect on response value which can be seen in Table 3. The concentration of alginate (factor A) was the most influencing (45.14%) factor. T_{90} was proportional to the degree of crosslinking and particle size. Higher concentration of alginate yielded larger beads with high T_{90} values. Higher calcium concentration and hardening time resulted in higher T_{90} due to higher degree of crosslinking[38].

Particle size

As shown in Table 3, all three parameters were significant for particle size amongst which sodium alginate concentration was the most affecting (54.84%) factor. The sizes of the beads are influenced by the size of the opening through which the alginate solution is allowed to pass (which was kept constant) and viscosity of the alginate solution. Viscosity increased with concentration of sodium alginate which resulted in larger particles. Calcium chloride concentration and hardening time had the negative effect (i.e. response decreases with increase in factor levels) on the particle size. Higher degree of crosskinking due to higher calcium chloride concentration and hardening time caused shrinkage of beads and resulted in smaller particle size[38].

Angle of Repose

Angle of repose was measured for estimating flowability of the beads. If the angle exceeds 50°, the material will not flow satisfactorily while materials having values near the minimum, flow easily and well[39]. The rougher and more irregular the surface of the particles, the higher will be the angle of repose. The angle also increases with decrease in particle size.

Here, too, all three factors exhibited significant effect on angle of repose. Particle size increased with increase in sodium alginate concentration and resulted in decreased angle. This was further confirmed by a negative coefficient of factor A in Table 3. Higher calcium chloride concentration and hardening time resulted in smaller beads with irregular surface due to shrinkage and showed increased angle. Concentration of sodium alginate concentration was the most influencing (61.33%) factor amongst all three.

Interactions between the factors

An interaction is the failure of a factor to produce the same effect on the response at the different levels of the other factor[40]. The ANOVA results (Table 3) showed that the interaction AB had significant influence on the % entrapment, T_{50} and particle size. The interaction AC had significant influence only on particle size while interaction BC was found to influence significantly on T_{50} and angle of repose.

The analysis of the results of the Table 2 by multiple regression leads to equations that adequately describe the influence of the selected factors on % entrapment, T_{50}, T_{90}, particle size and angle of repose. In Table 3 regression coefficients of these equations are presented.

Optimization of the process using the desirability function

Generally the aim of the optimization of pharmaceutical formulations is to find the optimum levels of the variables, which affect a process, where a product of good characteristics could be produced. Using the desirability function, all the selected responses were combined in one overall response, the overall desirability. As it has been already discussed, the overall desirability response was calculated from the individual desirability of each of the responses using the Eqs. (3)–(11). The results of each of these overall desirability responses are included in the optimization procedure and the equation found out was as follow (coded factors):

$$D = 0.609 - 0.184A - 0.189B - 0.110C - 0.046A^2 - 0.044B^2 - 0.016C^2 + 0.060AB + 0.004AC - 0.048BC \quad (r^2_{adj.} = 0.8530,\ P < 0.0001) \quad (12)$$

In Figures 3-5 the contour plots that describe the influence of the factors on the overall desirability, % entrapment and T_{50} are presented. The study of these plots showed that the highest values of the desirability could be obtained at low values of all three process variables. Especially the analysis of the Eq. (12) resulted to the optimum

rar productos con unas características buenas. Mediante la función de deseabilidad se conjugaron todas las respuestas seleccionadas en una respuesta general, la deseabilidad general. Como ya se ha visto anteriormente, la respuesta de deseabilidad general se calculó a partir de la deseabilidad individual de cada una de las respuestas mediante las ecuaciones (3)-(11). Los resultados de cada una de estas respuestas de deseabilidad general se incluyen en el procedimiento de optimización y la ecuación descubierta fue la siguiente (factores codificados):

$$D = 0{,}609 - 0{,}184A - 0{,}189B - 0{,}110C - 0{,}046A^2 - 0{,}044B^2 - 0{,}016C^2 + 0{,}060AB + 0{,}004AC - 0{,}048BC \quad (r^2_{adj.} = 0{,}8530,\ P < 0{,}0001) \quad (12)$$

Las Figuras 3-5 presentan las representaciones gráficas tridimensionales que describen la influencia de los factores de la deseabilidad general, el porcentaje de captura y el valor T_{50}. El estudio de estas representaciones mostró que podían obtenerse los valores más elevados de deseabilidad utilizando valores bajos en las tres variables del proceso. Sobre todo el análisis de la ecuación (12) resultó en la combinación óptima de las variables independientes donde un producto de las características deseadas y los resultados de este análisis se muestran en la Tabla 4.

combination of the independent variables where a product of desired characteristics may occur and results of this analysis are shown in Table 4.

FIGURA 3. Representaciones gráficas de deseabilidad, porcentaje de captura y T_{50} como función de la concentración de alginato sódico y la concentración de cloruro cálcico, con un tiempo de endurecimiento fijo de 20 min (C = - 1).

FIGURE 3.- Contour plots of desirability, % entrapment and T_{50} as function of sodium alginate concentration and calcium chloride concentration, with fixed hardening time of 20 min (C = - 1).

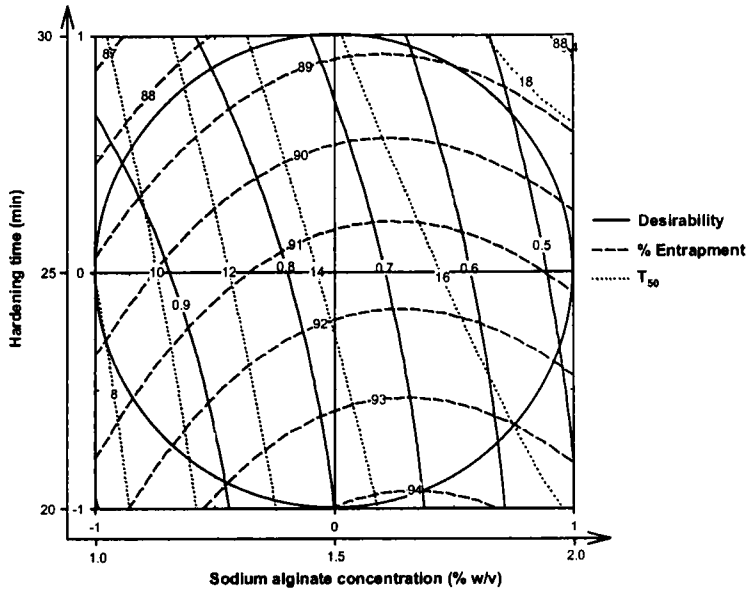

FIGURA 4. Representaciones gráficas de deseabilidad, porcentaje de captura y T_{50} como función de la concentración de alginato sódico y el tiempo de endurecimiento, con una concentración de cloruro cálcico fija de 0,05 M (B = – 1).

FIGURE 4.- Contour plots of desirability, % entrapment and T_{50} as function of sodium alginate concentration and hardening time, with fixed calcium chloride concentration of 0.05 M (B = – 1).

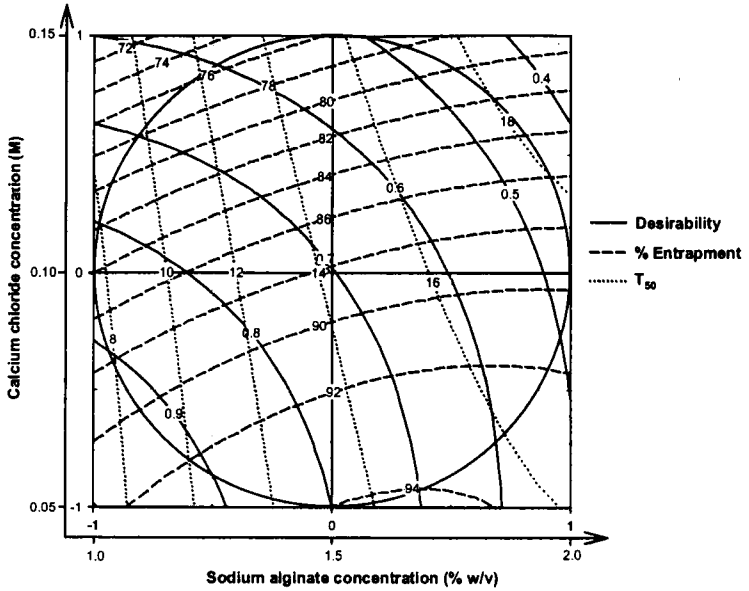

FIGURA 5. Representaciones gráficas de deseabilidad, porcentaje de captura y T_{50} como función de la concentración de cloruro cálcico y el tiempo de endurecimiento, con una concentración de alginato sódico fija de 1,0% p/v (A = – 1).

FIGURE 5.- Contour plots of desirability, % entrapment and T_{50} as function of calcium chloride concentration and hardening time, with fixed sodium alginate concentration of 1.0 % w/v (A = – 1).

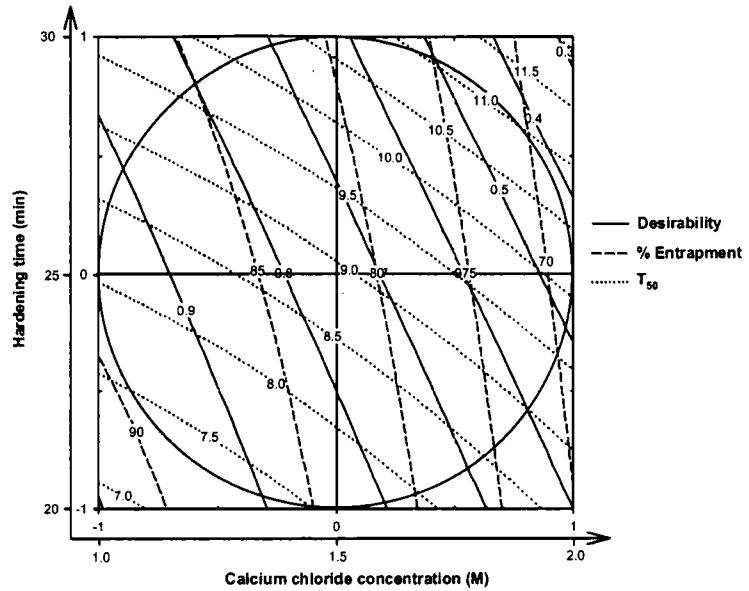

TABLE 4. Niveles óptimos para las variables del proceso independientes.

TABLE 4. Optimum levels for the independent process variables.

Variables independientes Independent variables	Valores óptimos Optimum values
Concentración de alginato sódico Sodium alginate concentration	1% p/v
Concentración de cloruro cálcico Calcium chloride concentration	0,05 M
Tiempo de endurecimiento Hardening time	20 min
Deseabilidad general Overall desirability	0,962

Evaluación de un modelo

Con el fin de evaluar la fiabilidad del modelo, se realizaron cinco experimentos modificando las variables del proceso en valores diferentes a los del modelo. En cada uno de estos experimentos de prueba se estimaron las respuestas mediante las ecuaciones y el procedimiento experimental. En la Tabla 5 se muestra la comparación entre los valores de previstos y experimentales de las respuestas para estos experimentos adicionales. El margen de error se calculó mediante la ecuación siguiente:

$$\text{Margen de error} = \left[\frac{(\text{valor previsto} - \text{valor experimental})}{\text{valor previsto}}\right] \times 100 \quad (13)$$

Se puede apreciar que en todos los casos hubo una correspondencia razonable entre el valor previsto y el experimental dado que se obtuvo un margen de error con un valor bajo. Por esta razón, se puede afirmar que las ecuaciones describen de forma adecuada la influencia de las variables de proceso seleccionadas sobre las respuestas sometidas a estudio.

Evaluation of model

In order to assess the reliability of the model, five experiments were conducted by varying the process variables at values other than that of the model. For each of these test experiments the responses were estimated by using the equations and experimental procedure. In Table 5 the comparison between the experimental and predicted values of the responses for these additional experiments is presented. Bios was calculated by the following equation:

$$\text{Bias} = \left[\frac{(\text{predicted value} - \text{experimental value})}{\text{predicted value}}\right] \times 100 \quad (13)$$

It can be seen that in all cases there was a reasonable agreement between the predicted and the experimental value, since low value of the bias were found. For this reason it can be concluded that the equations describe adequately the influence of the selected process variables on the responses under study.

TABLA 5. Comparación de los valores previstos y experimentales correspondientes a las formulaciones de prueba.

TABLE 5. Comparison between predicted and experimental values for the test formulations.

Respuestas *Responses*	Prueba *Test*	Factores/Niveles *Factors/levels*			Valores previstos *Predicted values*	Valores experimentales *Experimental values*	Margen de error (%) *Bias %*
		A	B	C			
Porcentaje de captura	1	-1	-0,6	-0,6	88,38	90,72	2,6
	2	-0,6	0	0,4	82,92	81,15	2,1
	3	-0,4	0,6	0	77,88	76,01	2,4
	4	0	-0,4	0,6	87,35	84,58	3,2
	5	0,4	0,4	-0,4	83,94	86,06	2,5
T_{50}	1	-1	-0,6	-0,6	7,56	7,41	1,9
	2	-0,6	0	0,4	12,65	12,83	1,5
	3	-0,4	0,6	0	14,16	14,47	2,1
	4	0	-0,4	0,6	15,97	16,23	1,7
	5	0,4	0,4	-0,4	17,31	17,09	1,2
T_{90}	1	-1	-0,6	-0,6	25,01	24,68	1,3
	2	-0,6	0	0,4	59,08	60,33	2,1
	3	-0,4	0,6	0	69,85	72,15	3,3
	4	0	-0,4	0,6	76,90	75,61	1,7
	5	0,4	0,4	-0,4	89,74	88,63	1,2
Tamaño de partículas	1	-1	-0,6	-0,6	196,74	181,71	7,6
	2	-0,6	0	0,4	170,61	180,72	5,9
	3	-0,4	0,6	0	181,17	172,76	4,6
	4	0	-0,4	0,6	267,43	285,91	6,9
	5	0,4	0,4	-0,4	383,66	414,58	8,1
Ángulo de reposo	1	-1	-0,6	-0,6	22,95	22,29	2,9
	2	-0,6	0	0,4	22,74	21,95	3,5
	3	-0,4	0,6	0	22,57	23,56	4,4
	4	0	-0,4	0,6	20,44	19,89	2,7
	5	0,4	0,4	-0,4	19,53	18,90	3,2
Deseabilidad general	1	-1	-0,6	-0,6	0,93	0,94	1,8
	2	-0,6	0	0,4	0,66	0,69	4,9
	3	-0,4	0,6	0	0,53	0,56	5,9
	4	0	-0,4	0,6	0,62	0,60	3,5
	5	0,4	0,4	-0,4	0,50	0,49	2,7

Calorimetría diferencial de barrido (DSC)

Los termogramas DSC a, b, c, d y e que representan el cloruro cálcico dihidratado, la papaína, el alginato sódico, los gránulos de alginato cálcico vacíos y los gránulos cargados de papaína, respectivamente, se realizaron con las mismas condiciones analíticas mostradas en la Figura 6. Los gránulos de alginato cálcico vacíos no mostraban temperatura exotérmica de degradación del alginato sódico a ~ 252°C y, a ~ 221°C, se observó una temperatura endodérmica correspondiente a la interacción del alginato y el calcio. La forma del pico de fusión de los gránulos de alginato cargados de papaína era similar a la de los gránulos vacíos, excepto por el hecho de que contenía un pico adicional de papaína. Esto indicó que la papaína se encontraba en la estructura reticular de los gránulos de alginato.

Differential scanning calorimetry (DSC)

The DSC thermograms a, b, c, d and e which represent calcium chloride dihydrate, papain, sodium alginate, blank calcium alginate beads and papain-loaded beads, respectively, made at the same analytical conditions are shown in Figure 6. The degradation exotherm of sodium alginate at ~ 252°C was absent in blank calcium alginate bead and at ~ 221°C, an endotherm corresponding to alginate-calcium interaction was observed. The melting peak shape of papain-loaded alginate beads was similar to the blank beads except it contained extra peak of papain. This indicated that papain was entrapped in the lattice structure of alginate beads.

FIGURA 6. Los termogramas DSC de (a) cloruro cálcico hexahidratado, (b) papaína, (c) alginato sódico, (d) gránulos de alginato cálcico vacíos y (e) gránulos de alginato cargados de papaína realizados en las mismas condiciones analíticas.

FIGURE 6.- The DSC thermograms of (a) calcium chloride hexahydrate, (b) papain, (c) sodium alginate, (d) blank calcium alginate beads and (e) papain-loaded alginate beads made at the same analytical conditions.

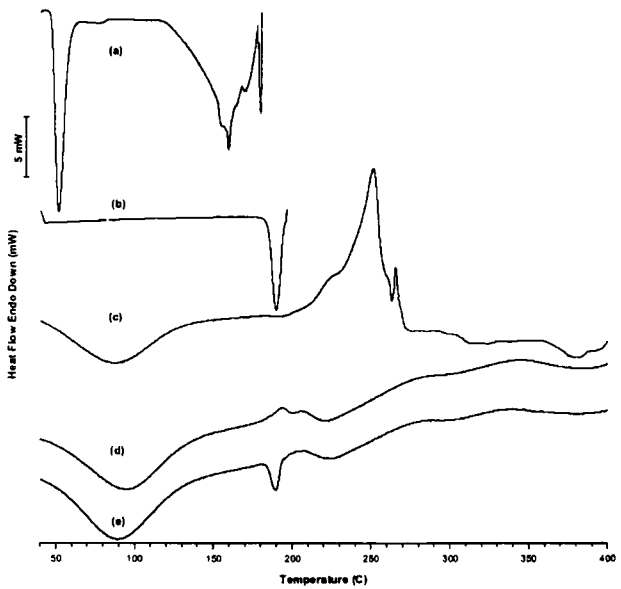

Morfología de los gránulos

La forma esférica de los gránulos cuando están húmedos se pierde normalmente una vez secos, especialmente en el caso de gránulos preparados con una baja concentración de alginato. En alginatos de 1,0% (p/v), los gránulos secos eran muy irregulares y tendían a aglomerarse debido a la baja fuerza mecánica. Con el aumento de la concentración de alginato (2,0% p/v), los gránulos adoptaron la forma de un disco esférico con el centro aplanado. En general, esta forma esférica se conservó cuando la concentración de alginato se elevó hasta el 5,0% (p/v)[41], pero la viscosidad de la solución de 5,0% p/v era demasiado alta para la preparación de los gránulos, así que no fue objeto de estudio. Estos resultados indicaron que la forma de los gránulos de alginato cálcico resultó gravemente afectada en el proceso de secado y que la forma esférica de los gránulos secos mejoró con el incremento de la concentración de alginato. De acuerdo con lo indicado por Skjåk-Bræk et al.[42], los gránulos de alginato cálcico presentaron una estructura heterogénea con una densa capa superficial y un núcleo menos denso debido al mecanismo de gelación heterogéneo, lo que resultó en el aplanamiento de los gránulos durante el proceso de secado[43].

Una característica evidente de la superficie de los gránulos era su alta porosidad al aumentar la concentración de cloruro cálcico (Figura 7; d–f). Este hecho sugirió que se creaban poros en la macromolécula soluble en el agua debido a que la formación de la estructura reticular de alginato cálcico se veía afectada durante la preparación de la unidad y porque se filtró a través de la membrana en el medio[44]. Además, se mejoró la morfología superficial (es decir, se redujo la rugosidad) al aumentar la concentración de alginato sódico (Figura 7; a–c)[41] debido a la alta viscosidad de la solución de alginato sódico.

Morphology of the beads

The spherical shape of beads in wet state was usually lost after drying especially for beads prepared with low alginate concentration. In 1.0% (w/v) alginate, the dried beads were very irregular and tend to agglomerate due to low mechanical strength. With the increasing of alginate concentration (2.0% w/v), the shape of beads changed to a spherical disc with a collapsed center. Normally the spherical shape was retained when the alginate concentration was as high as 5.0% (w/v)[41], but viscosity of 5.0% w/v solution was too high for bead preparation under present experimental conditions so it was not studied. These results indicated that the shape of calcium alginate beads was seriously destroyed in the drying process, and the spherical shape of dried beads improved with the increase of alginate concentration. It was reported by Skjåk-Bræk et al.[42] that calcium alginate beads usually have a heterogeneous structure with dense surface layer and loose core due to the heterogeneous gelation mechanism, which resulted in the collapse of beads during the drying process[43].

One noticeable characteristic of the beads surface was its high porosity when the concentration of calcium chloride increased (Figure 7; d–f). This suggested that the water-soluble macromolecule created pores both because it affected the calcium alginate network formation during the unit preparation and because it was leached from the membrane into the medium[44]. Further, the surface morphology was improved (i.e. decrease in roughness) with increase in sodium alginate concentration (Figure 7; a–c)[41] due to the high viscosity of the sodium alginate solution.

FIGURA 7. Micrografías SEM y morfología superficial de gránulos de alginato cálcico: (a–c) Efecto de la concentración de alginato sódico sobre la morfología superficial (concentración de cloruro cálcico 0,15 M) (a) 1,0% p/v; (b) 1,5% p/v y (c) 2,0% p/v de concentración de alginato sódico. (d–f) Efecto de la concentración de cloruro cálcico sobre la morfología superficial (concentración de alginato sódico 1,5 % p/v) (d) 0,10 M; (e) 0,15 M y (f) 0,20 M de concentración de cloruro cálcico.

FIGURE 7.- SEM micrographs and surface morphology of calcium alginate beads: (a–c) Effect of sodium alginate concentration on surface morphology (calcium chloride concentration 0.15 M) (a) 1.0% w/v; (b) 1.5% w/v and (c) 2.0% w/v sodium alginate concentration. (d–f) Effect of calcium chloride concentration on surface morphology (sodium alginate concentration 1.5 % w/v) (d) 0.10 M; (e) 0.15 M and (f) 0.20 M calcium chloride concentration.

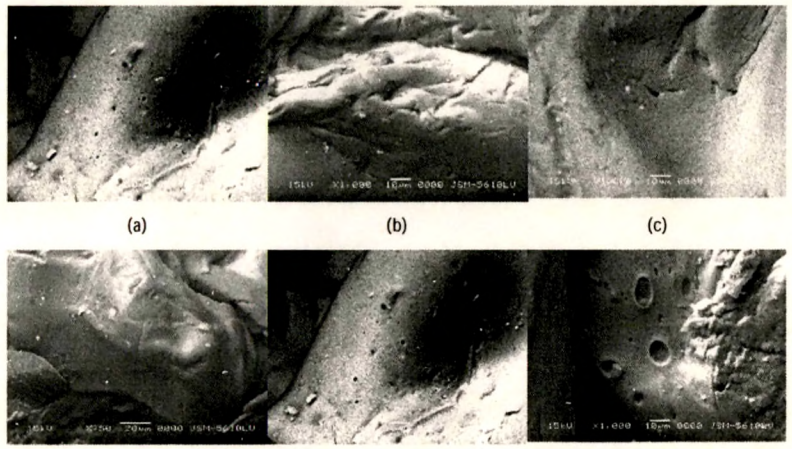

(a) (b) (c)

(d) (e) (f)

CONCLUSIONES

La capacidad de captura farmacológica de la papaína mejoró de forma significativa al reducir la concentración de cloruro cálcico y el tiempo de endurecimiento, así como al incrementar la concentración de alginato sódico. La concentración de alginato sódico, la concentración de cloruro cálcico y el tiempo de endurecimiento afectan al porcentaje de captura, los valores T_{50} y T_{90}, el tamaño de partículas y el ángulo de reposo de los gránulos de forma significativa. También se apreció que las condiciones de interacción eran importantes desde una perspectiva estadística. Además, el análisis de textura de las formulaciones de gránulos mostró que una mayor concentración de alginato sódico y cloruro cálcico afectan a la morfología superficial, así como a la forma de los gránulos. La captura de la enzima se confirmó con ayuda de la calorimetría diferencial de barrido. La optimización del proceso mediante la función de deseabilidad resultó en los valores óptimos de los factores con los que se podía alcanzar el objetivo de la producción de gránulos con características aceptables. Los estudios de disoluciones en un intervalo de pH similares al del tracto gastrointestinal de los seres humanos demostró que la velocidad de liberación del fármaco desde diferentes gránulos en pequeños entornos intestinales simulados depende principalmente de la concentración de alginato sódico y el tamaño de partículas. De acuerdo con las metodologías proporcionadas y según el lugar de aplicación de la papaína en el tracto gastrointestinal, es posible fabricar de forma fácil y sistemática gránulos adecuados a este fin. La aplicación de un solo polímero para la formación de gránulos permite al formulador predecir y producir gránulos sensibles al pH de diferentes geometrías, resistencia y características de liberación. Más concretamente, algunos de los problemas de formulación encontrados en la administración de fármacos o enzimas lábiles a la acción de ácidos o que irritan el aparato digestivo pueden resolverse mediante la aplicación de gránulos entrecruzados de varias unidades que responden ante el pH. Los resultados derivados de este estudio pueden ser de gran valor para aquellos científicos del campo farmacéutico especializados en la administración en lugares específicos, así como a la administración oral de enzimas, péptidos, proteínas y agentes ulcerogénicos.

AGRADECIMIENTOS

Los autores desean expresar su agradecimiento al AICTE (All India Council for Technical Education, Consejo para la educación técnica) de India por la financiación ofrecida al Dr. R. C. Mashru dentro del programa de I+D.

CONCLUSIONS

It was found that the drug entrapment capacity of papain was significantly enhanced by decreasing calcium chloride concentration and hardening time as well as by increasing in sodium alginate concentration. Sodium alginate concentration, calcium chloride concentration and hardening time affect % entrapment, T_{50}, T_{90}, particle size and angle of repose of the beads significantly. Interaction terms were also found to be statistically significant. Furthermore, texture analysis of the beads formulations illustrated that the higher concentration of sodium alginate and calcium chloride affect the surface morphology as well as shape of the beads. Enzyme entrapment was confirmed with the help of differential scanning calorimetry. The optimization of the process using the desirability function resulted to the optimum values of the factors at which the goal of the production of beads with acceptable characteristics could be fulfilled. Dissolution studies over a pH range similar to the human gastrointestinal tract demonstrated that the rate of drug release from the different beads in simulated small intestinal environments depends mainly on sodium alginate concentration and particle size. Based on the provided methodologies and depending on the site of action for papain within the gastrointestinal tract, desirable beads can be easily and reproducibly manufactured. The application of a single polymer for the formation of beads allows the formulator to predict and produce pH-sensitive beads of different geometries, strengths and release characteristics. More specifically, some of the formulation problems encountered for the delivery of gastric-irritating or acid-labile enzyme or drugs can be overcome by the application of multiple unit crosslinked pH-responsive beads. The results of this study may be of value to those pharmaceutical scientists who are engaged in site-specific delivery, as well as the oral delivery of enzymes, peptides, proteins and ulcerogenic agents.

ACKNOWLEDGEMENT

Authors are thankful to the AICTE (India) for funding under R&D scheme to Dr. R. C. Mashru.

BIBLIOGRAFÍA/BIBLIOGRAPHY

1. Perimann GE, Larand L. Proteolytic enzymes. Methods in Enzymology, 1970; pp 226-244.
2. Atkinson B, Mavituna F.Biochemical Engineering and Biotechnology Handbook, The Natural Press, Hong Kong, China, 1985; pp 508-509.
3. Shin CG, Kakusho T, Aral K, Seki M. Bull Chem Soc Jpn 1995; 68: 3549-3555.
4. Ulmann D, Bordusa F, Salchert K, Jakubke HD. Tetrahedron Asymmetry 1996; 7: 2047-2054.
5. Xin GW, Ye YH, Li ZX. Gaodeng Xuexiao Huaxue Xuebao 1998; 19: 1602-1607.

6. Uhlig H.Industrial Enzymes and their Applications, A Wiley-Interscience Publication John Wiley & Sons, Inc., New York, Singapore, Toronto, 1998; pp 147-150.
7. Smith EL, Kimmel JR. Ch. 5 Papain. In: Bayer PD, Lardy H, Myrback L (ed.) The Enzymes, Academic Press, New York & London, 1960; pp 133-312.
8. Singh R, Awasthi S, Vyas SP. New development on hydrogels: potential in drug delivery. Die Pharm 1993; 48: 728-731.
9. Ostberg T, Lund EM, Graffner C. Calcium alginate matrices for oral multiple unit administration. IV Release characteristics in different media. Int J Pharm 1994; 112: 241-248.
10. Monshipouri M, Rudolph AS. Liposome-encapsulated alginate: controlled hydrogel particle formation and release. J Microencapsulation 1995; 12: 117-127.
11. Garcia AM, Ghaly ES. Preliminary spherical agglomerates of water soluble drug using natural polymer and crosslinking technique. J Control Release 1996; 40: 179-186.
12. Kim H, Fassihi R. Application of a binary polymer system in drug release rete modulation. I. Characterization of release mechanism. J Pharm Sci 1997; 86: 316-322.
13. Yang L, Fassihi R. Modulation of Diclofenac release from a totally soluble controlled release drug delivery system. J Control Release 1997; 44: 135-140.
14. Heinamaki J, Marvola M, Happonen I, Westemarck E. The fate of multiple unit entric coated formulations in the stomach of the dog. Int J Pharm 1988; 42: 105-115.
15. Lin S-Y. Release kinetics of drug from different combined retios of micropellets. J Microencapsulation 1993; 10: 319-327.
16. Ritschel WA. Targeting in the gastrointestinal tract: new approaches. Methods Find Exp Clin Pharmacol 1991; 13: 313-336.
17. Chen H, Langer R. Magnetically-responsive polymerized liposomes as potential oral delivery vehicles. Pharm Res 1997; 14: 537-540.
18. Desai MP, Labhasetwar V, Walter E, Levy RJ, Amidon GL. The mechanism of uptake of biodegradable microparticles in Caco-2 cells is size dependent. Pharm Res 1997; 14: 1568-1573.
19. Technical information - alginates, Pronove Biopolymer, 1994; pp 3-14.
20. Alginate as immobilization material for cells, Pronove Biopolymer, 1994; pp 1-4.
21. Park PG, Shalaby WSW, Park H. Ch. 5. Biodegradable Hydrogels for Drug Delivery, Technomic, Lancaster, 1993; pp 99-140.
22. Kibat PG, Igari Y, Wheatley MA, Eisen HN, Langer R. Enzymatically activated microencapsulated liposomes can provide pulsative drug release. FASEB J 1990; 4: 2533-2539.
23. Yotsuyanagi T, Ohkubo T, Ohhashi T, Ikeda K. Calcium-induced gelation of alginic acid and pH-sensitive reswelling of dried gels. Chem Pharm Bull 1987; 35: 1555-1563.
24. Perka C, Spitzer R-S, Lendenhayn K, Sittinger M, Schultz O. Matrix-mixed culture: new methodology for chondrocyte culture and preparation of cartilage transplants. J Biomed Mater Res 2000; 49: 305-311.
25. Lanza RP, Ecker D, Huntreiber WM, Staruk JE, Marsh J, Chick WL. A simple method for transplanting discordant islets into rats using alginate gel spheres. Transplantation 1995; 59: 1485-1487.
26. Zimmerberg J, Cohen FS, Finkelstein A. Micromolar Ca^{2+} stimulates fusion of lipid vesicles with planar bilayers containing a calcium-binding protein. Science 1980; 210: 906-908.
27. Chowdary KPR, Babu KVVS. A comparative evaluation of ethyl cellulose, gelatin and calcium alginate microcapsules prepared by complex emulsion methods. Ind J Pharm Sci 1988; 50: 173-175.
28. Bodmeier R, Chen H, Paeratakul O. A novel approach to the oral delivery of mocro- or napartilces. Pharm Res 1989; 3: 413-417.
29. Rajaonarivony M, Vauthier C, Couarraze G, Puisieux F, Couvreur P. Development of a new drug carrier made from alginate. J Pharm Sci 1993; 82: 912-917.
30. Pillay V, Dangor CM, Govender T, Moopanar KR, Hurbans N. Ionotropic gelation: encapsulation of indomethacin in calcium alginate gel discs. J Microencapsulation 1998; 15: 215-226.
31. Pillay V, Dangor CM, Govender T, Moopanar KR, Hurbans N. Drug release modulation from crosslinked calcium alginate microdiscs. 1. Evaluation of the concentration dependency of sodium alginate on drug entrapment capacity, morphology and dissolution rate. Drug Deliv 1998; 5: 25-34.
32. Pillay V, Dangor CM, Govender T, Moopanar KR, Hurbans N. Drug release moldulation from crosslinked calcium alginate microdiscs. 2. Swelling, compression and stability of the hydronamically-sensitive calcium alginate matrix and the associated drug release mechanisms. Drug Deliv 1998; 5: 35-46.
33. Lewis G, Mathieu D, Phan-Tan-Luu R.Pharmaceutical Experimental Design, Marcel Dekker, New York, 1999; pp 265-276.
34. Kim C-K, Lee E-J. The controlled release of blum dextran from alginate beads. Int J Pharm 1992; 79: 11-19.
35. Lee B-J, Min G-H. Preparation and release characteristics of polymer-reinforced and coated alginate beads. Arch Pharm Res 1995; 18: 183-188.
36. Ostberg T, Vesterhus L, Graffner C. Calcium alginate matrices for oral multiple unit administration: II. Effect of process and formulation factors on matrix properties. Int J Pharm 1993; 97: 183-193.
37. Lee B-J, Min G-H. Oral controlled release of melatonin using polymer-reinforced and coated alginate beads. Int J Pharm 1996; 144: 37-46.

38. Wang K, He Z. Alginate-konjac glucomannan-chitosan beads as controlled release matrix. Int J Pharm 2002; 244: 117-126.
39. Carter SJ (eds.).Tutorial Pharmacy, CBS Publishers & Distributors, New Delhi, India, 1986; pp 225-226.
40. Montgomery DC. Ch 1. Introduction. Design and Analysis of Experiments, John Wiley & Sons, Inc., New York, 2001; pp 1-20.
41. Shu XZ, Zhu KJ. The release behavior of brilliant blue from calcium-alginate gel beads coated by chitosan: the preparation method effect. Eur J Pharm Biopharm 2002; 53: 193-201.
42. Skjak-Brae G, Grasdalen KH, Draget KI, Smidsrod O. Inhomogeneous poysaccharide ionic gels. Carbohydr Polym 1989; 10: 31-54.
43. Polk A, Amsden B, Yao KD, Peng T, Goosen MFA. Controlled release of albumin from chitosan-alginate microcapsules. J Pharm Sci 1994; 83: 178-185.
44. Iannuccelli V, Coppi G, Bernabei MT, Cameroni R. Air compartment multiple-unit system for prolonged gastric residence. Part I. Formulation study. Int J Pharm 1998; 174: 47-54.

Papain Entrapment in Alginate Beads for Stability Improvement and Site-Specific Delivery: Physicochemical Characterization and Factorial Optimization Using Neural Network Modeling

Submitted: September 22, 2004; Accepted: March 10, 2005; Published: September 30, 2005

Mayur G. Sankalia,[1] Rajshree C. Mashru,[1] Jolly M. Sankalia,[1] and Vijay B. Sutariya[1]

[1]Center of Relevance and Excellence in NDDS, Pharmacy Department, The M.S. University of Baroda, Vadodara, Gujarat, India 390 002

ABSTRACT

This work examines the influence of various process parameters (like sodium alginate concentration, calcium chloride concentration, and hardening time) on papain entrapped in ionotropically cross-linked alginate beads for stability improvement and site-specific delivery to the small intestine using neural network modeling. A 3^3 full-factorial design and feed-forward neural network with multilayer perceptron was used to investigate the effect of process variables on percentage of entrapment, time required for 50% and 90% of the enzyme release, particle size, and angle of repose. Topographical characterization was conducted by scanning electron microscopy, and entrapment was confirmed by Fourier transform infrared spectroscopy and differential scanning calorimetry. Times required for 50% (T_{50}) and 90% (T_{90}) of enzyme release were increased in all 3 of the process variables. Percentage entrapment and particle size were found to be directly proportional to sodium alginate concentration and inversely proportional to calcium chloride concentration and hardening time, whereas angle of repose and degree of cross-linking showed exactly opposite proportionality. Beads with ~90% entrapment and T_{50} of ~10 minutes could be obtained at the low levels of all 3 of the process variables. The inability of beads to dissolve in acidic environment, with complete dissolution in buffer of pH ≥6.8, showed the suitability of beads to release papain into the small intestine. The shelf-life of the capsules prepared using the papain-loaded alginate beads was found to be 3.60 years compared with 1.01 years of the marketed formulation. It can be inferred from the above results that the proposed methodology can be used to prepare papain-loaded alginate beads for stability improvement and site-specific delivery.

KEYWORDS: alginate beads, neural network, multilayer perceptron, optimization, papain

Corresponding Author: Rajshree C. Mashru, Pharmacy Department, G.H. Patel Building, Donor's Plaza, The Maharaja Sayajirao University of Baroda, Fatehgunj, Vadodara, Gujarat, India 390 002. Tel: +91-265-2434187/2794051; Fax: +91-265-2418927; E-mail: sankalia_mayur@hotmail.com

INTRODUCTION

Papain (EC 3.4.22.2) is one of the thiol proteases, and its active site consists of Cys-25, His-159, and Asp-158. Papain shows extensive proteolytic activity toward proteins, short-chain peptides, amino acid esters, and amide links and is applied extensively in the fields of food and medicine. The reverse reaction of "papain hydrolysis," can be used in the synthesis of peptides and oligomers. Most marketed formulations containing papain and other digestive enzymes need to be stored at cold (2 to 8°C) or cool (8 to 25°C) temperatures conditions and still have the shelf-life of < 1 year. Entrapment of the papain in ionotropically cross-linked biodegradable hydrogels may improve the stability of the parent enzymes and make it less prone to interference of various formulation excipients. Immobilized enzymes are stable at higher temperatures and might be stored at room temperature with extended shelf-life.[1] The optimum pH for activity of papain is in the range of 3 to 9, which varies with different substrates.[2] However, papain is almost inactive at a gastric pH of 1.2, so the ideal place for papain delivery is the small intestine. Multiple-unit dosage forms are particularly useful for the following purposes: (1) for delivering highly irritant drugs, such as nonsteroidal antiinflammatory drugs;[3] (2) for site-specific targeting of acid-labile drugs within the gastrointestinal tract;[4] and (3) for the delivery of enzymes, peptides/proteins, and vaccines.[5] The above advantages are of great commercial interest for the pharmaceutical industries; hence, it was the objective of the research to develop an extended shelf-life formulation for site-specific delivery of papain by immobilization in ionotropically cross-linked biodegradable alginate beads, which results in better and efficient utilization of enzymes. This article also deals with "in vitro" dissolution studies of beads, physicochemical characterization for evaluating the bead formation, and its release behavior.

Alginate, a high-molecular-mass polysaccharide, is a naturally occurring biodegradable copolymer of 1,4-linked β-D-mannuronic acid (M) and α-L-guluronic acid (G) that is extracted from brown seaweeds (*Phacophyceae*, mainly *Laminaria*). It has been shown that the G and M units are joined together in blocks, and, as such, the following 3 types of blocks may be found: homo-polymeric G blocks

(GG), homopolymeric M blocks (MM), and heteropolymeric sequentially alternating blocks (MG). The reactivity with calcium and the subsequent gel formation capacity is a direct function of the average chain length of the G blocks. Hence, alginates containing the highest GG fractions possess the strongest ability to form gels. This initially arises from the ability of the divalent calcium cation to fit into the guluronate structures like eggs in an "egg box junction." Consequently, this binds the alginate chains together by forming junction zones, sequentially leading to gelling of the solution mixture and bead formation. When an aqueous solution of sodium alginate is added dropwise to an aqueous solution of calcium chloride, it forms a spherical gel with regular shape and size, also known as an "alginate bead." Alginate beads have the advantages of being nontoxic orally and having high biocompatibility.[6] Another advantageous property is their inability to reswell in acidic environment, whereas they easily reswell in an alkaline environment, so acid-sensitive drugs incorporated into the beads would be protected from gastric juice.[7] Therefore, alginate is used as an entrapment matrix for cells and enzymes, as well as for pharmaceutical and food adjuvants. In the past, conventional cross-linked calcium-alginate beads have been investigated for the development of a multiple-unit drug-delivery system.[8-11] However, not even a single reference could be cited in the literature to date for entrapment of papain in alginate beads for improvisation of shelf-life.

Neural network (NN) models might generalize better than regression models, because regression analyses are dependent on predetermined statistical significance levels (ie, less significant terms are not included in the model).[12,13] With the NN method, all of the data are used, potentially making the models more accurate. Hence, NN was selected as a modeling and evaluating tool in this article. The use of at least 1 hidden layer enables the NNs to describe nonlinear systems.[12] One layer is usually sufficient to provide an adequate prediction, even if continuous variables are adopted as the units in the output layer. Additionally, there is a little evidence to suggest that a larger number of hidden layers improves performance.[14]

The multilayer perceptron (MLP) with back propagation algorithm is one of the most widely implemented NN topologies and is important in the study of nonlinear dynamics. Two important characteristics of the MLP are its smooth nonlinear neurons (sigmoidal function) and its massive interconnectivity.

NN has been successfully applied to many pharmaceutical areas in recent years,[15] such as quantitative structure activity relationship analysis and drug modeling,[16] pharmacokinetic[17]-pharmacodynamic studies,[18] optimization and pharmaceutical formulation development,[14] powder flow,[19] compound determination using high-performance liquid chromatography,[20] analysis of nuclear magnetic resonance spectra,[21] prediction of drug release profile,[22] prediction of physicochemical properties,[23] prediction of octanol-water partition coefficient,[24] prediction of solubility,[25] and so forth.

MATERIALS AND METHODS

Materials

Hammersten-type casein US Pharmacopeia ([USP] Himedia Laboratories Pvt Ltd, Mumbai, India) and trichloroacetic acid (98.0%, Qualigens Fine Chemicals, Mumbai, India) were used as received. Purified papain Indian Pharmacopeia (IP), sodium alginate IP, calcium chloride dihydrate (98.0%), dibasic sodium phosphate (99.5%), disodium ethylenediaminetetraacetate (99.5%), cystein hydrochloride (99.0%), and citric acid (98.0%) were purchased from S. D. Fine-Chem Ltd (Mumbai, India). All of the other chemicals and solvents were of analytical grade and were used without additional purification. Deionized double-distilled water was used throughout the study.

Preparation of Beads

Concentrated sodium alginate solution in distilled water was prepared well before required. The required quantity of the enzyme (200 mg of papain in 50 mL of final sodium alginate solution) was dissolved in a small quantity of water and mixed with concentrated sodium alginate solution. The final concentration of sodium alginate was adjusted in the range of 1% to 2% w/v and was used after being degassed under a vacuum. The beads were prepared by dropping the sodium alginate solution (10 mL) containing papain from the dropping device, such as a syringe with a 26-gauge × 0.5-in flat-tip hypodermic needle, to a magnetically stirred calcium chloride solution (40 mL) at a rate of 5 mL/min and were allowed to harden for specific time. Different levels (Table 1) of sodium alginate, calcium chloride, and hardening time were selected. The beads were collected by decanting the calcium chloride solution, washed with deionized water, and dried to a constant weight in vacuum desiccator (Tarsons Products Pvt Ltd, Kolkata, India) at room temperature for 36 hours.

Factorial Design

In this study, a 3^3 full-factorial design was used to determine the effect of the sodium alginate concentration, the calcium chloride concentration, and the hardening time. Before the application of the design, a number of preliminary trials were conducted to determine the conditions at which the process resulted to beads. The matrix of the experiments and the results of the responses are listed in

Table 1. Process Variables and Their Levels for 3^3 Full-Factorial Design

Factors	Low Level	Middle Level	High Level
Sodium alginate (% w/v)	1.0	1.5	2.0
Calcium chloride (M)	0.05	0.10	0.15
Hardening time (min)	20	25	30

Table 2. To determine the experimental error, the experiment at the center point was repeated 5 times at different days. The mean (±SD) percentage of entrapment, time required for 50 (T_{50}) and 90 (T_{90}) percent of enzyme release, particle size, and angle of repose of these experiments were 85.88 ± 1.02%, 15.57 ± 0.28 min, 82.43 ± 0.33 min, 261.1 ± 0.9 μm, and 20.61 ± 0.29°, respectively. The above-mentioned values showed good reproducibility of the process.

NN Software and Network Topology

The Microsoft Windows-based NN software NeuroSolutions Version 4.24 (NeuroDimension, Inc) was used. The MLP with single hidden-layer architecture was chosen. The experimental matrix of 32 input-to-desired output data sets (Table 2) was introduced in to the model, with 3 input neurons (process variables), 1 hidden layer, and 5 output neurons (response variables). Various adjustable parame-

Table 2. Matrix of the Experiments and Results for the Measured Responses

	Factors/ Levels			Responses				
ES*	Na Alginate (% w/v)	Calcium chloride (M)	Hardening Time (min)	% Entrapment	T_{50}	T_{90}	Size (μm)	Angle of Repose
1	1.0	0.05	20	91.80	6.50	23.80	211.1	22.62
10	1.0	0.05	25	89.00	8.30	25.70	207.3	22.88
19	1.0	0.05	30	86.20	9.35	28.40	202.6	23.27
4	1.0	0.10	20	85.00	7.80	27.50	184.3	23.39
13	1.0	0.10	25	82.60	9.10	30.55	181.1	23.75
22	1.0	0.10	30	80.71	10.70	34.00	178.3	24.15
7	1.0	0.15	20	68.80	8.60	34.60	176.0	24.07
16	1.0	0.15	25	67.79	10.30	39.00	171.4	24.94
25	1.0	0.15	30	65.28	12.05	59.25	169.7	26.33
2	1.5	0.05	20	93.40	13.35	48.00	297.0	19.50
11	1.5	0.05	25	90.80	14.45	57.40	291.6	19.76
20	1.5	0.05	30	88.00	16.30	57.40	285.5	20.02
5	1.5	0.10	20	87.70	14.35	75.00	266.9	20.27
29	1.5	0.10	25	87.01	15.30	82.50	261.5	20.56
32	1.5	0.10	25	86.29	15.90	82.90	259.8	20.20
31	1.5	0.10	25	85.06	15.20	82.40	260.3	20.98
28	1.5	0.10	25	84.35	15.80	81.90	261.9	20.44
14	1.5	0.10	25	86.78	15.70	82.30	262.0	20.89
30	1.5	0.10	25	85.80	15.50	82.60	261.3	20.58
23	1.5	0.10	30	83.50	16.80	87.65	255.4	20.97
8	1.5	0.15	20	77.30	15.55	80.55	258.2	21.20
17	1.5	0.15	25	75.30	16.90	83.50	252.7	21.84
26	1.5	0.15	30	72.00	19.30	86.50	246.0	22.20
3	2.0	0.05	20	94.40	15.90	83.80	715.3	16.14
12	2.0	0.05	25	91.39	17.05	91.50	708.0	16.49
21	2.0	0.05	30	88.50	18.60	95.60	701.3	16.87
6	2.0	0.10	20	88.40	17.70	90.80	682.7	17.00
15	2.0	0.10	25	86.00	18.60	94.20	677.1	17.26
24	2.0	0.10	30	84.00	20.20	96.15	671.9	17.77
9	2.0	0.15	20	79.50	19.40	95.60	673.5	18.03
18	2.0	0.15	25	76.60	20.40	96.30	668.2	18.56
27	2.0	0.15	30	73.70	22.80	97.20	662.7	18.89

*ES indicates experimental sequence.

ters, like the number of neurons in the hidden layer, the step size, the momentum of the hidden layer and the output layer, and so forth, were optimized. Training was repeated 3 times for optimization of all of the parameters. At the start of the training run, weights were initialized with random values. During training, 5 additional data sets of input-to-desired output ratio were used for the cross-validation and were back-propagated through the network to evaluate the trained network. The training termination criterion was the rise in minimum standard error of the cross-calibration set compared with that of the training set for 100 continuous epochs. The network trained under optimum conditions was used to predict the responses at different factor values and response surfaces were generated for interpretation.

Characterization of Beads

Estimation of Papain

Papain was estimated by modified casein digestion method of USP XXVI in the presence of cysteine hydrochloride. Different aliquots of standard papain solution in phosphate-cysteine disodium ethylenediaminetetraacetate buffer were added to 5 mL of buffered substrate (hammersten-type casein 10 mg/mL, pH 6.0 ± 0.1) and incubated for 60 minutes at 40°C. The digestion process of casein was stopped by adding 3 mL of 30% w/v trichloroacetic acid solution and was allowed to stand for 30 to 40 minutes at 40°C. Digested amino acids were filtered through Whatman filter paper no. 42 by discarding first 3 mL of filtrate, and absorbance was measured at 280 nm against their respective blanks. The method was found to be linear over an analytical range of 3 to 100 μg/mL with a correlation coefficient (r) of 0.9996. Limit of detection, limit of quantitation, and regression equation were found to be 0.77 μg/mL, 2.57 μg/mL, and $y = 0.0042x - 0.0033$, respectively.

Determination of Entrapment Efficiency

Entrapment efficiency was determined by dissolving the enzyme-loaded beads in a magnetically stirred simulated intestinal fluid without enzyme (USP XXVI) for about 45 minutes. The resulting solution was centrifuged at 2,500 rpm for 10 minutes (Remi Instruments Ltd, Mumbai, India), and the supernatant was assayed (n = 3) for enzyme content by the modified casein digestion method of USP XXVI. Entrapment efficiency was calculated as:

$$\text{Entrapment efficiency} = \frac{\text{Enzyme loaded}}{\text{Theoratical enzyme loading}} \times 100 \quad (1)$$

Effect of pH on Release Profile

To study the effect of pH on the papain release profile, an in vitro dissolution study was conducted using the USP XXVI dissolution apparatus 2 (TDT-60T, Electrolab, Mumbai, India) in 500 mL of different pH media (simulated gastric juice pH 1.2 [USP], phosphate buffer pH 4.0 [IP], neutralized phthalate buffer pH 5.4 [IP], simulated intestinal fluid without enzyme pH 6.8 [USP], phosphate buffer pH 7.4 [IP], and phosphate buffer pH 8.0 [IP]) on the optimized batch at 37 ± 0.5°C with a paddle speed of 75 rpm. Accurately weighed samples (n = 3) equivalent to about 40 mg of papain were introduced to dissolution media, and samples of 2 mL were collected at 0, 0.25, 0.50, 0.75, 1.0, 1.5, 2.0, 2.5, 3.0, 3.5, 4.0, 4.5, 5.0, 5.5, and 6.0 hours. Samples were filtered through a 0.4-μm Whatman membrane filter and assayed for enzyme content as before.

Determination of T_{50} and T_{90}

T_{50} and T_{90} are important parameters for the enzyme release study and were used to evaluate the onset of action and duration of action, respectively. For optimization purposes, a dissolution study of all of the batches was conducted in 500 mL of simulated intestinal fluid without enzyme as before. Accurately weighed samples (n = 3) equivalent to about 40 mg of papain were subjected to dissolution, and aliquots of 2 mL were assayed at 0, 5, 10, 15, 20, 30, 45, 60, 90, and 120 minutes. T_{50} and T_{90} were found by extrapolating the percentage of enzyme released versus time plot.

Particle Size Measurements

Particle size is an important parameter for the formulation development. An optimized batch of the beads was filled in the capsules during which the particle size was the evolutionary parameter. Larger particles show higher weight variation during capsule filling; hence, the experimental conditions resulting in smaller particles are preferable. Particle size was determined with the laser diffraction particle size analyzer (MAN 0244/HYDRO 2000 SM, Malvern Instruments Ltd, Malvern, United Kingdom) using isopropyl alcohol as a vehicle.

Angle of Repose Measurements

Angle of repose was measured for estimating flowability of the beads. If the angle exceeds 50°, the material will not flow satisfactorily, whereas materials having values near the minimum flow easily and well. The rougher and more irregular the surface of the particles, the higher the angle of repose. The angle also increases with decrease in particle size. The angle of repose was measured by passing beads through a funnel on the horizontal surface. The height (h) of the heap formed was measured with a cathetometer, and the radius (r) of the cone base was also determined. The angle of repose (Φ) was calculated from:

$$\tan \Phi = \frac{h}{r} \quad (2)$$

Fourier Transform Infrared Spectroscopy

Infrared transmission spectra were obtained using a Fourier transform infrared spectroscopy (FTIR) spectrophotometer (FTIR-8300, Shimadzu, Japan). A total of 5% (w/w) of sample, with respect to the potassium bromide (KBr) disk, was mixed with dry KBr (S. D. Fine Chem Ltd, Mumbai, India). The mixture was ground into a fine powder using an agate mortar before compressing into the KBr disk under a hydraulic press at 10,000 psi. Each KBr disk was scanned at 4 mm/s at a resolution of 2 cm over a wave number region of 400 to 4,500 cm^{-1}. The characteristic peaks were recorded.

Differential Scanning Calorimetry

Differential scanning calorimetric analysis was used to characterize the thermal behavior of the isolated substances, their physical mixture, and empty and loaded beads. Differential scanning calorimetry (DSC) thermograms were obtained using an automatic thermal analyzer system (DSC-60, Shimadzu, Japan). Temperature calibration was performed using indium as a standard. Samples were crimped in a standard aluminum pan and heated from 40 to 400°C at a heating rate of 10°C/min under constant purging of dry nitrogen at 30 mL/min. An empty pan, sealed in the same way as the sample, was used as a reference. The characteristic endothermic peaks and specific heat of the melting endotherm were recorded.

Scanning Electron Microscopy

The purpose of the scanning electron microscopy study was to obtain a topographical characterization of beads. The beads were mounted on brass stubs using double-sided adhesive tape. Scanning electron microscopy photographs were taken with a scanning electron microscope (JSM-5610LV, Jeol Ltd, Tokyo, Japan) at the required magnification at room temperature. The working distance of 39 mm was maintained, and the acceleration voltage used was 15 kV, with the secondary electron image as a detector.

Preparation of Capsule Formulation, Packaging, and Stability Study

Accurately weighed alginate beads equivalent to 40 mg of papain were filled into a hard gelatin capsule manually. The joint of the capsule body and cap was carefully sealed by pressing them to fit in the lock mechanism. The capsules were packaged in high-density polyethylene bottles with polypropylene caps (foamed polyethylene and pressure sensitive liner). The capsules were subjected to stability testing according to the International Conference on Harmonization guidelines for zone III and IV. The packed containers of prepared capsules along with marketed formulation and bulk papain were kept for accelerated (40 ± 2°C/75 ± 5% relative humidity) and long-term (30 ± 2°C/65 ± 5% relative humidity) stability in desiccators with saturated salt solution for up to 12 months. A visual inspection (for discoloration of capsule content), dissolution testing, and papain content estimation was conducted every 15 days for the entire period of stability study.

Results and Discussion

Optimization of NN

For the optimum number of neurons in the hidden layer, the NN was trained with 1 to 35 hidden neurons with 2,000 training epochs, and performance was tested after the addition of each neuron and was found to be 17. Step size, momentum of hidden, and output layer were optimized by varying the parameters from 0.1 to 1 at the increment of 0.1. The optimum step size for hidden layer and output layer was found to be 0.9 and 1, respectively, whereas the optimum momentum for hidden layer and output layer was found to be 0.9. The NN was constructed using the optimum conditions and was used to predict the experimental matrix (Table 3) and to generate the response surfaces for interpreting the effect of various process variables.

Effect of the Factors on Responses

Percentage of Entrapment

Contour plots of response surface for percentage of entrapment are shown in Figure 1A, C, and E, from which it can be concluded that the ~90% of the entrapment value was obtained at the high level (2% w/v) of the sodium alginate concentration, especially when the high level of the sodium alginate concentration was followed by the low levels of the other 2 factors (94.4% entrapment, experiment 3; Table 2). Whereas the calcium chloride concentration and hardening time were affecting negatively (ie, response decreases with an increase in factor level) in a significant amount, their interaction was synergistic at higher levels (experiment 25, 26, and 27; Table 2).

On the addition of sodium alginate solution to a calcium chloride solution, instantaneous interfacial cross-linking takes place with precipitation of calcium alginate followed by a more gradual gelation of the interior, which causes loss of enzyme from the surface of the beads. This can be

Table 3. Matrix of the Experiments and NN-Predicted Responses

Sr. No.	Factors/ Levels: Na Alginate (% w/v)	Calcium Chloride (M)	Hardening Time (min)	Responses: % Entrapment	T_{50}	T_{90}	Size (μm)	Angle of Repose
1	1.0	0.05	20	91.81	7.45	22.09	151.0	22.45
2	1.0	0.05	25	89.93	8.31	23.26	150.3	22.92
3	1.0	0.05	30	87.28	9.44	24.94	149.4	23.43
4	1.0	0.10	20	84.23	8.00	26.94	151.0	23.37
5	1.0	0.10	25	81.61	9.28	31.09	150.0	23.89
6	1.0	0.10	30	78.63	10.87	36.27	148.8	24.43
7	1.0	0.15	20	69.87	8.46	34.30	150.5	24.31
8	1.0	0.15	25	68.70	10.14	43.54	149.2	24.84
9	1.0	0.15	30	67.78	12.21	54.11	147.7	25.33
10	1.5	0.05	20	93.04	12.29	51.25	300.2	19.10
11	1.5	0.05	25	91.31	13.77	57.76	292.1	19.50
12	1.5	0.05	30	88.69	15.11	62.82	283.9	19.94
13	1.5	0.10	20	88.81	13.96	72.34	275.5	20.18
14	1.5	0.10	25	86.17	15.89	80.51	269.5	20.65
15	1.5	0.10	30	82.90	17.49	85.84	262.6	21.17
16	1.5	0.15	20	76.07	14.94	81.70	257.0	21.32
17	1.5	0.15	25	74.14	17.20	89.34	250.9	21.86
18	1.5	0.15	30	72.35	18.94	93.72	242.5	22.48
19	2.0	0.05	20	92.80	16.31	84.32	699.8	16.67
20	2.0	0.05	25	91.04	17.59	88.50	698.5	16.82
21	2.0	0.05	30	88.54	18.64	91.26	696.6	16.99
22	2.0	0.10	20	89.04	17.89	92.74	684.8	17.18
23	2.0	0.10	25	86.16	19.16	95.39	682.1	17.40
24	2.0	0.10	30	82.77	20.13	97.03	678.6	17.67
25	2.0	0.15	20	79.81	19.23	96.34	661.9	17.93
26	2.0	0.15	25	76.91	20.38	98.09	657.4	18.25
27	2.0	0.15	30	74.28	21.20	99.10	651.5	18.63

noticed from the pores on the bead surface (Figure 2) created by the water-soluble macromolecules both because it affected the calcium alginate network formation during the unit preparation and because it was leached from the membrane into the medium.[26] Loss of surface enzyme was found to be proportional to the degree of cross-linking. Increase in viscosity with an increase in sodium alginate concentration retarded penetration of calcium to the interior of the bead, resulted in decreased cross-linking (also decreased surface roughness and porosity; Figure 2A–C), and increased entrapment efficiency. Degree of cross-linking increases with an increase in calcium concentration and contact time;[27] hence, entrapment efficiency decreased.

T_{50}

As shown in Figure 1A, C, and E, all 3 of the factors had significant positive (ie, response increases with increase in factor level) effects on the response value. However, immediate release of enzyme for quicker onset of action and, hence, shorter T_{50} was the desirable criteria for the optimum formulation; hence, low value of all 3 of the variables resulted in the beads with T_{50} as low as 6.5 minutes (experiment 1, Table 2). T_{50} was found to be proportional to the particle size and degree of cross-linking. As the concentration and, hence, the viscosity of alginate solutions increases, larger beads (discussed under "Particle Size," below) with less surface porosity (Figure 2A–C) were obtained, which took a long time for complete dissolution and resulted in higher T_{50} (16 to 23 minutes; Table 2). Higher calcium concentration and hardening time caused penetration of calcium to the interior of the bead, resulted in increased cross-linking[27] (also increased surface roughness and porosity; Figure 2D–F), and delayed dissolution (hence, higher T_{50}).

T_{90}

As with T_{50}, all 3 of the factors had positive effects on this response, which can be observed in Figure 1B, D, and F.

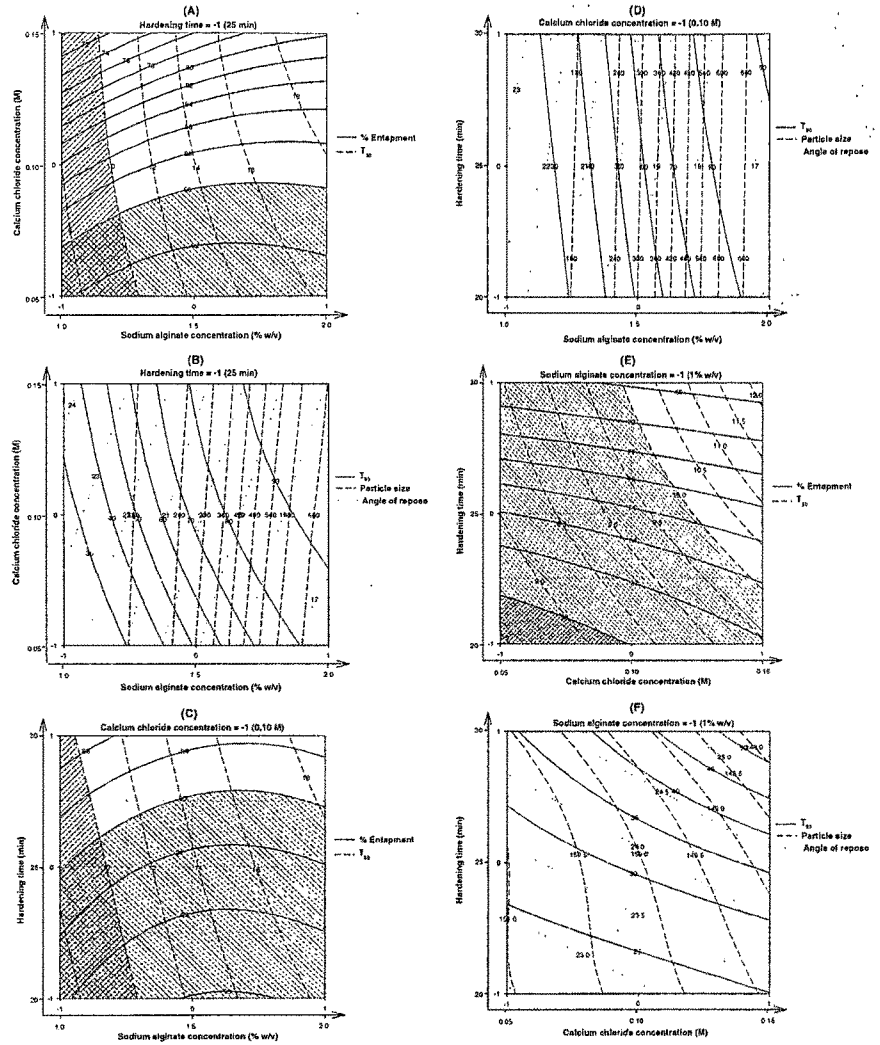

Figure 1. Contour plots of percentage of entrapment, T_{50}, T_{90}, particle size, and angle of repose as a function of sodium alginate concentration, calcium chloride concentration, and hardening time.

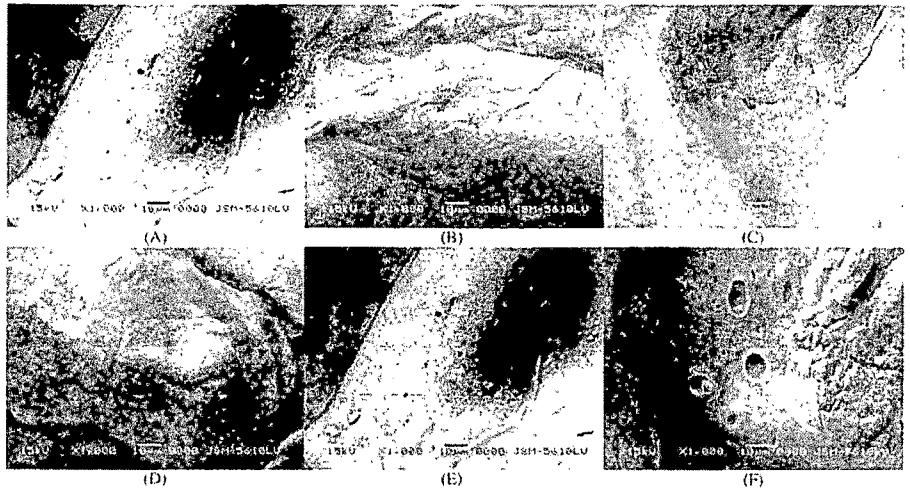

Figure 2. Scanning electron microscopy micrographs and surface morphology of calcium alginate beads. (A–C) Effect of sodium alginate concentration on surface morphology (calcium chloride concentration 0.15 mol/L): (A) 1.0% w/v, (B) 1.5% w/v, and (C) 2.0% w/v sodium alginate concentration. (D–F) Effect of calcium chloride concentration on surface morphology (sodium alginate concentration 1.5% w/v): (D) 0.10 mol/L, (E) 0.15 mol/L, and (F) 0.20 mol/L calcium chloride concentration.

The sodium alginate concentration was the most positively influencing factor among all 3 (higher T_{90} of the magnitude of 83 to 98 minutes; Table 2). None of the remaining 2 factors was affecting T_{90} significantly. However, both calcium chloride concentration and hardening time at higher levels had a synergistic positive action (experiment 25, 26, and 27; Table 2). T_{90} was also found to be proportional to the particle size and degree of cross-linking. For additional explanation, see "T_{50}" section, above.

Particle Size

As shown in Figure 1B, D, and F, the sodium alginate concentration was the most affecting factor. The bead size is influenced by the opening through which the alginate solution is allowed to pass (which was kept constant) and the viscosity of the alginate solution. Increased viscosity at a higher concentration of sodium alginate resulted in larger particles (660 to 715 μm; Table 2). Calcium chloride concentration and hardening time had a negative effect on the particle size. High calcium chloride concentration and hardening time caused shrinkage of beads and resulted in smaller particle size (experiment 25, 26, and 27; Table 2) because of a high degree of cross-linking.[27] Although the negative effect of calcium chloride concentration and hardening time was of less magnitude, they contribute to the morphology of the beads, and the surface became rougher and porous (Figure 2D–F).

Angle of Repose

Here, too, the sodium alginate concentration had a significant positive effect on the angle of repose. However, calcium chloride concentration and hardening time had a synergistic positive effect at higher levels (experiment 25, 26, and 27; Table 2); their individual effects were negligible. Particle size increased with the increase in sodium alginate concentration and resulted in a decreased angle (lowest angle of 16.14, experiment 3; Table 2). Higher calcium chloride concentration and hardening time resulted in smaller beads with irregular surface because of shrinkage and showed an increased angle (from 16.14 to 18.89 in experiments 3 to 27, respectively).

Optimization of the Process Using the Graphical Evaluation

Generally, the aim of the optimization of pharmaceutical formulations is to find the optimum levels of the variables, which affect a process, where a product of good characteristics could be produced. NN can be trained for predicting the response surface and can be used for optimization within the experimental region. Contour plot of the NN-predicted responses affected by 2 chosen variables are shown in Figure 1A–F. The contours represent different combinations of 2 variables with the same response. Two responses, namely the percentage of entrapment and T_{50}, were selected for optimization of the process. The criteria for the optimum formulation selection were >90% entrapment and T_{50} of <10 minutes. From observing these figures, it is clear that the >90% entrapment area coincides with the T_{50} area of <10 minutes. The study of these plots showed that the highest values of the entrapment and lowest value of T_{50} could be obtained at low values of all 3 of the process variables (ie, at −1, −1, and −1; experiment 1, Table 2).

Table 4. Comparison of Responses Between Predicted and Experimental Values for the Cross-Validation Set

		Factors/Levels					
Responses	**Test**	**A**	**B**	**C**	**Experimental Values**	**Predicted Values**	**Bias %**
% Entrapment	1	−1	−0.6	−0.6	90.72	89.04	1.9
	2	−0.6	0	0.4	81.15	82.98	2.2
	3	−0.4	0.6	0	76.01	77.65	2.1
	4	0	−0.4	0.6	84.58	87.13	2.9
	5	0.4	0.4	−0.4	86.06	84.17	2.2
T_{50}	1	−1	−0.6	−0.6	7.81	8.04	2.9
	2	−0.6	0	0.4	12.83	12.79	0.4
	3	−0.4	0.6	0	14.47	14.31	1.1
	4	0	−0.4	0.6	16.23	16.07	1.0
	5	0.4	0.4	−0.4	17.09	17.58	2.7
T_{90}	1	−1	−0.6	−0.6	24.68	24.27	1.7
	2	−0.6	0	0.4	56.33	54.47	3.4
	3	−0.4	0.6	0	72.15	73.18	1.4
	4	0	−0.4	0.6	75.61	76.88	1.7
	5	0.4	0.4	−0.4	88.63	90.90	2.5
Particle Size	1	−1	−0.6	−0.6	161.7	150.7	7.3
	2	−0.6	0	0.4	180.7	166.2	8.8
	3	−0.4	0.6	0	172.8	182.6	5.4
	4	0	−0.4	0.6	285.9	273.8	4.4
	5	0.4	0.4	−0.4	414.6	435.0	4.7
Angle of Repose	1	−1	−0.6	−0.6	22.29	23.01	3.1
	2	−0.6	0	0.4	21.95	22.98	4.5
	3	−0.4	0.6	0	23.56	22.78	3.4
	4	0	−0.4	0.6	19.89	20.47	2.8
	5	0.4	0.4	−0.4	18.90	19.44	2.8

Evaluation of Model Using Cross-Validation

To assess the reliability of the model, 5 cross-validation experiments were conducted by varying the process variables at values other than that of the model, and responses were predicted using the trained network. A comparison between the experimental and predicted values of the responses for these additional experiments is presented in Table 4. Bias was calculated by the following equation:

$$\text{Bias} = \left[\frac{(\text{predicted value} - \text{experimental value})}{\text{predicted value}}\right] \times 100 \quad (3)$$

It can be seen that in all of the cases there was a reasonable agreement between the NN predicted and the experimental value, because a low value of the bias was found. For this reason, it can be concluded that the NN-predicted responses describe adequately the influence of the selected process variables on the responses under study, and NN can be used successfully as a predictive and optimizing tool.

Characterization of Optimal Formulation

Effect of pH on Release Profile

The effect of pH on the release of papain from calcium alginate beads in different pH (1.2, 4.0, 5.4, 6.8, 7.4, and

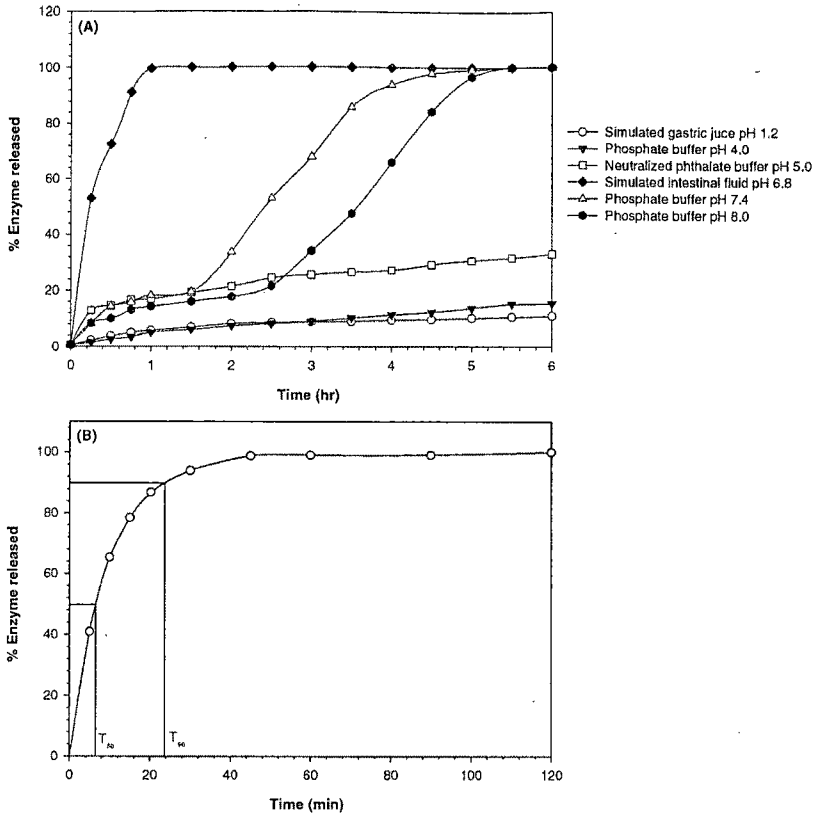

Figure 3. (A) The effect of pH on the release profile of papain in different buffers simulating the human gastrointestinal tract; (B) In vitro release profile of optimized batch in simulated intestinal fluid without enzyme.

8.0) buffers simulating the human gastrointestinal tract is given in Figure 3A. Release profile of optimized batch in simulated intestinal fluid without enzyme is shown in Figure 3B. Generally, higher molecular weight and poorly water-soluble drugs are not released from calcium alginate beads because of stability and nonswelling property in the acidic environment, whereas swell and disintegrate is found in intestinal fluid.[7,28] This was additionally confirmed by the very low amount of papain release in the acidic media (pH 1.2, 4.0, and 5.4) because of higher molecular weight. The swelling and disintegration of calcium alginate beads are dependent on compositions of dissolution medium, for example, sodium and phosphate, and solubility of drug entrapped into alginate beads.[29] The swelling and disintegration of alginate beads in intestinal fluid (pH 6.8) were attributable to the affinity of calcium to phosphate and sodium/calcium exchange. However, the complete release profile was delayed up to 6 hours as the pH increased (7.4 and 8.0) despite the presence of sodium and phosphate. This study confirms the site-specific papain delivery to the intestine rather than the stomach.

FTIR

FTIR spectra of papain, sodium alginate, calcium alginate blank beads, papain-loaded optimized batch, and the

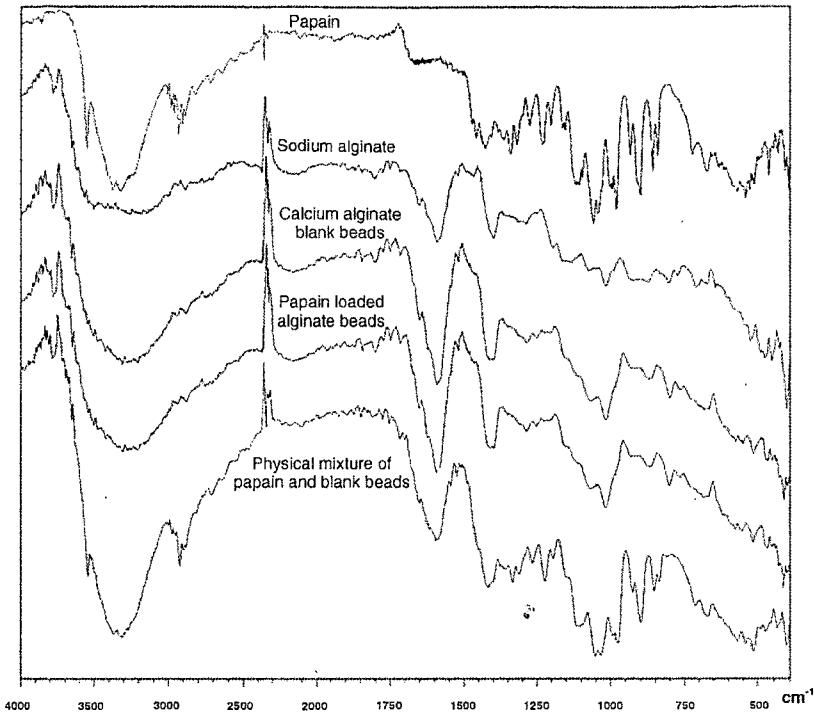

Figure 4. The FTIR spectra of papain, sodium alginate, blank calcium alginate beads, papain-loaded alginate beads, and physical mixture of papain and blank calcium alginate beads.

physical mixture of papain and blank beads are shown in Figure 4. FTIR spectrum of sodium alginate powder showed various distinct peaks of alginate: hydroxyl at 3,263.33 cm^{-1}, carbonyl at 1,600.81 cm^{-1}, and carboxyl and carboxylate at about 1,000 to 1,400 cm^{-1} (Figure 4). Cross-linking of alginate by Ca^{2+} was shown by a decrease in the wave number of the carbonyl peak from 1,600.81 to 1,579.32 cm^{-1}. The hydroxyl peak of calcium alginate had a higher value of wave number than that of the sodium alginate (Figure 4). This was probably because of a negative effect on bond formation involving adjacent hydroxyl groups as a result of conformational changes of alginate after reacting with Ca^{2+}.[30] With incorporation of papain, the spectrum of beads (Figure 4) was similar to that of the calcium alginate blank beads (Figure 4). However, the physical mixture of papain and calcium alginate blank beads showed the peaks attributable to both papain and calcium alginate. This confirms the papain entrapment into the alginate beads at the molecular level.

DSC

The DSC thermograms of papain, sodium alginate, blank calcium alginate beads, and papain-loaded beads are shown in Figure 5. The degradation exotherm of sodium alginate at 252°C was absent in blank calcium alginate bead, and an additional endothermic peak at 221°C corresponding to alginate-calcium interaction was observed. Similar results were reported by Fernandez-Hervas et al.[31] The papain exhibits a sharp endothermic peak at 196°C, whereas the melting peak shape of papain-loaded alginate beads was similar to the blank beads and did not show any peak at 196°C. This confirms that most of the enzyme was uniformly dispersed at the molecular level in the beads.

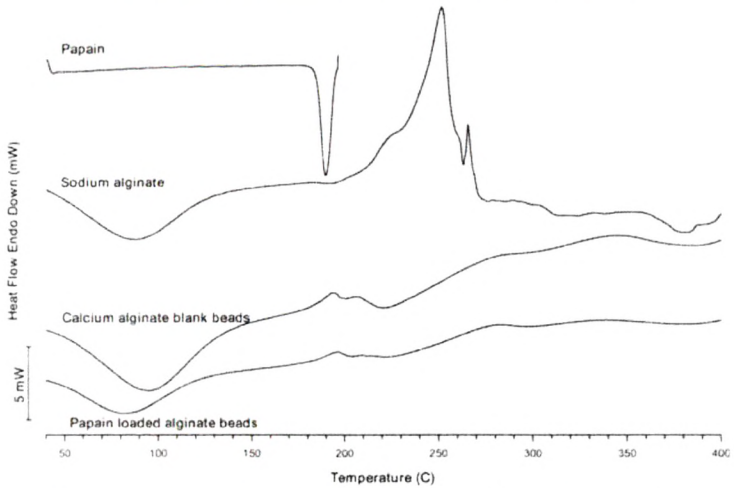

Figure 5. The DSC thermograms of papain, sodium alginate, blank calcium alginate beads, and papain-loaded alginate beads made at the same analytical conditions.

Morphology of the Beads

The spherical shape of beads in the wet state was usually lost after drying, especially for beads prepared with low alginate concentration. In 1% (w/v) alginate, the dried beads were very irregular and tended to agglomerate because of low mechanical strength. With the increasing of alginate concentration (2% w/v), the shape of beads changed to a spherical disk with a collapsed center (Figure 6). Normally the spherical shape was retained when the alginate concentration was as high as 5% (w/v), but viscosity of 5% w/v solution was too high for bead preparation under the present experimental conditions, so it was not studied. These results indicated that the shape of calcium alginate beads was seriously destroyed in the drying process, and the spherical shape of dried beads improved with the increase of alginate concentration. It was reported by Skjak-Brae et al[32] that calcium alginate beads usually have a heterogeneous structure with a dense surface layer and a loose core because of the heterogeneous gelation mechanism, which resulted in the collapse of beads during the drying process.

Stability Study

For the developed formulation, the similarity factor was calculated by a comparison of the dissolution profiles at each storage condition with the control at the initial condition. Results of similarity factors ranged from 76 to 98 or 2% to 5% average difference. In addition to the dissolution profiles, capsule potency results for all of the stability conditions were within 90% to 110% of the label claim. Overall, results from the stability studies indicated that capsules were physically and chemically stable for $\geq$12 months at 40 $\pm$ 2°C/75 $\pm$ 5% relative humidity and for >12 months (approximately for double time period) at 30 $\pm$ 2°C/65 $\pm$ 5% relative humidity.

An approach for analyzing the data on a quantitative attribute that is expected to change with time is to determine the time at which the 95% 1-sided confidence limit for the mean curve intersects the acceptance criterion ($\leq$5% change in assay from its initial value). The accelerated stability data for prepared formulation, marketed formulation,

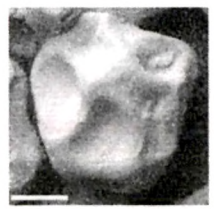

Figure 6. The scanning electron micrograph of dried alginate bead at ×100 magnification (bar at the left bottom = 100 μm).

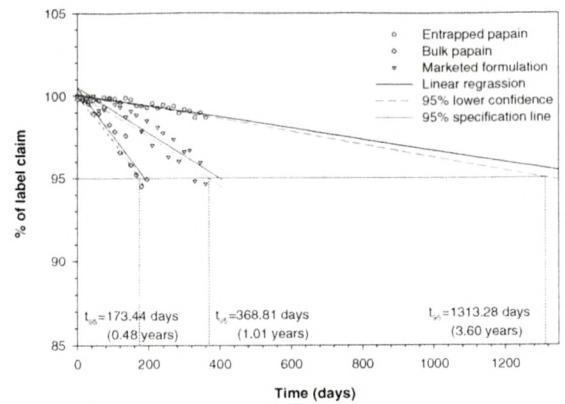

Figure 7. Extrapolation of accelerated stability data of developed formulation, marketed formulation, and bulk papain for shelf-life calculation.

and the bulk papain were extrapolated to calculate the shelf-life (Figure 7) and were found be 3.60 years, 1.01 years, and 0.48 years, respectively. Hence, the stability of the entrapped papain was significantly more improved than the conventional dosage forms.

CONCLUSIONS

The optimization of the process using the NN-predicted responses resulted in >90% entrapment and < 10 minutes of T_{50} at low levels of all 3 of the process variables (1.0% sodium alginate, 0.05 mol/L calcium chloride, and 20 minutes hardening time). Entrapment of papain in alginate beads was confirmed using FTIR and DSC study. Texture analysis of the beads formulations illustrated that the degree of cross-linking decreased with an increase in sodium alginate concentration, whereas it increased with an increase in calcium chloride concentration and hardening time. Dissolution studies over a pH range similar to the human gastrointestinal tract demonstrated that alginate beads can be used for site-specific intestinal delivery of papain. An accelerated and long-term stability study illustrated considerable improvement in the shelf-life of papain entrapped in alginate beads than the conventional dosage form.

ACKNOWLEDGMENTS

The authors thank the University Grants Commission (India) for funding Mayur G. Sankalia under a Junior Research Fellowship scheme.

REFERENCES

1. Bickerstaff GF. Immobilization of enzymes and cells: some practical considerations. In: Bickerstaff GF, ed. *Immobilization of Enzymes and Cells.* Totowa, NJ: Humana Press; 1997;1-12.

2. Uhlig H. *Industrial Enzymes and their Applications.* New York: Wiley; 1998.

3. Lin SY. Release kinetics of drug from different combined ratios of micropellets. *J Microencapsul.* 1993;10:319-322.

4. Ritschel WA. Targeting in the gastrointestinal tract: new approaches. *Methods Find Exp Clin Pharmacol.* 1991;13:313-336.

5. Chen H, Langer R. Magnetically-responsive polymerized liposomes as potential oral delivery vehicles. *Pharm Res.* 1997;14:537-540.

6. Park PG, Shalaby WSW, Park H. Physical Gels. In: *Biodegradable Hydrogels for Drug Delivery.* Lancaster, PA: CRC Press; 1993:99-140.

7. Yotsuyanagi T, Ohkubo T, Ohhashi T, Ikeda K. Calcium-induced gelation of alginic acid and pH-sensitive reswelling of dried gels. *Chem Pharm Bull.* 1987;35:1555-1563.

8. Pillay V, Dangor CM, Govender T, Moopanar KR, Hurbans N. Drug release modulation from crosslinked calcium alginate microdiscs. 1. Evaluation of the concentration dependency of sodium alginate on drug entrapment capacity, morphology and dissolution rate. *Drug Deliv.* 1998;5:25-34.

9. Arica B, Calis S, Kas HS, Sargon MF, Hincal AA. 5-Fluorouracil encapsulated alginate beads for the treatment of breast cancer. *Int J Pharmaceut.* 2002;242:267.

10. Gu F, Amsden B, Neufeld R. Sustained delivery of vascular endothelial growth factor with alginate beads. *J Control Release.* 2004;96:463.

11. Almeida FP, Almeida AJ. Cross-linked alginate-gelatine beads: a new matrix for controlled release of pindolol. *J Control Release.* 2004;97:431-439.

12. Agatonovic-Kustrin S, Zecevic M, Zivanovic LJ, Tucker IG. Application of artificial neural networks in HPLC method development. *J Pharm Biomed Anal.* 1998;17:69-76.

13. Sathe PM, Venitz J. Comparison of neural network and multiple linear regression as dissolution predictors. *Drug Dev Ind Pharm.* 2003;29:349-355.

14. Takayama K, Fujikawa M, Obata Y, Morishita M. Neural network based optimization of drug formulations. *Adv Drug Del Rev.* 2003;55:1217-1231.

15. Agatonovic-Kustrin S, Beresford R. Basic concepts of artificial neural network (ANN) modeling and its application in pharmaceutical research. *J Pharm Biomed Anal.* 2000;22:717-727.

16. Winkler DA, Burden FR. Bayesian neural nets for modeling in drug discovery. *Drug Discovery Today: BIOSILICO.* 2004;2:104-111.

17. Turner JV, Maddalena DJ, Cutler DJ. Pharmacokinetic parameter prediction from drug structure using artificial neural networks. *Int J Pharm.* 2004;270:209-219.

18. Veng-Pedersen P, Modi NB. Application of neural networks to pharmacodynamics. *J Pharm Sci.* 1993;82:918-926.

19. Kachrimanis K, Karamyan V, Malamataris S. Artificial neural networks (ANNs) and modeling of powder flow. *Int J Pharm.* 2003;250:13-23.

20. Havlis J, Madden JE, Revilla AL, Havel J. High-performance liquid chromatographic determination of deoxycytidine monophosphate and methyldeoxycytidine monophosphate for DNA demethylation monitoring: experimental design and artificial neural networks optimisation. *J Chromatogr B Biomed Sci Appl.* 2001;755:185-194.

21. Dow LK, Kalelkar S, Dow ER. Self-organizing maps for the analysis of NMR spectra. *Drug Discovery Today: BIOSILICO.* 2004;2:157-163.

22. Lim CP, Quek SS, Peh KK. Prediction of drug release profiles using an intelligent learning system: an experimental study in transdermal iontophoresis. *J Pharm Biomed Anal.* 2003;31:159-168.

23. Taskinen J, Yliruusi J. Prediction of physicochemical properties based on neural network modelling. *Adv Drug Deliv Rev.* 2003;55:1163-1183.

24. Molnar L, Keseru GM, Papp A, Gulyas Z, Darvas F. A neural network based prediction of octanol-water partition coefficients using atomic5 fragmental descriptors. *Bioorg Med Chem Lett.* 2004;14:851-853.

25. Jouyban A, Majidi M-R, Jalilzadeh H, Asadpour-Zeynali K. Modeling drug solubility in water-cosolvent mixtures using an artificial neural network. *Farmaco.* 2004;59:505-512.

26. Iannuccelli V, Coppi G, Bernabei MT, Cameroni R. Air compartment multiple-unit system for prolonged gastric residence. Part I. Formulation study. *Int J Pharm.* 1998;174:47-54.

27. Wang K, He Z. Alginate-konjac glucomannan-chitosan beads as controlled release matrix. *Int J Pharm.* 2002;244:117-126.

28. Kim C-K, Lee E-J. The controlled release of blum dextran from alginate beads. *Int J Pharm.* 1992;79:11-19.

29. Ostberg T, Lund EM, Graffner C. Calcium alginate matrices for oral multiple unit administration. IV Release characteristics in different media. *Int J Pharm.* 1994;112:241-248.

30. Wong TW, Chan LW, Kho SB, Heng PWS. Design of controlled-release solid dosage forms of alginate and chitosan using microwave. *J Control Release.* 2002;84:99-114.

31. Fernandez-Hervas MJ, Holgado MA, Fini A, Fell JT. In vitro evaluation of alginate beads of a diclofenac salt. *Int J Pharm.* 1998;163:23-34.

32. Skjak-Brae G, Grasdalen KH, Draget KI, Smidsrod O. Inhomogeneous polysaccharide ionic gels. *Carbohydr Polym.* 1989;10:31-54.

Available online at www.sciencedirect.com
SCIENCE DIRECT
International Journal of Pharmaceutics xxx (2006) xxx–xxx
INTERNATIONAL JOURNAL OF PHARMACEUTICS
www.elsevier.com/locate/ijpharm

Stability improvement of alpha-amylase entrapped in kappa-carrageenan beads: Physicochemical characterization and optimization using composite index

Mayur G. Sankalia, Rajshree C. Mashru *, Jolly M. Sankalia, Vijay B. Sutariya

Centre of Relevance and Excellence in Novel Drug Delivery Systems, Pharmacy Department, G.H. Patel Building, The M.S. University of Baroda, Vadodara 390002, India

Received 12 July 2005; received in revised form 1 November 2005; accepted 24 November 2005

Abstract

Purpose: This work examines the influence of various process parameters on α-amylase entrapped in crosslinked κ-carrageenan beads for stability improvement. A three level full factorial design was employed to investigate the effect of three process variables namely κ-carrageenan concentration, potassium chloride concentration and hardening time on % entrapment, time required for 50% (T_{50}) and 90% (T_{90}) of enzyme release and particle size.

Methods: The beads were prepared by dropping the κ-carrageenan-containing α-amylase to magnetically stirred potassium chloride solution. The composite index was applied to optimize the process under study. 'In vitro' enzyme release profile of the beads was fitted to various release kinetics models to understand the release mechanism. Topographical characterization was carried out by SEM and entrapment was confirmed by FTIR and DSC. Stability testing according to the ICH guidelines for zone III and IV was carried out.

Results: With the use of ionotropic gelation method, a polymeric matrix prepared by 3.5% (w/v) κ-carrageenan, 0.7 M potassium chloride and hardening time of 30 min resulted in the production of beads characterized by disc shaped with collapsed centre, absence of aggregates, % entrapment of 73.79, T_{50} of 74.4 min, and composite index of 83.01. Moreover, shelf-life of the enzyme loaded beads was found to increase up to 3.53 years compared to 0.99 year of the conventional formulation.

Conclusions: It can be inferred that the proposed method can be used to prepare α-amylase loaded κ-carrageenan beads for stability improvement. Also the proper selection of rate-controlling carrageenan concentration and its interactive potential for crosslinking is important and will determine the overall size and shape of beads, the duration and pattern of dissolution profiles and enzyme loading capacity.

Keywords: α-Amylase; κ-Carrageenan; Ionotropic gelation; Release kinetics; Composite index; Stability study

1. Introduction

α-Amylase, a major enzyme used for replacement of pancreatic enzymes, need not be reabsorbed in the intestine like other proteins, which are used for systemic therapy. Fungal α-amylases (EC 3.2.1.1; CAS 9000-90-2) are obtained from various strains of *Aspergillus* (mainly *A. niger*, *A. awamori*, and *A. usamii*) species. The α-amylases consist of three domains called A, B and C (Nielsen et al., 1999). The active site, situated in a cleft at the interface between domains A and B, is consist of three acids Asp231, Glu261 and Asp328, which are essential for catalytic activity (Uitdehaag et al., 1999). α-Amylases catalyze the hydrolysis of α-1,4 glycosidic linkages in starch and other related carbohydrates. α-Amylases are used in several industrial processes such as starch liquefaction, laundering, dye removal and feed preprocessing, but the largest volume is sold to the starch industry for the production of high-fructose syrups and ethanol (Guzman-Maldano and Paredes-Lopez, 1995).

Formulations containing α-amylase and other digestive enzymes need to be stored at cold (2–8 °C) or cool (8–25 °C) temperature conditions and still have the shelf-life of not more than 1 year. Entrapment of the α-amylase in ionotropically crosslinked biodegradable hydrogels may improve the stability of the parent enzymes and make it less prone to interference of various formulation excipients. Immobilized enzymes are stable at higher temperature and might be stored at room temperature with extended shelf-life (Bickerstaff, 1997). Optimum pH for activity of α-amylase (*A. oryzae*) is 5.0 (Uhlig, 1998). Multiple unit dosage forms are particularly useful for delivery of enzymes, peptides/proteins and vaccines (Chen and Langer, 1997). Above advantages are of great commercial interest for the pharmaceutical industries hence it was the objective of the research to develop an extended shelf-life formulation of α-amylase by entrapment in ionotropically crosslinked biodegradable κ-carrageenan beads which results in better and efficient utilization of enzyme. This paper also deals with 'in vitro' dissolution studies and physicochemical characterization for evaluating the beads and its release behavior.

Carrageenan has been used increasingly in pharmaceutical formulation studies (Picker, 1999), for example, microcapsules for sustained delivery (Suzuki and Lim, 1994), crosslinked spheres for controlled release (Garcia and Ghaly, 1996; Sipahigil and Dortunc, 2001), or tablet for reducing inactivation of α-amylase (Schmidt et al., 2003). Carrageenans are naturally occurring high molecular weight polysaccharides extracted from red seaweed. They are made up of alternating copolymers of 1,3-linked β-D-galactose and 1,4-linked 3,6-anhydro-α-D-galactose. The units are joined by alternating α-1,4 and β-1,4 glycosidic linkages. Depending on the algae from which they are extracted and the preparative technique, three main types of carrageenans (Scheme 1) are available: kappa (κ), lambda (λ), and iota (ι). Because of the ionic nature of the polymer, gelation is strongly influenced by the presence of electrolytes. κ-Carrageenan forms a gel with potassium ions, but also shows gelation under salt-free

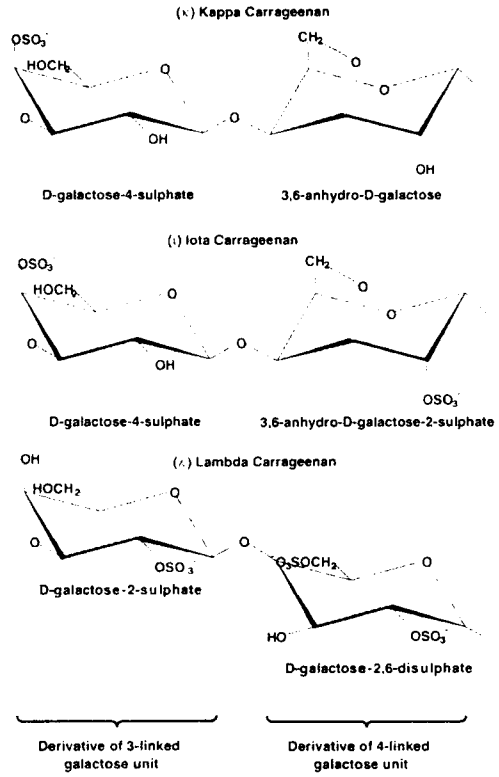

Scheme 1. Different types of carrageenan

* Corresponding author. Tel.: +91 265 2434187/94051; fax: +91 265 2418927.
E-mail addresses: sankalia_mayur@hotmail.com (M.G. Sankalia), rajshree-mashru@yahoo.com (R.C. Mashru), jollymayur@hotmail.com (J.M. Sankalia).

0378-5173/$ – see front matter © 2006 Elsevier B.V. All rights reserved.
doi:10.1016/j.ijpharm.2005.11.048

conditions. However, gels prepared in the presence of metallic ions were substantially stronger than those obtained under salt-free conditions. (Hossain et al., 2001) The gelling and melting temperatures of κ-carrageenan are dependent almost solely on the concentration of potassium ions.

When a polyelectrolyte (like carrageenan) is combined with a uni/multivalent ion of the opposite charge, it may form a physical hydrogel known as an 'ionotropic' hydrogel. Ionotropic hydrogel, which may degrade and eventually disintegrate and dissolve, are held together by molecular entanglements, and/or secondary forces including ionic, H-bonding or hydrophobic forces. (Prestwich et al., 1998) All of these interactions are reversible, and can be disrupted by changes in physical conditions such as ionic strength, pH, temperature, application of stress, or addition of specific solutes that compete with the polymeric ligand for the affinity site on the protein.

From these characteristics, κ-carrageenan is used as an entrapment matrix for cells and enzymes as well as for pharmaceuticals and food adjuvants. In the past, conventional crosslinked potassium-κ-carrageenan beads have been investigated for the development of a multiple unit drug delivery system. However, not even a single reference could be cited in literature till date for entrapment of α-amylase in κ-carrageenan beads for improvisation of shelf-life, hence it was the objective of the study.

2. Materials and methods

2.1. Materials

Potassium dihydrogen phosphate, sodium hydroxide, hydrochloric acid (Qualigens Fine Chemicals, Mumbai, India) and soluble starch (Himedia Laboratories Pvt. Ltd., Mumbai, India) were used as received. Fungal α-amylase, κ-carrageenan (obtained from Irish moss, *Chondrus crispus*), potassium chloride, iodine, and potassium iodide were purchased from S.D. Fine-Chem Ltd., Mumbai, India. All the other chemicals and solvents were of analytical grade and were used without further purification. Deionized double-distilled water was used throughout the study.

2.2. Characterization of carrageenan

The carrageenan procured was derived from Irish moss (*C. crispus*), which is known to contain kappa (gelling fraction) and lambda (non-gelling fraction) carrageenan as major constituents. Carrageenan sample was tested according to the identification test B (gel constancy test) and D (FTIR study) of USP-27 NF-22, and was found to be kappa-carrageenan with non-gelling fraction (lambda-carrageenan) of less than 5%. Moreover, the kappa-carrageenan was confirmed by observing the syneresis phenomenon, which is not observed with iota-carrageenan gels.

2.3. Preparation of beads

Concentrated κ-carrageenan solution in distilled water was prepared by heating the powder dispersion at 70 °C to get homogenous solution and cooled to 40 °C. Required quantity of enzyme (200 mg α-amylase in 50 ml of final κ-carrageenan solution) was dissolved in small quantity of water and mixed with concentrated κ-carrageenan solution. Final concentration of κ-carrageenan was adjusted in the range of 2.5–3.5% (w/v) and was used after being degassed under vacuum. The beads were prepared by dropping the κ-carrageenan solution (10 ml) containing α-amylase from the dropping device such as syringe with 18-G × 1/2 in. flat-tip hypodermic needle to a magnetically stirred potassium chloride solution (40 ml) at a rate of 5 ml/min and were allowed to harden for specific time. Different levels (Table 1) of κ-carrageenan, potassium chloride and hardening time were selected. The beads were collected by decanting potassium chloride solution, washed with deionized water and dried to a constant weight in vacuum desiccator (Tarsons Products Pvt. Ltd., Kolkata, India) at room temperature for 48 h.

Table 1
Process variables and their levels for 3^3 full factorial design

Factors	Coded levels	Actual levels
A: κ-carrageenan concentration (%, w/v)	−1	2.5% (w/v)
	0	3.0% (w/v)
	1	3.5% (w/v)
B: potassium chloride concentration (M)	−1	0.3 M
	0	0.5 M
	1	0.7 M
C: hardening time (min)	−1	10 min
	0	20 min
	1	30 min

2.4. Factorial design

Before the application of the design, number of preliminary trials were conducted by changing one variable at a time and keeping other variables fixed to determine the conditions at which the process resulted to beads. In the present study three-level full factorial design (FFD) was employed to generate response surfaces. To determine the experimental error, the experiment at the centre point was repeated five times at different days. The mean % entrapment, T_{50}, T_{90}, and particle size at the center-replicated points were 73.96 ± 0.46%, 33.64 ± 0.65 min, 44.12 ± 1.21 min, and 1.92 ± 0.008 mm, respectively and showed good reproducibility of the process. The quadratic coefficients were estimated using the least-squares multiple regression to the observed response. The analysis of variance (ANOVA) was performed in order to determine significance of the fitted equation. All analytical treatments were supported by NCSS software. The process variables with their coded experimental values and the results of the responses are reported in Table 2.

2.5. Composite index

On completion of the individual experiments, a weighted composite index was used to designate a single score utilizing two responses, i.e., % entrapment, and T_{90}. Many researchers have utilized the technique of multiple responses for optimization studies. Derringer and Suich illustrated how several response variables can be transformed into one response (Derringer and Suich, 1980). The applications of one-sided transformations are also demonstrated by different researchers (Bodeam and Leucata, 1997; Gohel et al., 2003). The application of generalized distance function to incorporate several objectives into a single function has been reported (Shigeo et al., 1994). As the relative contribution of each individual constraint to the "true" composite score was unknown, a decision was made to assign an arbitrary value of one-half to each of the two response variables (Taylor et al., 2000). The empirical composite index was devised to yield a score 100 for an optimum result for each of the two responses and each formulation result was transformed to a value between 0 and 50. For % entrapment, highest value (84.7) was assigned a score equal to 50, and lowest value (52.59) was assigned zero score. For T_{90}, lowest value (25.5) was assigned to zero score and the highest value (74.4) was assigned to 50. The batch having the highest composite index would be considered as a batch fulfilling the desired criteria. The raw data transformations were as follows:

$$\text{transformed value of \% entrapment or } T_{90} = \frac{Y_i - Y_{\min}}{Y_{\max} - Y_{\min}} \times 50 \quad (1)$$

where Y_i is the experimental value of individual response variable, $Y_{\max}$ and $Y_{\min}$ are maximum and minimum values of individual response variable, respectively.

$$\text{composite index} = \text{transformed value of \% entrapment} + \text{transformed value of } T_{50} \quad (2)$$

2.6. Curve fitting

The 'in vitro' release pattern was evaluated to check the goodness of fit to the zero-order release kinetics Eq. (3), first-order release kinetics (Gibaldi and Feldman, 1967; Wagner, 1969) Eq. (4), Higuchi's square root of time equation (Higuchi, 1963) Eq. (5), Korsmeyer–Peppas' power law equation (Korsmeyer et al., 1983; Peppas, 1985) Eq. (6), and Hixson–Crowell's cube root of time equation (Hixson and Crowell, 1931) Eq. (7). The goodness of fit was evaluated by r (correlation coefficient) values. For better understanding residual analysis (Pather et al., 1998) of above models was performed on the optimized formulation

$$Q_t = Q_0 + K_0 t \quad (3)$$

where Q_t is the amount of drug dissolved in time t, Q_0 is the initial amount of drug in the solution (most times, $Q_0 = 0$), K_0 is

Table 2
Factorial 3^3; matrix of the experiments and results for the measured responses and the composite index

ES[a]	Factors/levels			Responses				Transformed		Composite index (CI)
	Carrageenan (%, w/v)	KCl (M)	Hardening time (min)	% Immobilization	T_{50}	T_{90}	Particle size ± S.D.[b] (mm)	% Immobilization	T_{90}	
9	−1	−1	−1	65.34	17.15	25.50	1.83 ± 0.19	19.85	50.00	19.85
13	−1	−1	0	62.40	19.20	29.70	1.80 ± 0.17	15.28	45.71	19.57
2	−1	−1	1	60.29	22.10	33.65	1.76 ± 0.18	11.99	41.67	20.32
24	−1	0	−1	62.11	22.30	32.50	1.68 ± 0.20	14.82	42.84	21.98
17	−1	0	0	59.25	25.45	38.60	1.65 ± 0.19	10.37	36.61	23.77
6	−1	0	1	57.24	29.10	44.10	1.61 ± 0.20	7.24	30.98	26.26
1	−1	1	−1	57.27	28.86	42.35	1.63 ± 0.19	7.29	32.77	24.52
27	−1	1	0	54.49	32.65	46.10	1.60 ± 0.20	2.96	28.94	24.02
10	−1	1	1	52.59	36.40	49.70	1.56 ± 0.17	0.00	25.26	24.74
23	0	−1	−1	78.79	24.50	35.30	2.09 ± 0.20	40.80	39.98	50.82
8	0	−1	0	75.97	28.75	41.10	2.06 ± 0.16	36.41	34.05	52.36
15	0	−1	1	73.96	33.05	46.05	2.02 ± 0.17	33.28	28.99	54.29
12	0	0	−1	76.65	30.75	41.50	1.95 ± 0.20	37.46	33.64	53.82
26	0	0	0	73.92	33.70	44.15	1.92 ± 0.19	33.21	30.93	52.28
19	0	0	1	72.02	37.75	50.90	1.88 ± 0.20	30.26	24.03	56.23
3	0	1	−1	70.68	37.86	50.83	1.90 ± 0.22	28.17	24.10	54.07
18	0	1	0	68.00	42.05	55.20	1.87 ± 0.19	24.00	19.63	54.36
21	0	1	1	66.18	44.60	62.95	1.83 ± 0.18	21.16	11.71	59.45
4	1	−1	−1	84.70	31.50	45.40	2.43 ± 0.19	50.00	29.65	70.35
25	1	−1	0	82.02	35.90	49.30	2.41 ± 0.19	45.83	25.66	70.16
11	1	−1	1	80.13	40.95	56.20	2.38 ± 0.18	42.88	18.61	74.27
22	1	0	−1	82.30	38.47	51.90	2.29 ± 0.17	46.26	23.01	73.26
14	1	0	0	79.79	42.10	56.05	2.27 ± 0.19	42.35	18.76	73.59
7	1	0	1	78.03	45.50	62.00	2.24 ± 0.19	39.61	12.68	76.93
5	1	1	−1	77.80	45.60	60.50	2.26 ± 0.18	39.26	14.21	75.04
16	1	1	0	75.42	48.30	67.80	2.24 ± 0.18	35.55	6.75	78.80
20	1	1	1	73.79	51.40	74.40	2.21 ± 0.18	33.01	0.00	83.01

[a] ES, experimental sequence.
[b] S.D., standard deviation ($n = 50$).

the zero order release constant and t is release time

$$Q_t = Q_0 e^{-K_1 t} \quad (4)$$

where Q_t is the amount of drug dissolved in time t, Q_0 is the initial amount of drug in the solution, K_1 is the first order release constant and t is release time

$$Q_t = K_H \sqrt{t} \quad (5)$$

where Q_t is the amount of drug dissolved in time t, K_H is the Higuchi dissolution constant and t is release time

$$\frac{Q_t}{Q_\infty} = K_K t^n \quad (6)$$

where Q_t is the amount of drug dissolved in time t, Q_∞ is the amount of drug dissolved in ∞ time (the drug loaded in the formulation), Q_t/Q_∞ is the fractional release of the drug in time t, K_K is a constant incorporating structural and geometric characteristic of dosage form, n is the release (diffusional) exponent that depends on the release mechanism and the shape of the matrix tested (Ritger and Peppas, 1987) and t is release time. Interpretation of diffusional exponent is given in Table 3

$$Q_0^{1/3} - Q_t^{1/3} = K_\lambda t \quad (7)$$

where Q_0 is the initial amount of drug in the pharmaceutical dosage form, Q_t is the remaining amount of drug in pharmaceutical dosage form at time t, K_λ is a constant incorporating the surface–volume relation and t is release time.

In order to understand the release mechanism, the release data of the optimized batch was fitted to empirical equations proposed by Kopcha (Kopcha et al., 1991) Eq. (8)

$$M = At^{1/2} + Bt \quad (8)$$

In the above equations, M (~70%) is the percentage of drug released at time t, while A and B are, respectively, diffusion and erosion terms. According to this equation, if diffusion and erosion ratio, $A/B = 1$, then the release mechanism includes both diffusion and erosion equally. If $A/B > 1$, then diffusion prevails, while for $A/B < 1$, erosion predominates.

2.7. Characterization of beads

2.7.1. Estimation of α-amylase (dextrinogenic assay)

The iodine test of Smith and Roe (Smith and Roe, 1957; Hsiu et al., 1964) was modified as follows: 2 ml of a 0.2% starch solution was added to 1.0 ml of enzyme diluted in 0.05 M phosphate buffer pH 6.8. The mixture was incubated for 3 min at 25 °C and then reaction was stopped with 1 ml of 1 N HCl. Finally, 20 ml of water and 0.5 ml of 0.01 N iodine solution prepared according to Rice (1959) were added and the absorbance A was recorded on a spectrophotometer (Shimadzu UV-1601, Japan) at 660 nm. The instrument was adjusted to zero reading with iodine blank containing neither enzyme nor substrate. The dextrinogenic activity is expressed in arbitrary units as follows:

$$D = \frac{A_B - A}{A_B} E \quad (9)$$

where A_B is the absorbance of the starch–iodine complex in the absence of enzyme and E is the enzyme dilution. Best results were obtained when the enzyme solution was diluted in such a manner as to make the ratio $(A_B - A)/A_B$, approach 0.20–0.25.

Table 3
Interpretation of Korsmeyer–Peppas power law release exponent

Release exponent (n)	Drug transport mechanism	Rate as a function of time
0.5	Fickian diffusion	$t^{-0.5}$
0.5 < n < 1.0	Anomalous transport	$t^{(n-1)}$
1.0	Case-II transport	Zero order release
Higher than 1.0	Super case-II transport	t^{n-1}

2.7.2. Determination of entrapment efficiency

Entrapment efficiency was determined by dissolving the enzyme loaded beads in a magnetically stirred simulated gastric fluid (SGF) without enzyme (USP XXVI) for about 90 min. An aliquot of 2 ml was taken and neutralized to pH 6.8 using 0.01 N sodium hydroxide. The resulting solution was centrifuged at 2500 rpm for 10 min (Remi Instruments Ltd., Mumbai, India) and supernatant was assayed ($n = 3$) for enzyme content by dextrinogenic assay as above. Entrapment efficiency was calculated as

$$\text{entrapment efficiency} = \frac{\text{enzyme loaded}}{\text{theoretical enzyme loading}} \times 100 \quad (10)$$

2.7.3. Determination of T_{50} and T_{90}

Time required for 50 (T_{50}) and 90 (T_{90}) percent of enzyme release were used to evaluate the onset and duration of action, respectively. For optimization purpose, dissolution study of all batches was carried out in 500 ml of SGF without enzyme using the USP XXVI dissolution apparatus 2 (TDT-60T, Electrolab, Mumbai, India) at 37 ± 0.5 °C with paddle speed of 75 rpm. Accurately weighed samples ($n = 3$) equivalent to about 40 mg of α-amylase were subjected to dissolution and aliquots of 2 ml were collected, neutralized to pH 6.8 using 0.01 N sodium hydroxide, and assayed at 0, 5, 10, 15, 20, 30, 45, 60, 90 and 120 min. T_{50} and T_{90} were found by extrapolating the % enzyme released versus time plot.

2.7.4. Particle size measurements

The particle sizes of 50 gel beads were measured with a gauge type micrometer (0.01 mm least count, Durga Scientific Pvt. Ltd., Vadodara, India) for each formulation and the mean particle size was determined.

2.7.5. Fourier transform infra-red spectroscopy (FTIR)

IR transmission spectra were obtained using a FTIR spectrophotometer (FTIR-8300, Shimadzu, Japan). A total of 2% (w/w) of sample, with respect to the potassium bromide (KBr; S.D. Fine Chem Ltd., Mumbai, India) disc, was mixed with dry KBr. The mixture was ground into a fine powder using an agate mortar before compressing into KBr disc under a hydraulic press at 10,000 psi. Each KBr disc was scanned at 4 mm/s at a resolution of 2 cm over a wavenumber region of 400–4000 cm^{-1}. The characteristic peaks were recorded.

2.7.6. Differential scanning calorimetry (DSC)

Differential scanning calorimetric analysis was used to characterize the thermal behavior of the isolated substances, empty and enzyme loaded beads. DSC thermograms were obtained using an automatic thermal analyzer system (DSC-60, Shimadzu, Japan). Temperature calibration was performed using indium as a standard. Samples were crimped in a standard aluminum pan and heated from 40 to 400 °C at a heating rate of 10 °C/min under constant purging of dry nitrogen at 30 ml/min. An empty pan, sealed in the same way as the sample, was used as a reference.

Table 4
ANOVA results (P values), effect of the variables on % entrapment, T_{50}, T_{90}, particle size and composite index

Factors	% Entrapment		T_{50}		T_{90}		Particle size		Composite index	
	Coefficient	P	Coefficient	P	Coefficient	P	Coefficient	P	Coefficient	P
Intercept	73.73	<0.0001*	33.97	<0.0001*	45.10	<0.0001*	1.92	<0.0001*	52.96	<0.0001*
A	10.17	<0.0001*	8.14	<0.0001*	10.08	<0.0001*	0.31	<0.0001*	26.13	<0.0001*
B	3.74	<0.0001*	6.37	<0.0001*	8.20	<0.0001*	0.09	<0.0001*	2.56	<0.0001*
C	−2.30	<0.0001*	3.55	<0.0001*	5.23	<0.0001*	−0.03	<0.0001*	1.77	<0.0001*
A^2	3.85	<0.0001*	0.58	0.0068*	0.98	0.0929	0.04	<0.0001*	4.99	<0.0001*
B^2	1.37	<0.0001*	0.74	0.0009*	2.03	0.0016*	0.05	<0.0001*	0.06	0.8971
C^2	0.30	0.0609	0.24	0.2173	0.98	0.0939	0.005	0.0126*	1.47	0.0060
AB	0.32	0.0120*	0.21	0.1672	0.21	0.6308	0.008	<0.0001*	0.71	0.0664
AC	0.15	0.2228	0.25	0.1032	0.64	0.1484	0.005	0.0025*	0.88	0.0256
BC	0.10	0.3757	−0.24	0.1169	0.30	0.4820	0.000	1.0000	0.48	0.2083
ABC	0.02	0.8688	−0.78	0.0003*	0.49	0.3622	0.000	1.0000	0.54	0.2466
r^2_{adj}	0.9979		0.9965		0.9820		0.9996		0.9962	

Regression coefficients are in coded values.
* Statistically significant ($P < 0.05$).

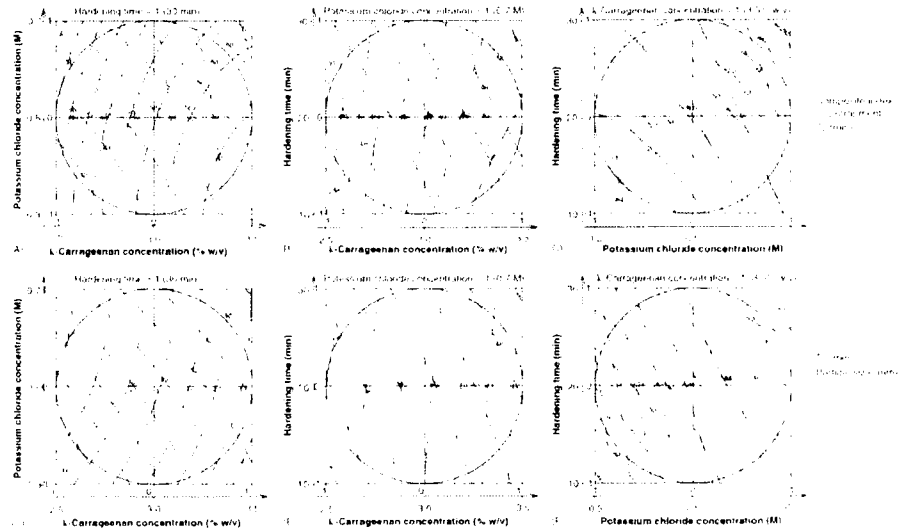

Fig. 1. Contour plots of composite index, % entrapment, T_{50}, T_{90} and particle size as a function of sodium carrageenan concentration, potassium chloride concentration, and hardening time.

2.7.7. Scanning electron microscopy (SEM)

The purpose of SEM study was to obtain a topographical characterization of beads. The beads were mounted on brass stubs using carbon paste. SEM photographs were taken with scanning electron microscope (JSM-5610LV, Jeol Ltd., Japan) at the required magnification at room temperature. The working distance of 39 mm was maintained and acceleration voltage used was 5 kV, with the secondary electron image (SEI) as a detector.

2.8. Preparation of capsule formulation, packaging, and stability study

Accurately weighed carrageenan beads equivalent to 40 mg of α-amylase were filled into a hard gelatin capsule manually. The joint of the capsule body and cap was carefully sealed by pressing them to fit in the lock mechanism. The capsules were packed in high density polyethylene (HDPE) bottles with polypropylene (PP) caps (foamed polyethylene and pressure sensitive liner). The capsules were subjected to stability testing according to the International Conference on Harmonization guidelines for zone III and IV. The packed containers of prepared capsules along with marketed formulation and bulk α-amylase were kept for accelerated (40 ± 2 °C/75 ± 5% relative humidity) and long term (30 ± 2 °C/65 ± 5% relative humidity) stability in desiccators with saturated salt solutions for up to 12 months. For accelerated and long term stability, desiccators containing saturated sodium chloride and potassium iodide solutions were kept into ovens at 40 and 30 °C to maintain a constant relative humidity of 74.68 ± 0.13 and 67.98 ± 0.23, respectively. A visual inspection (for discoloration of capsule content), dissolution testing and α-amylase content estimation was carried out every 15 days for the entire period of stability study.

3. Results and discussion

3.1. Effect of the factors on responses

3.1.1. % Entrapment

ANOVA results and regression coefficients of response variables are shown in Table 4. All three process variables were

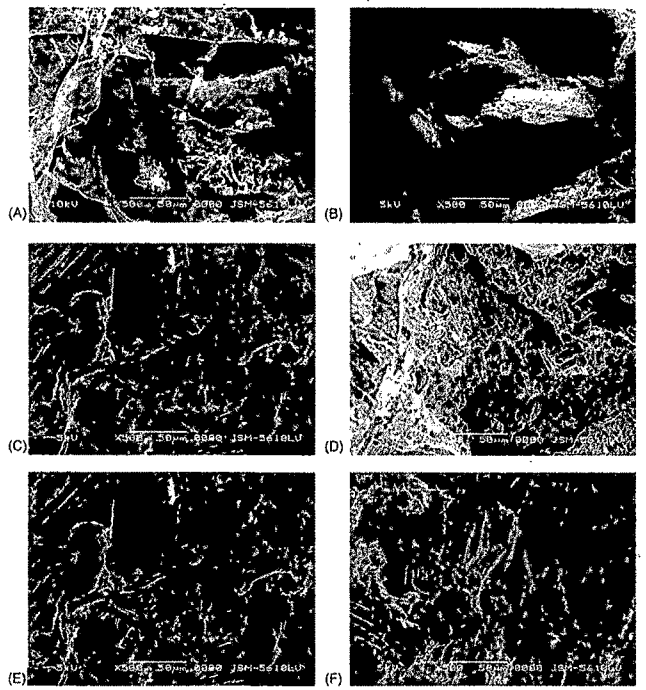

Fig. 2. SEM micrographs and surface morphology of carrageenan beads: (A–C) Effect of potassium chloride concentration (κ-carrageenan concentration 3.0%, w/v) (A) 0.3 M, (B) 0.5 M, and (C) 0.7 M potassium chloride concentration. (D–F) Effect of κ-carrageenan concentration (potassium chloride concentration 0.7 M) (D) 2.5%, w/v, (E) 3.0%, w/v, and (F) 3.5%, w/v κ-carrageenan concentration.

statistically significant ($P < 0.05$). From the contour plots of response surface for % entrapment (Fig. 1A–C) and Table 2, it can be concluded that concentration of κ-carrageenan was the most influencing factor (45.53%) and affecting positively (positive coefficient; Table 4; i.e. response increases with increase in factor level). However, potassium chloride concentration and hardening time were affecting negatively (negative coefficient; Table 4; i.e. response decreases with increase in factor level) in significant amount. More than 84% entrapment (experiment 4) was obtained at the high level of the κ-carrageenan concentration especially when it was followed by the low levels of the other two factors.

On addition of κ-carrageenan solution to a potassium chloride solution, instantaneous interfacial crosslinking takes place followed by a more gradual gelation of the interior and causes loss of enzyme from the beads, which was found to be proportional to the degree of crosslinking. Increase in viscosity with increase in κ-carrageenan concentration may retard penetration of potassium to the interior of the bead, resulted in decreased crosslinking (also decreased surface roughness and porosity; Fig. 2D and E) and hence increased entrapment efficiency. Degree of crosslinking increased with increase in potassium concentration and contact time, and so entrapment efficiency decreased. The entrapment efficiency of the α-amylase containing beads prepared with calcium alginate (sodium alginate and calcium chloride) and chitosan-alginate was 91% and 90%, respectively, using κ-carrageenan the α-amylase entrapment efficiency in our study did not exceed 85%, although the same method was used. So with chitosan or alginate more efficient entrapment was achieved (Bodmeier and Wang, 1993).

3.1.2. T_{50} and T_{90}

As shown in Fig. 1 and Table 4, all three factors had significant positive effect on both response values. The concentration of κ-carrageenan concentration (factor *A*) had the most significant effect. For maximum activity of enzyme in the intestine longer T_{50} and T_{90} were the desired criteria for the optimum formulation. Thus, extreme level of all three variables resulted the beads with T_{50} and T_{90} as high as 51.4 and 74.4 min, respectively (experiment 20, Table 2). T_{50} and T_{90} were found to be proportional to particle size and degree of crosslinking. As the concentration and hence the viscosity of κ-carrageenan increeases, larger beads (discussed under 'particle size') were obtained which took long time for complete dissolution and resulted in higher T_{50} and T_{90}. The increase of the in vitro release rates of α-amylase from carrageenan beads prepared with low concentrations of potassium chloride solutions may be due to the less crosslinked structure of the beads which may result in a more porous matrix (Fig. 2A–C) and higher drug release (Garcia and Ghaly, 1996; Sipahigil and Dortunc, 2001). Higher hardening time caused penetration of potassium to the interior of the bead, resulted in increased crosslinking, and hence higher T_{50} and T_{90}.

Table 5
Comparison of responses between predicted and experimental values for the cross-validation set

Responses	Test	Factors/levels			Experimental values	Predicted values	Bias %
		A	*B*	*C*			
% Entrapment	1	−1	−0.6	−0.6	63.26	62.50	1.2
	2	−0.6	0	0.4	65.34	63.70	2.5
	3	−0.4	0.6	0	66.23	68.08	−2.8
	4	0	−0.4	0.6	73.71	71.79	2.6
	5	0.4	0.4	−0.4	76.44	78.28	−2.4
T_{50}	1	−1	−0.6	−0.6	19.88	20.44	−2.8
	2	−0.6	0	0.4	30.28	31.10	−2.7
	3	−0.4	0.6	0	34.76	33.68	3.1
	4	0	−0.4	0.6	33.82	34.66	−2.5
	5	0.4	0.4	−0.4	38.44	37.96	1.2
T_{90}	1	−1	−0.6	−0.6	29.48	29.22	0.9
	2	−0.6	0	0.4	41.51	42.39	−2.1
	3	−0.4	0.6	0	46.83	46.09	1.6
	4	0	−0.4	0.6	45.57	46.66	−2.4
	5	0.4	0.4	−0.4	50.81	51.37	−1.1
Particle size	1	−1	−0.6	−0.6	1.75	1.71	2.1
	2	−0.6	0	0.4	1.73	1.76	−1.8
	3	−0.4	0.6	0	1.76	1.74	1.3
	4	0	−0.4	0.6	1.94	1.98	−2.2
	5	0.4	0.4	−0.4	2.03	2.06	−1.6
Composite index	1	−1	−0.6	−0.6	20.69	19.24	7.0
	2	−0.6	0	0.4	36.22	34.58	4.5
	3	−0.4	0.6	0	43.05	45.19	−4.9
	4	0	−0.4	0.6	53.41	51.54	3.5
	5	0.4	0.4	−0.4	63.02	66.45	−5.4

3.1.3. Particle size

As depicted in Table 4, the κ-carrageenan concentration (factor *A*, most influential; 56.77%) had positive coefficient, while potassium chloride concentration and hardening time had negative coefficient. In contrast to the finding of Sipahigil (Sipahigil and Dortunc, 2001) and Bhardwaj (Bhardwaj et al., 1995), all three process variables were statistically significant ($P < 0.05$). Freely water soluble drug always entrapped in higher ratio and results in bigger particles. (Sipahigil and Dortunc, 2001) The bead size is influenced by the opening through which the κ-carrageenan is allowed to pass (which was kept constant) and the viscosity of the carrageenan solution. Increased viscosity at higher concentration of κ-carrageenan resulted in larger particles. High potassium chloride concentration and hardening time resulted in smaller particle size due to high degree of crosslinking. Though the negative effect of potassium chloride concentration and hardening time was of less magnitude, they contribute to the morphology of the beads (Fig. 2A–C).

3.2. Interactions between the factors

An interaction is the failure of a factor to produce the same effect on the response at the different levels of the other factor. The ANOVA results (Table 4) showed that interaction AB had significant influence on % entrapment, ABC had significant influence on T_{50}, while AB and AC had significant influence on particle size. The analysis of the results by multiple regression (Table 4) leads to equations that adequately describe the influence of the selected factors on % entrapment, T_{50}, T_{90}, particle size, and composite index.

3.3. Optimization of the process using the composite index

Generally the aim of the optimization is to find the optimum levels of the variables, which affect a process, where a product of desired characteristics could be produced easily and reproducibly. Using the composite index, both selected responses (% entrapment and T_{90}) were combined in one response. As it has been already discussed, the composite index was calculated from the individually calculated transformed value of each of the responses using the Eqs. (1) and (2). The equation found out using multiple regression was as follow (coded factors):

$$CI = 62.87 + 5.53A - 14.22B - 8.93C - 7.00A^2 - 4.22B^2 - 0.53C^2 + 0.28AB - 0.43AC - 0.15BC - 0.46ABC \quad (R^2_{adj} = 0.9822,\ P < 0.0001) \quad (11)$$

In Fig. 1A–C the contour plots that describe the influence of the independent factors on the composite index is presented. The study of these plots and Table 2 showed that the highest values of the CI (83.01) could be obtained at high level of all three independent factors (experiment 20) and was considered as a batch fulfilling all the constraints favorable for the bead preparation.

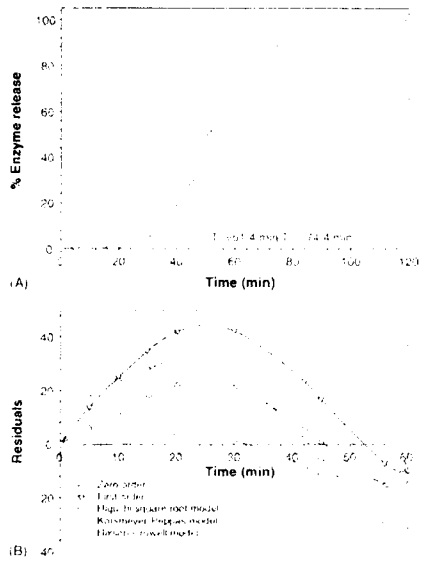

Fig. 3. (A) 'In vitro' release profile of optimized formulation (experiment 20) in SGF without enzyme. (B) Residual plot of different release models for the same formulation.

3.4. Evaluation of model using cross-validation

In order to assess the reliability of the model, five experiments were conducted by varying the process variables at values other than that of the model. For each of these test experiments the responses were estimated by using the multiple regression equations and experimental procedure for comparison between both responses (Table 5). Bias was calculated by the following equation:

$$\text{bias} = \left[\frac{\text{predicted value} - \text{experimental value}}{\text{predicted value}}\right] \times 100 \quad (12)$$

It can be seen that in all cases there was a reasonable agreement between the predicted and the experimental value, since low value of the bias were found. For this reason it can be concluded that the equations describe adequately the influence of the selected process variables on the responses under study.

3.5. Curve fitting and release mechanism

'In vitro' dissolution profile of the optimized batch is shown in Fig. 3A. Release of α-amylase from κ-carrageenan beads in simulated gastric fluid is conceivably attributed to the presence of strongly acidic sulphate groups in the carrageenan molecule,

Table 6
Comparison of different dissolution kinetics models

ES[a]	Release model										
	Zero-order		First-order		Higuchi matrix		Korsmeyer–Peppas			Hixson–Crowell	
	K_0	r_0	K_1	r_1	K_H	r_H	n	K_k	r_k	K_s	r_s
9	3.19	0.97	−0.11	0.74	14.13	0.87	1.30	1.22	0.98	0.02	0.87
13	2.53	0.96	−0.08	0.90	13.06	0.87	1.33	0.83	0.97	0.02	0.94
2	2.31	0.96	−0.07	0.85	11.91	0.84	1.62	0.27	0.98	0.01	0.92
24	2.33	0.96	[b]	[b]	12.04	0.85	1.38	0.61	0.97	0.02	0.87
17	2.08	0.96	[b]	[b]	10.87	0.82	1.56	0.27	0.98	0.02	0.82
6	1.75	0.95	[b]	[b]	10.30	0.83	1.71	0.12	0.97	0.01	0.90
1	1.79	0.96	0.06	0.86	10.60	0.84	1.50	0.27	0.97	0.01	0.92
27	1.65	0.94	0.05	0.83	9.68	0.81	1.94	0.04	0.98	0.01	0.90
10	1.51	0.93	−0.05	0.79	8.93	0.78	2.21	0.01	0.96	0.01	0.87
23	2.18	0.97	[b]	[b]	11.38	0.85	1.29	0.76	0.98	0.02	0.84
8	1.93	0.95	0.06	0.76	10.18	0.81	1.50	0.29	0.98	0.01	0.86
15	1.65	0.95	0.05	0.83	9.74	0.81	1.81	0.07	0.99	0.01	0.90
12	1.86	0.94	0.06	0.72	9.83	0.79	1.47	0.30	0.97	0.01	0.83
26	1.66	0.94	0.05	0.85	9.78	0.81	2.00	0.04	0.99	0.01	0.90
19	1.32	0.92	0.04	0.90	9.15	0.83	2.03	0.02	0.97	0.01	0.92
3	1.50	0.94	[b]	[b]	8.90	0.79	1.81	0.06	0.97	0.01	0.80
18	1.24	0.93	−0.05	0.86	8.59	0.81	2.04	0.02	0.97	0.01	0.91
21	1.16	0.94	−0.04	0.84	8.09	0.80	2.14	0.01	0.94	−0.01	0.91
4	1.70	0.96	[b]	[b]	10.10	0.84	1.40	0.35	0.97	0.01	0.89
25	1.55	0.95	0.05	0.80	9.24	0.81	1.64	0.12	0.97	0.01	0.88
11	1.25	0.94	[b]	[b]	8.73	0.82	1.77	0.05	0.96	0.01	0.91
22	1.47	0.94	0.05	0.71	8.83	0.80	1.69	0.09	0.98	0.01	0.85
14	1.24	0.94	−0.04	0.88	8.61	0.82	2.01	0.02	0.98	0.01	0.92
7	1.16	0.93	−0.04	0.86	8.02	0.80	2.42	0.00	0.98	0.01	0.91
5	1.17	0.94	−0.04	0.82	8.17	0.81	1.61	0.08	0.96	0.01	0.91
16	1.09	0.93	−0.04	0.79	7.58	0.79	2.22	0.01	0.97	0.01	0.89
20	1.02	0.93	−0.03	0.80	7.13	0.78	2.23	0.00	0.95	0.01	0.88

[a] ES, experimental sequence.
[b] Not possible.

that allow a certain degree of ionization to be maintained also at low pH (Bonferoni et al., 1994). Values of release exponent (n) and kinetic constant (K) were derived using Eqs. (3) to (7) and are presented in Table 6. The enzyme release data show a good fit to the Korsmeyer–Peppas' power law release kinetics Eq. (6), which can be confirmed by comparing the values of correlation coefficient (r) with that of the other models. The values of Korsmeyer–Peppas' release exponent (n) determined for the various formulations studied ranged from 1.29 to 2.42 suggesting the probable release by super case-II transport. The K_k values ranged from 0.0033 to 1.22 where low K_k value may suggest near to zero release from the beads initially. If one considers the correlation coefficient (r) values of zero-order and Korsemeyer–Peppas release models, both models describe the dissolution data reasonably well. Where there are competing models (with similar r values), residuals analysis can be used to distinguish between the models (Pather et al., 1998). Fig. 3B is the residual plot for optimized formulation. The residuals are high for the zero-order, first-order, Higuchi, and Hixson–Crowell models (and least for the Korsemeyer–Peppas model), which also shows systematic deviation; the models overpredict initially and underpredict at the later stages of the dissolution process. This indicates that the Korsemeyer–Peppes' power low is the best fit model in describing the dissolution behavior of α-amylase from κ-carrageenan beads.

Finally, in order to know whether the enzyme release was due to erosion or diffusion, the release data of the optimized formulation was fitted to Kopcha model Eq. (8) and parameters like A and B at different time intervals were determined

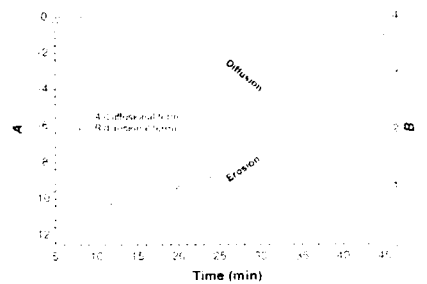

Fig. 4. Kopcha model parameters (A and B) versus time profile for optimized batch (experiment 20).

(Fig. 4). Throughout the release profile, A was <0 and B was >0, and expressed the predominance of erosion relative to diffusion. This probably may be due to the lower gel strength of carrageenan gels. During dissolution study carrageenan gel swell but is unable to maintain the gel matrix due to low gel strength and start to erode. However, the rate of hydration initially was found to be the rate limiting step of erosion rate and explain the biphasic nature of release profile (plateau initially followed by steep rise in erosion rate). The erosion term B increases with time because erosion of the hydrated layer is easier.

3.6. Characterization of optimal formulation

3.6.1. Fourier transform infra-red spectroscopy (FTIR)

FTIR spectra of κ-carrageenan powder, carrageenan blank beads, α-amylase loaded carrageenan beads, physical mixture of α-amylase and blank beads, and α-amylase are shown in Fig. 5. FTIR spectrum of κ-carrageenan powder showed various distinct peaks: very broad band spreading 3150–3600 cm^{-1} (strong; s) due to polyhydroxy $(-OH)_n$ group; 2968 cm^{-1} (s), 2920 cm^{-1} (s), and 2850 cm^{-1} (medium; m) due to C–H stretch; 1425 cm^{-1} (s) and 1375 cm^{-1} (s) due to C–H deformation; 1225 cm^{-1} (s) due to S=O stretch of sulfate ester salt; 1070 cm^{-1} due to C–O stretch of cyclic ethers; 925 cm^{-1} (s) due to C–O stretch of polyhydroxy groups attached to carbons; etc. Crosslinking of carrageenan by K^+ was shown by a decrease in the intensity of S=O stretch (1225 cm^{-1}) of sulfate ester group which was same as C–O stretch (1070 cm^{-1}) of cyclic ethers in intensity for the κ-carrageenan powder. This was probably because of some negatively charged sulfate ester reacted with positively charged K^+ and resulted in physicochemical changes of carrageenan. α-Amylase also showed various distinct peaks: one predominant band at 3190–3380 cm^{-1} (s) due to N–H stretch of secondary N-substituted amides; 2980 cm^{-1} (weak; w) due to C–H stretch, medium bands at 1500–1650 cm^{-1} due to C–C, while 898 cm^{-1} (s) and 875 cm^{-1} (s) due to p-substituted aromatic out of plane C–H deformation of aromatic residue of tryptophan or tyrosine; 2931 cm^{-1} (s) and 2898 cm^{-1} (s) due to C–H stretch, while 1425 cm^{-1} (s), 1382 cm^{-1} (m), 1361 cm^{-1} (m), and 1340 cm^{-1} (m) due to C–H deformation of alkyl chain of amino acids; 1670 cm^{-1} due to C=O stretch of carboxylate anion and amide group; strong peaks between 1050 and 1200 cm^{-1}, weak bands at 550–600 cm^{-1}, and 400–450 cm^{-1} due to C–S stretch of sulfides and disulfides. With incorporation of α-amylase, the spectrum of beads was similar to that of the κ-carrageenan blank beads. However, the physical mixture of α-amylase and blank beads showed the peaks due to both α-amylase and κ-carrageenan. This confirms the amylase entrapment into the κ-carrageenan beads at molecular level.

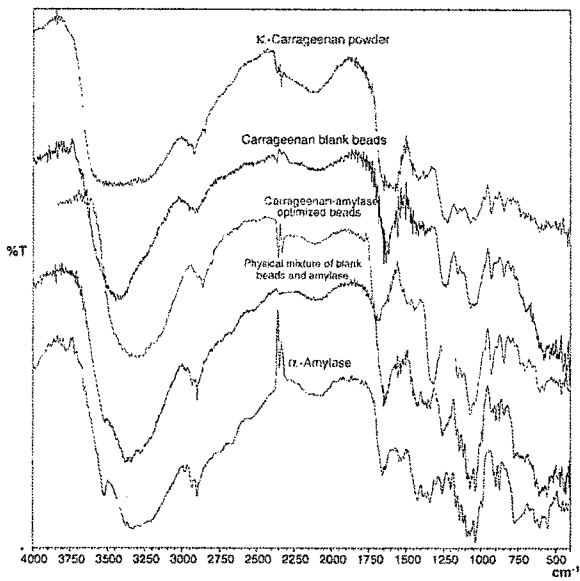

Fig. 5. The FTIR spectra of κ-carrageenan powder, carrageenan blank beads, α-amylase loaded carrageenan beads, physical mixture of α-amylase and blank beads, and α-amylase.

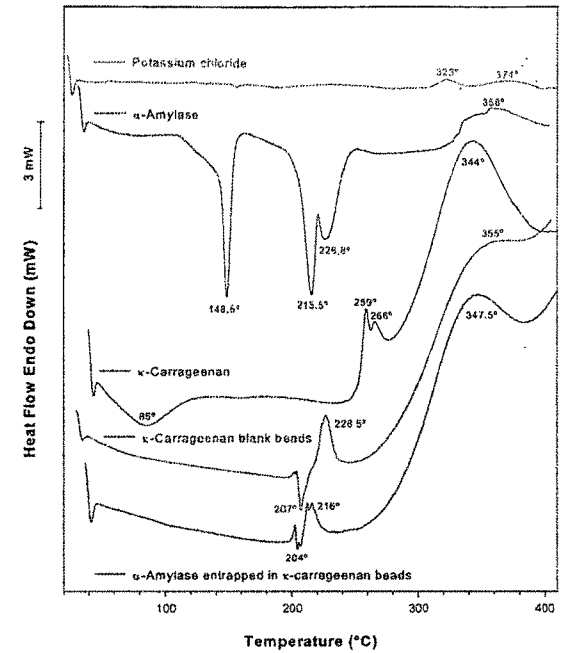

Fig. 6. The DSC thermograms of potassium chloride, α-amylase, κ-carrageenan powder, blank beads, and α-amylase loaded carrageenan beads made at the same analytical conditions.

3.6.2. Differential scanning calorimetry (DSC)

The DSC thermograms of potassium chloride, α-amylase, κ-carrageenan, blank beads, and α-amylase-loaded beads are shown in Fig. 6. Potassium chloride showed two non-significant exothermic peaks at 323 and 374 °C. α-Amylase exhibited three endothermic peaks at 148.5, 215.5, and 226.8 °C and one minor exothermic peak at 358 °C. Broad endothermic peak at 85 °C in the thermogram of κ-carrageenan was observed due to the presence of water molecules. Two minor peaks at 259 and 266 °C in the degradation exotherm of κ-carrageenan were absent in blank beads and α-amylase loaded beads, while major exothermic peak at 344 °C was found to be shifted towards higher temperature (355 °C) in blank beads. This showed that, κ-carrageenan-KCl beads are more stable than κ-carrageenan. However, additional two peaks (one endothermic at 207 and one exothermic at 226.5 °C) were observed in the thermogram of blank beads due to the potassium-κ-carrageenan interaction. DSC thermogram of enzyme loaded beads was similar to that of blank beads except all corresponding peaks were shifted to lower temperature, might be due to the presence of α-amylase. However, it did not showed any peak analogous to α-amylase. This confirms that most of the enzyme was uniformly dispersed at the molecular level in the beads.

3.6.3. Morphology of the beads

The spherical shape of beads in wet state was usually lost after drying especially for beads prepared with low carrageenan concentration. In 2.5% (w/v) carrageenan, the dried beads were very irregular and tend to agglomerate due to low mechanical strength. With the increase of κ-carrageenan concentration (3.5%, w/v), the shape of beads retained considerably. However, the shape of beads changed to disc with a collapsed center (Fig. 7) during drying process due to aggregation of the helical fibers into bundles and the squeezing out of some water from the gel (Iborra et al., 1997). Normally the spherical shape was retained when the carrageenan concentration was as high as 5.0% (w/v), but viscosity of 5.0% (w/v) solution was too high for bead preparation under present experimental conditions so it was not studied. Crosslinked hydrogels reach an equilibrium swelling level in aqueous solutions, which depends mainly on the crosslink density. In some cases, depending on the solvent composition, temperature and solids concentration

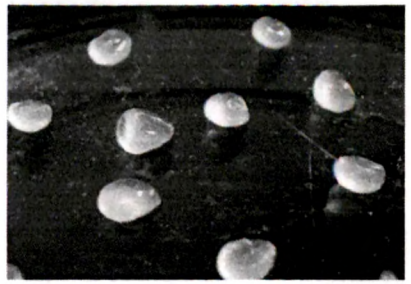

Fig. 7. Photograph of wet κ-carrageenan beads showing spherical disk shape with collapsed centre during drying process.

during gel formation, phase separation can occur, and water-filled 'voids' or 'macropores' can form which can be observed Fig. 2. One noticeable characteristic of the beads' surface is high degree of crosslinking when the concentration of potassium chloride increased (Fig. 2A–C). Further, the surface morphology was improved (i.e. decrease in roughness) with increase in κ-carrageenan concentration (Fig. 2D–F) due to the high viscosity of the κ-carrageenan solution.

3.7. Stability study

For the formulation developed, the similarity factor (f_2) was calculated by a comparison of the dissolution profiles at each storage condition with the control at the initial condition. Results of f_2 factors ranged from 73 to 97 with 2–5% average difference. Overall, results from the stability studies indicated that capsules were physically and chemically stable for at least 12 months at 40 ± 2 C/75 ± 5% relative humidity and for more than 12 months (approximately for double time period) at 30 ± 2 C/65 ± 5% relative humidity.

An approach for analyzing the data on a quantitative attribute that is expected to change with time is to determine the time at which the 95% one-sided confidence limit for the mean curve intersects the acceptance criterion (not more than 5% change in assay from its initial value). The accelerated stability data for prepared formulation, marketed formulation and the bulk α-amylase were extrapolated to calculate the shelf-life (Fig. 8) and were found be 3.53, 0.99 and 0.41 year, respectively. Hence, the stability of the entrapped α-amylase was significantly improved than that of the conventional dosage forms.

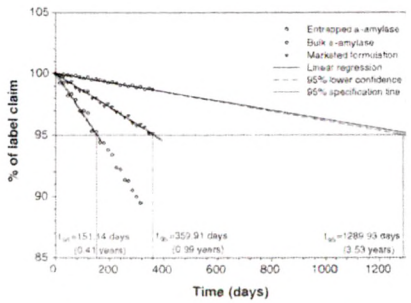

Fig. 8. Extrapolation of accelerated stability data for shelf-life calculation.

4. Conclusions

Ionotropically corsslinked κ-carrageenan beads exhibit promising stability improvement of entrapped α-amylase and can find a place in the design of multiparticulate drug delivery systems. The optimization of the process using the composite index resulted in more than 73% entrapment and more than 74 min of T_{90} at high levels of all three process variables. T_{50} and T_{90} were increased with increase in all three process variables. Percentage entrapment and particle size were found to be directly proportional to κ-carrageenan concentration and inversely proportional to potassium chloride concentration and hardening time. Mathematical analysis of the different drug release modalities has evidenced that enzyme release from carrageenan beads follows Korsmeyer–Peppas' power law equation with super case-II transport mechanism. Furthermore, investigation of release profile by Kopcha model revealed that enzyme release is due to erosion and not by diffusion. FTIR and DSC study showed uniform dispersion of α-amylase at molecular level in the carrageenan beads. Texture analysis discovered directly proportional relation of degree of crosslinking with potassium chloride concentration. In addition, the surface roughness decreased with increase in κ-carrageenan concentration. Accelerated and long term stability study illustrated considerably improved shelf-life of α-amylase entrapped in carrageenan than the conventional dosage form. The application of a single polymer (as used traditionally) for the formation of beads allows the formulator to predict and produce beads of different geometries, strengths and release characteristics. Results of presented experiments seem to be of value for the pharmaceutical industries associated with digestive enzymes formulations.

Acknowledgements

This research was supported by a grant from the All India Council for Technical Education (New Delhi, India, 8019/RDII/R&D/PHA (207)/2000–2001), for which R.C. Mashru was the principal investigator. We acknowledge the University Grants Commission (New Delhi, India) for availing Senior Research Fellowship to Mr. Mayur G. Sankalia. We greatly appreciate the Vaibhav Analytical Services Ltd. (Ahmedabad, India) for skillful assistance and providing FTIR testing facility in this study.

References

Bhardwaj, S.B., Shukla, A.J., Collins, C.C., 1995. Effect of varying drug loading on particle size distribution and drug release kinetics of verapamil hydrochloride microspheres prepared with cellulose esters. J. Microencapsul. 12, 71–81.

Bickerstaff, G.F., 1997. Immobilization of enzymes and cells: some practical considerations. In: Bickerstaff, G.F. (Ed.), Immobilization of Enzymes and Cells, Methods in Biotechnology, vol. 1. Humana Press, Totowa, New Jersey, pp. 1–12.

Bodeam, X., Leucata, S.E., 1997. Optimization of hydrophilic matrix tablets using a D-optimal design. Int. J. Pharm. 153, 247–255.

Bodmeier, R., Wang, J., 1993. Microencapsulation of drugs with aqueous colloidal polymer dispersions. J. Pharm. Sci. 82, 191–194.

Bonferoni, M.C., Rossi, S., Tamayo, M., Pedraz, J.L., Dominguez Gil, A., Caramella, C., 1994. On the employment of λ-carrageenan in a matrix system. II. λ-Carrageenan and hydroxypropylmethylcellulose mixtures. J. Control. Rel. 30, 175–182.

Chen, H., Langer, R., 1997. Magnetically-responsive polymerized liposomes as potential oral delivery vehicles. Pharm. Res. 14, 537–540.

Derringer, G., Suich, R., 1980. Simultaneous optimization of several responses variables. J. Qual. Technol. 2, 214–219.

Garcia, A.M., Ghaly, E.S., 1996. Preliminary spherical agglomerates of water soluble drug using natural polymer and cross-linking technique. J. Control. Rel. 40, 179–186.

Gibaldi, M., Feldman, S., 1967. Establishment of sink conditions in dissolution rate determinations - theoretical considerations and application to non-disintegrating dosage forms. J. Pharm. Sci. 56, 1238–1242.

Gohel, M.C., Patel, M.M., Amin, A.F., 2003. Development of modified release diltiazem HCl tablets using composite index to identify optimal formulation. Drug Dev. Ind. Pharm. 29, 565–574.

Guzman-Maldano, H., Paredes-Lopez, O., 1995. Amylolytic enzymes and products derived from starch; a review. Crit. Rev. Food. Nutr. 36, 373–403.

Higuchi, T., 1963. Mechanism of sustained-action medication. Theoretical analysis of rate of release of solid drugs dispersed in solid matrices. J. Pharm. Sci. 52, 1145–1149.

Hixson, A.W., Crowell, J.H., 1931. Dependence of reaction velocity upon surface and agitation. Ind. Eng. Chem. 23, 923–931.

Hossain, K.S., Miyanaga, K., Maeda, H., Nemoto, N., 2001. Sol–gel transition behavior of pure ι-carrageenan in both salt-free and added salt states. Biomacromolecules 2, 442–449.

Hsiu, J., Fischer, E.H., Stein, E.A., 1964. Alpha-amylase as calcium-metalloenzymes. II. Calcium and the catalytic activity. Biochemistry 3, 61–66.

Iborra, J.L., Manjon, A., Canovas, M., 1997. Immobilization in carrageenans. In: Bickerstaff, G.F. (Ed.), Immobilization of Enzymes and Cells, Methods in Biotechnology, vol. 1. Humana Press, Totowa, New Jersey, pp. 53–60.

Kopcha, M., Lordi, N., Tojo, K.J., 1991. Evaluation of release from selected thermosoftening vehicles. J. Pharm. Pharmacol. 43, 382–387.

Korsmeyer, R.W., Gurny, R., Doelker, E.M., Buri, P., Peppas, N.A., 1983. Mechanism of solute release from porous hydrophilic polymers. Int. J. Pharm. 15, 25–35.

Nielsen, J.E., Beier, L., Otzen, D., Borchert, T.V., Frantzen, H.B., Andersen, K.V., Svendsen, A., 1999. Electrostatics in the active site of an α-amylase. Eur. J. Biochem. 264, 816–824.

Pather, S.I., Russell, I., Syce, J.A., Neau, S.H., 1998. Sustained release theophylline tablets by direct compression. Part 1. Formulation and in vitro testing. Int. J. Pharm. 164, 1–10.

Peppas, N.A., 1985. Analysis of Fickian and non-Fickian drug release from polymers. Pharm. Acta Helv. 60, 110–111.

Picker, K.M., 1999. Matrix tablets of carrageenans. II. Release behavior and effect of added cations. Drug Dev. Ind. Pharm. 25, 339–346.

Prestwich, G.D., Marecak, D.M., Marecak, J.F., Vercruysse, K.P., Ziebell, M.R., 1998. Controlled chemical modification of hyaluronic acid. J. Control. Rel. 53, 93–103.

Rice, E.W., 1959. Improved spectrophotometric determination of amylase with a new stable starch substrate solution. Clin. Chem. 5, 592–596.

Ritger, P.L., Peppas, N.A., 1987. A simple equation for description of solute release. II. Fickian and anomalous release from swellable devices. J. Control. Rel. 5, 37–42.

Schmidt, A.G., Wartewig, S., Picker, K.M., 2003. Potential of carrageenans to protect drugs from polymorphic transformation. Eur. J. Pharm. Biopharm. 56, 101–110.

Shigeo, O., Toshihiko, K., Yousuke, M., Horoshima, S., Kozo, T., Nagai, T., 1994. A new attempt to solve the scale up problem for granulation using response surface methodology. J. Pharm. Sci. 83, 439–443.

Sipahigil, O., Dortunc, B., 2001. Preparation and in vitro evaluation of verapamil HCl and ibuprofen containing carrageenan beads. Int. J. Pharm. 228, 119–128.

Smith, B.W., Roe, J.H., 1957. A micromodification of the Smith and Roe method for the determination of amylase in body fluids. J. Biol. Chem. 227, 357–362.

Suzuki, S., Lim, J.K., 1994. Microencapsulation with carrageenan-locust bean gum in a multiphase emulsification technique for sustained drug release. J. Microencapsul. 11, 197–203.

Taylor, M.K., Ginsburg, J., Hickey, A.J., Gheyas, F., 2000. Composite method to quantify powder flow as a screening method in early tablet or capsule formulation development. AAPS PharmSciTech 1, article 18 (http://www.pharmascitech.com).

Uhlig, H., 1998. Description of Enzymes. in: Industrial Enzymes and their Applications. A Wiley-Interscience Publication John Wiley & Sons. Inc., New York, pp. 37–202.

Uitdehaag, J.C., Mosi, R., Kalk, K.H., van der Veen, B.A., Dijkhuizen, L., Withers, S.G., Dijkstra, B.W., 1999. X-ray structures along the reaction pathway of cyclodextrin glycosyltransferase elucidate catalysis in the α-amylase family. Nat. Struct. Biol. 6, 432–436.

Wagner, J.G., 1969. Interpretation of percent dissolved-time plots derived from in vitro testing of conventional tablets and capsules. J. Pharm. Sci. 58, 1253–1257.